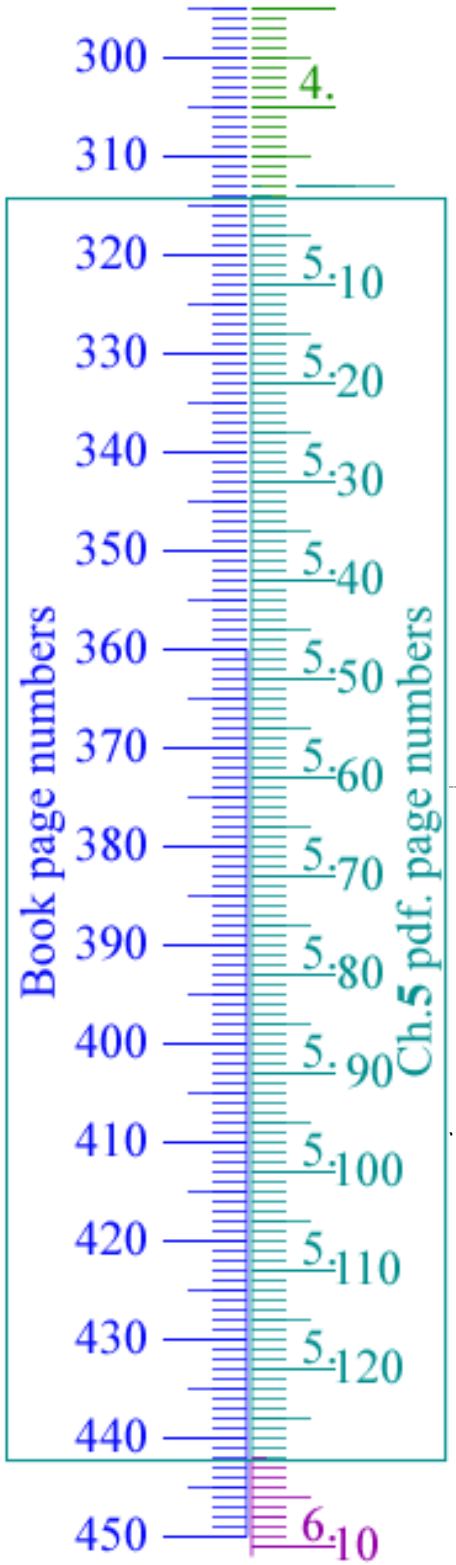

5 REPRESENTATIONS OF CONTINUOUS ROTATION GROUPS AND APPLICATIONS

CHAPTER 5

REPRESENTATIONS OF CONTINUOUS ROTATION GROUPS AND APPLICATIONS

We consider now the symmetry of a vacuum occupied by a single point or a perfect sphere. This symmetry is higher than all the point symmetries discussed earlier since it contains all their symmetry operations along with an infinite number more. A rotation about any axis through the point of origin, by any angle 1.0001°, 19°, or whatever, is now a symmetry operation. So is inversion or any reflection. The resulting symmetry group is called the three-dimensional ORTHOGONAL GROUP O_3.

The theory of the orthogonal groups O_2 and O_3 in two and three dimensions is known to physicists as ANGULAR-MOMENTUM CALCULUS. This will be the main topic of this chapter. To mathematicians O_2 and O_3 are two fundamental examples of LIE (pronounced Lee) groups, which are named after mathematician Sophus Lie. This chapter also contains a brief introduction to other important Lie groups including O_4, and the UNITARY GROUPS U_2 and U_3.

Lie groups appear to be very different from the finite or discrete symmetry groups which have been discussed so far. In the place of group tables and tables of representations for finite group algebras there will be analytic functions which give the same information for Lie groups. However, it is possible to find finite subalgebras called LIE ALGEBRAS which help one to analyze Lie groups and their representations. Then some of the algebraic methods developed in the preceding chapters can be used again.

One of the important applications of the R_3 Lie-group representations involves the theory of the free quantum rotor and the hindered quantum rotor. The theory of hindered quantum rotors is related to crystal field splitting. This theory is a generalization of the Bohr orbital level splitting

treated in Section 2.12 or 3.6, and it is introduced in Section 5.6. This is a very important part of the theoretical spectroscopy which is discussed in later chapters.

5.1 BASIC THEORY OF ORTHOGONAL GROUPS O_2 AND O_3

The group O_n consists of all real linear transformations of n-dimensional vectors which leave all vector lengths and angles between all pairs of vectors unchanged. For example, consider the set of all 3×3 orthogonal transformation matrices:

$$\mathscr{O} = \begin{pmatrix} \mathscr{O}_{11} & \mathscr{O}_{12} & \mathscr{O}_{13} \\ \mathscr{O}_{21} & \mathscr{O}_{22} & \mathscr{O}_{23} \\ \mathscr{O}_{31} & \mathscr{O}_{32} & \mathscr{O}_{33} \end{pmatrix}. \tag{5.1.1}$$

Suppose that their action on column vectors

$$u = \begin{pmatrix} u_1 \\ u_2 \\ u_3 \end{pmatrix}, \qquad v = \begin{pmatrix} v_1 \\ v_2 \\ v_3 \end{pmatrix}, \ldots \tag{5.1.2}$$

gives new or transformed vectors:

$$\begin{pmatrix} u'_3 \\ u'_2 \\ u'_3 \end{pmatrix} = \begin{pmatrix} \mathscr{O}_{11} & \mathscr{O}_{12} & \mathscr{O}_{13} \\ \mathscr{O}_{21} & \mathscr{O}_{22} & \mathscr{O}_{23} \\ \mathscr{O}_{31} & \mathscr{O}_{32} & \mathscr{O}_{33} \end{pmatrix} \begin{pmatrix} u_1 \\ u_2 \\ u_3 \end{pmatrix}, \qquad \begin{pmatrix} v'_1 \\ v'_2 \\ v'_3 \end{pmatrix} = \begin{pmatrix} \mathscr{O}_{11} & \mathscr{O}_{12} & \mathscr{O}_{13} \\ \mathscr{O}_{21} & \mathscr{O}_{22} & \mathscr{O}_{23} \\ \mathscr{O}_{31} & \mathscr{O}_{32} & \mathscr{O}_{33} \end{pmatrix} \begin{pmatrix} v_1 \\ v_2 \\ v_3 \end{pmatrix}, \tag{5.1.3}$$

for which all scalar products are unchanged:

$$u' \cdot u' = u \cdot u, \qquad u' \cdot v' = u \cdot v, \qquad v' \cdot v' = v \cdot v. \tag{5.1.4}$$

This implies the following for arbitrary u_i or v_j:

$$\sum_{j=1}^{3} u'_j v'_j = \sum_{j=1}^{3} \sum_{u=1}^{3} \sum_{l=1}^{3} (\mathscr{O}_{jk} u_k)(\mathscr{O}_{jl} v_l) = \sum_{k=1}^{3} \sum_{l=1}^{3} \left(\sum_{j=1}^{3} \mathscr{O}_{jk} \mathscr{O}_{jl} \right) u_k v_l = \sum_{n=1}^{3} u_n v_n.$$

In particular, setting $u_i = \delta_{ik}$ and $v_j = \delta_{jl}$, one finds the following constraint on the $\mathscr{O}$ matrices:

$$\sum_{j=1}^{3} \mathscr{O}_{jk} \mathscr{O}_{jl} = \delta_{kl}. \tag{5.1.5}$$

This equation implies that the columns of each $\mathscr{O}$ matrix must be three mutually orthogonal column vectors of unit length. It also implies that the transpose $\mathscr{O}^T$ of the matrix $\mathscr{O}$ must be the inverse of $\mathscr{O}$:

$$\mathscr{O}^T\mathscr{O} = 1 = \mathscr{O}\mathscr{O}^T. \tag{5.1.6}$$

Note that if the columns of any finite square matrix are components of mutually orthogonal vectors, then the same must be true of the rows:

$$\sum_{j=1}^{3} \mathscr{O}_{kj}\mathscr{O}_{lj} = \delta_{kl}. \tag{5.1.7}$$

Equations (5.1.5) and (5.1.7) are special cases of the orthogonal and completeness relations discussed in Section 1.2.B(b). [Compare with Eqs. (1.2.19) and (1.2.20).]

One may imagine that these operations $\mathscr{O}$ transform physical objects in space. Physical objects are composed of particles whose position vectors $u, v, w, \ldots$ get moved by $\mathscr{O}$, as indicated in Figure 5.1.1.

After an orthogonal transformation all the particles in the object will end up having the same interparticle distances, since all scalar products stay the same. While thinking of this one might conclude that $\mathscr{O}_3$ is the set of all rigid rotations. In fact $\mathscr{O}_3$ does contain all rotations in a subgroup labeled R_3. However, this accounts for only half of O_3. The other half consists of discontinuous or IMPROPER transformations such as INVERSION (I) through a point [see Figure 5.1.1(b)] or combinations of I with rotations. The improper transformations change left-handed objects into right-handed ones and vice versa. It is easy to snap a left-handed surgeon's glove into a right-handed one, but if you try the same transformation on most objects you will break or tear them.

In Section 2.11 we introduced another example of an improper transformation in O_3 represented by a matrix having only ± 1 on its diagonal:

$$\sigma_{xy} \to \begin{pmatrix} 1 & 0 & 0 \\ 0 & 1 & 0 \\ 0 & 0 & -1 \end{pmatrix}.$$

This transformation is inversion through a plane (the xy or 12 plane is used here) or REFLECTION. A related transformation,

$$i_z = \sigma_{xy} I \to \begin{pmatrix} -1 & 0 & 0 \\ 0 & -1 & 0 \\ 0 & 0 & 1 \end{pmatrix},$$

could be called inversion through an axis. (The z or 3 axis is used here.)

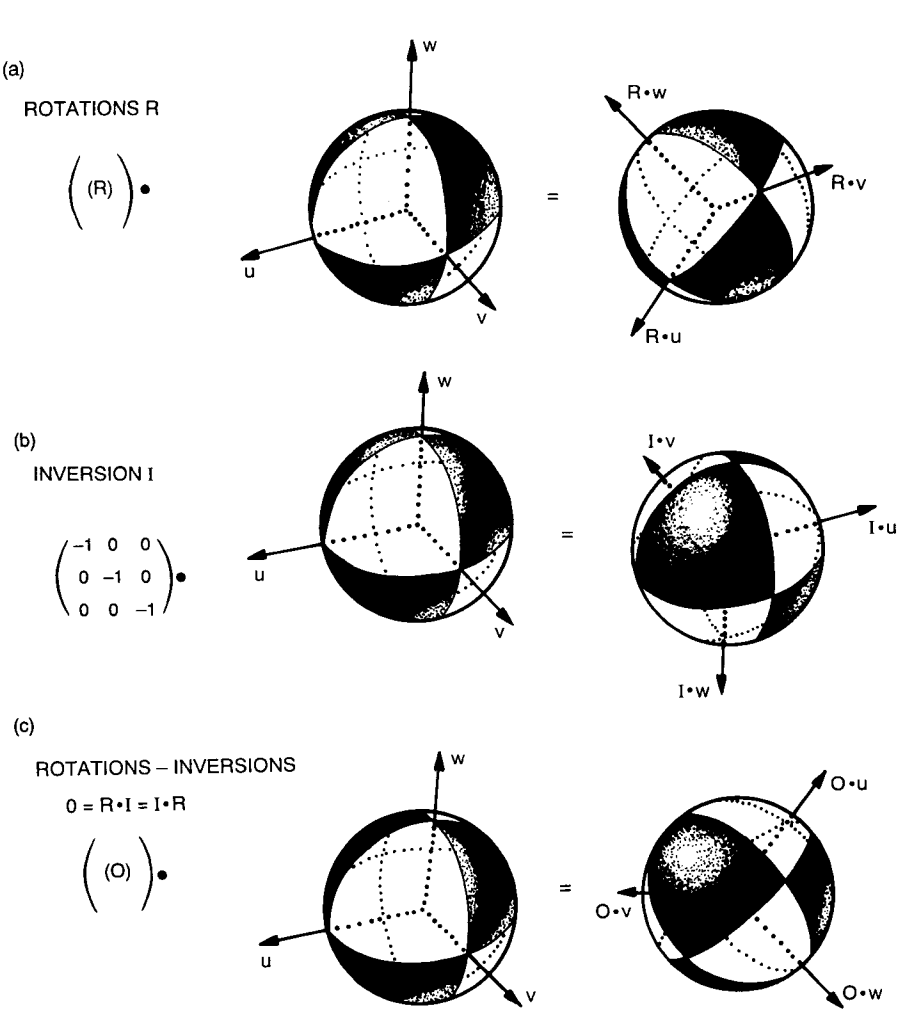

Figure 5.1.1 Action of orthogonal transformations on a unit vector triad. (a) Rotations are proper operations. (b) Inversion or (c) rotation inversions are improper operations.

However, it is actually quite proper, since it is just a 180° rotation around the z axis. To check the propriety of a general orthogonal transformation matrix, one may evaluate its determinant. The determinant gives the volume spanned by the transformed unit vectors $\hat{x}'_j = \mathscr{O}\hat{x}_j$:

$$\det \mathscr{O} = \hat{x}'_1 \cdot \hat{x}'_2 \times \hat{x}'_3 = \begin{cases} 1, & \text{if } \mathscr{O} \text{ is proper,} \\ -1, & \text{if } \mathscr{O} \text{ is improper.} \end{cases} \tag{5.1.8}$$

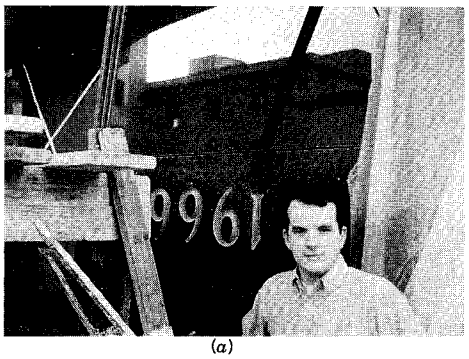

(a)

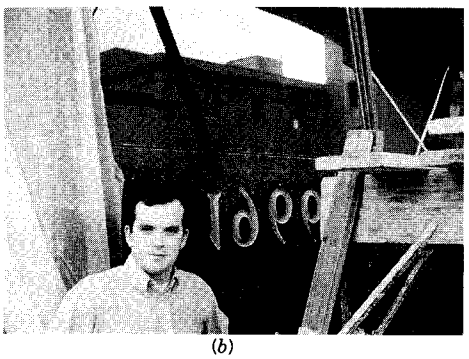

(b)

Figure 5.1.2 (*a*) Early Cal Tech experiment on parity and time reversal. (*b*) Later experiment.

You might try to determine whether proper or improper operations have been applied in Figures 5.1.2.

Note that O_3 and R_3 are not Abelian groups; that is, a general pair of elements will not necessarily commute ($\mathscr{O}\mathscr{O}' \neq \mathscr{O}'\mathscr{O}$). However, the inversion operator I is seen to commute with all elements in $\mathscr{O}_3$. This allows us to express $\mathscr{O}_3$ as an OUTER PRODUCT $R_3 \times C_i$ of the rotation group R_3 with the finite group $C_i = \{1, I\}$ as depicted in Figure 5.1.3. (The formal definition of the outer product was given in Section 2.10.) This allows one to obtain the representations of O_3 directly from products of those of R_3 and C_i.

Let us consider briefly the mathematical definition of the two-dimensional orthogonal group O_2. The four components of 2×2 orthogonal matrices $\mathscr{O}_{ij}$ obey Eqs. (5.1.5). Of these, the following three are independent:

$$\mathscr{O}_{11}\mathscr{O}_{11} + \mathscr{O}_{21}\mathscr{O}_{21} = 1, \tag{5.1.9a}$$

$$\mathscr{O}_{12}\mathscr{O}_{12} + \mathscr{O}_{22}\mathscr{O}_{22} = 1, \tag{5.1.9b}$$

$$\mathscr{O}_{11}\mathscr{O}_{21} + \mathscr{O}_{12}\mathscr{O}_{21} = 0. \tag{5.1.9c}$$

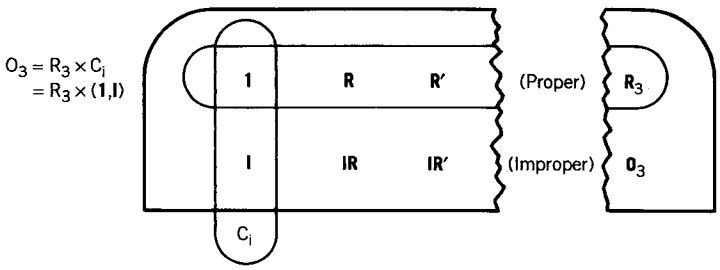

Figure 5.1.3 Diagram of orthogonal group O_3. O_3 is an outer product of rotation group R_3 and the cyclic (C_2-like) inversion group C_i.

This leaves only one undetermined variable or parameter. Equation (5.1.9a) suggests that we set $\mathscr{O}_{11} \equiv \cos\phi$ and $\mathscr{O}_{21} = \sin\phi$. Then we see that the following two types of solutions to the orthogonal equations are possible:

$$\mathscr{O} = \begin{pmatrix} \cos\phi & -\sin\phi \\ \sin\phi & \cos\phi \end{pmatrix}, \tag{5.1.10a}$$

$$\mathscr{O}' = \begin{pmatrix} \cos\phi & \sin\phi \\ \sin\phi & -\cos\phi \end{pmatrix} = \begin{pmatrix} \cos\phi & -\sin\phi \\ \sin\phi & \cos\phi \end{pmatrix}\begin{pmatrix} 1 & 0 \\ 0 & -1 \end{pmatrix}. \tag{5.1.10b}$$

The first matrix has $\det \mathscr{O} = +1$ and corresponds to a proper rotation by angle ϕ, while the second matrix has $\det \mathscr{O}' = -1$ and corresponds to an improper inversion or reflection through the 1 axis, followed by a rotation of angle ϕ. (The second transformation is equal to a single reflection through a line with slope angle $\phi/2$.)

From this it is clear that the group R_2 of proper rotations is a subgroup of O_2, and that R_2 is Abelian. However, the reflections such as $\left(\begin{smallmatrix} 1 & 0 \\ 0 & -1 \end{smallmatrix}\right)$ do not commute with elements of R_2, and so it is not possible to express O_2 as an outer product involving R_2. Furthermore, O_2 is not Abelian. Note, also, that the improper two-dimensional reflection $\left(\begin{smallmatrix} 1 & 0 \\ 0 & -1 \end{smallmatrix}\right)$ could be accomplished by a proper three-dimensional rotation about the 1 axis.

Similar reasoning can be applied to any of the orthogonal Lie groups O_n. For example, each of the n^2 real components $\mathscr{O}_{ij}$ of O_n can assume any values that satisfy the orthogonality equations,

$$\sum_{i=1}^{3} \mathscr{O}_{ij}\mathscr{O}_{ik} = \delta_{jk}, \qquad j, k = 1, 2, \ldots, n. \tag{5.1.11}$$

Of these, exactly $n(n+1)/2$ are independent ($j \geq k = 1, 2, \ldots, n$). This implies that only $n^2 - n(n+1)/2 = n(n-1)/2$ independent parameters

are needed to define all elements of O_n:

$$\begin{aligned} O_n &= O_1, O_2, O_3, O_4, O_5, O_6 \cdots, \\ \text{number of parameters} &= n(n-1)/2 = 0,\ 1,\ 3,\ 6,\ 10,\ 15 \cdots. \end{aligned} \tag{5.1.12}$$

(Note that O_1 contains only two elements. No continuous parameters are needed.) In general, R_n and O_n have the same number of parameters since they differ only by the inclusion of discrete parity or inversion operations.

5.2 REPRESENTATIONS OF R_2, O_2, AND RELATED SYMMETRY GROUPS

Two-dimensional rotational symmetry R_2 is the limiting case of C_n symmetry when n approaches infinity. Let the angle of rotation ($0 \leq \phi < 2\pi$) be the single parameter of R_2. For C_n, ϕ was restricted to integral multiples of $2\pi/n$. C_n symmetry was discussed in Sections 2.7 and 2.12.

The irreps of R_2 are obtained from those of C_n by taking the limit $n \to \infty$. They are given by

$$D^m(\phi) = e^{im\phi}, \tag{5.2.1}$$

where all integers $m = 0, \pm 1, \pm 2, \ldots, \infty$ are allowed now. In the case of C_n, these integers had been restricted by Eq. (2.7.2) so as to give only the nth roots of unity. (Recall also Figure 2.7.2.)

Section 2.1.7 contains a discussion of the physical significance of the irreps in terms of waves. The case $m = |m|$ (positive) corresponds to an angular wave with m crests running around the circle in the counterclockwise direction, while $m = -|m|$ (negative) corresponds to the same wave running in the clockwise direction.

If the full O_2 symmetry is present, these two wave states $|+m\rangle$ and $|-m\rangle$ must have the same frequency or phase velocity. This follows since one is the (improper) reflection of the other. We may therefore combine them to make cosine ($|c_m\rangle$) and sine ($|s_m\rangle$) standing waves which are also stationary states or normal modes:

$$|c_m\rangle = (|+m\rangle + |-m\rangle)/\sqrt{2}, \qquad |s_m\rangle = (-|+m\rangle + |-m\rangle)/i\sqrt{2}. \tag{5.2.2}$$

Then the resulting representation of the proper rotations is

$$\begin{pmatrix} \frac{1}{\sqrt{2}} & \frac{1}{\sqrt{2}} \\ -\frac{i}{\sqrt{2}} & \frac{i}{\sqrt{2}} \end{pmatrix} \begin{pmatrix} e^{im\phi} & 0 \\ 0 & e^{-im\phi} \end{pmatrix} \begin{pmatrix} \frac{1}{\sqrt{2}} & \frac{i}{\sqrt{2}} \\ \frac{1}{\sqrt{2}} & -\frac{i}{\sqrt{2}} \end{pmatrix}$$

$$= \begin{pmatrix} \cos m\phi & -\sin m\phi \\ \sin m\phi & \cos m\phi \end{pmatrix} \equiv \mathscr{D}^m(\phi). \tag{5.2.3}$$

This is the real irrep $\mathscr{D}^m$ of O_2 rotations for $m \geq 1$. These O_2 irreps are listed in the following on the left-hand side. Two of the most commonly used irrep notations are given. The equivalent complex moving-wave representations are given below the table for the standing-wave ones.

Irrep notations			Standing-Wave Representations: z-Axis Rotation ϕ	Standing-Wave Representations: x-Plane Reflection $\updownarrow$
A_1	Σ^+	$m = 0$	$\mathscr{D}^{\Sigma^+}(\phi) = 1$	$D^{\Sigma^+}(\updownarrow) = 1$
A_2	Σ^-	0	$\mathscr{D}^{\Sigma^-}(\phi) = 1$	$D^{\Sigma^-}(\updownarrow) = -1$
E_1	Π	± 1	$\mathscr{D}^{\Pi}(\phi) = \begin{pmatrix} \cos\phi & -\sin\phi \\ \sin\phi & \cos\phi \end{pmatrix}$	$\mathscr{D}^{\Pi}(\updownarrow) = \begin{pmatrix} 1 & 0 \\ 0 & -1 \end{pmatrix}$
E_2	Δ	± 2	$\mathscr{D}^{\Delta}(\phi) = \begin{pmatrix} \cos 2\phi & -\sin 2\phi \\ \sin 2\phi & \cos 2\phi \end{pmatrix}$	$\mathscr{D}^{\Delta}(\updownarrow) = \begin{pmatrix} 1 & 0 \\ 0 & -1 \end{pmatrix}$
E_3	Φ	± 3	$\mathscr{D}^{\Phi}(\phi) = \begin{pmatrix} \cos 3\phi & -\sin 3\phi \\ \sin 3\phi & \cos 3\phi \end{pmatrix}$	$\mathscr{D}^{\Phi}(\updownarrow) = \begin{pmatrix} 1 & 0 \\ 0 & -1 \end{pmatrix}$
$\vdots$	$\vdots$	$\vdots$	$\vdots$	$\vdots$
			Moving-Wave Representations: z-Axis Rotation ϕ	Moving-Wave Representations: x-Plane Reflection $\updownarrow$
A_1	Σ^+	$m = 0$	$\mathscr{D}^{\Sigma^+}(\phi) = 1$	$D^{\Sigma^+}(\updownarrow) = 1$
A_2	Σ^-	0	$\mathscr{D}^{\Sigma^-}(\phi) = -1$	$D^{\Sigma^-}(\updownarrow) = -1$
E_1	Π	± 1	$D^{\Pi}(\phi) = \begin{pmatrix} e^{i\phi} & 0 \\ 0 & e^{-i\phi} \end{pmatrix}$	$D^{\Pi}(\updownarrow) = \begin{pmatrix} 0 & 1 \\ 1 & 0 \end{pmatrix}$
E_2	Δ	± 2	$D^{\Delta}(\phi) = \begin{pmatrix} e^{2i\phi} & 0 \\ 0 & e^{-2i\phi} \end{pmatrix}$	$D^{\Delta}(\updownarrow) = \begin{pmatrix} 0 & 1 \\ 1 & 0 \end{pmatrix}$
E_3	Φ	± 3	$D^{\Phi}(\phi) = \begin{pmatrix} e^{3i\phi} & 0 \\ 0 & e^{-3i\phi} \end{pmatrix}$	$D^{\Phi}(\updownarrow) = \begin{pmatrix} 0 & 1 \\ 1 & 0 \end{pmatrix}$
			$\vdots$	$\vdots$

(5.2.4)

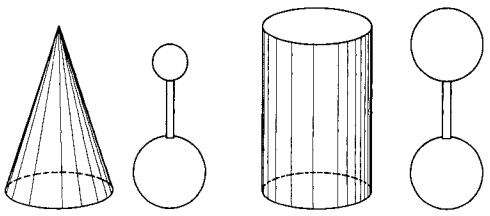

Figure 5.2.1 Examples of objects with (a) $C_{\infty v}$ symmetry, and (b) $D_{\infty h}$ symmetry.

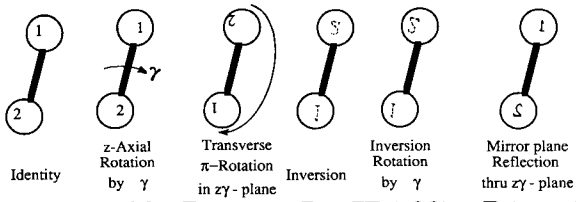

$D_{\infty h}$	1	$\mathbf{R}(\gamma 00)$	$\mathbf{R}(-\gamma\pi\gamma)$	$\mathbf{I}$	$\mathbf{IR}(\gamma 00)$	$\mathbf{R}(-\gamma\pi\gamma)$
$A_{1g}=\Sigma_g^+$	1	1	1	1	1	1
$A_{1u}=\Sigma_u^+$	1	1	-1	-1	-1	1
$A_{2g}=\Sigma_g^-$	1	1	-1	1	1	-1
$A_{2u}=\Sigma_u^-$	1	1	1	-1	-1	-1
$E_{1g}=\Pi_g$	2	$2\cos\gamma$	0	2	$2\cos\gamma$	0
$E_{1u}=\Pi_u$	2	$2\cos\gamma$	0	-2	$-2\cos\gamma$	0
$E_{2g}=\Delta_g$	2	$2\cos 2\gamma$	0	2	$2\cos 2\gamma$	0
$E_{2u}=\Delta_u$	2	$2\cos 2\gamma$	0	-2	$-2\cos 2\gamma$	0
$E_{3g}=\Phi_g$	2	$2\cos 3\gamma$	0	2	$2\cos 3\gamma$	0
⋮	⋮	⋮	⋮	⋮	⋮	⋮

Figure 5.2.2 Classes and characters of $D_{\infty h}$ molecular symmetry. Operations are indicated by their effect on a diatomic (X_2) molecule. The notation [$R(\alpha 00)$, etc.] for Euler angles will be explained in Section 5.3.

The spatial symmetry isomorphic to O_2 is known as $C_{\infty v}$. It is the limiting case of C_{nv} as $n \to \infty$, and is the symmetry of a right circular cone or of a diatomic or linear molecule composed of different nuclei. [See Figure 5.2.1(a).] Another related spatial symmetry is

$$D_{\infty h} = C_{\infty v} \times C_i \sim O_2 \times C_i. \tag{5.2.5}$$

This includes all the $O_2 \sim C_{\infty v}$ operations as well as all of them in combination with the 3-space inversion I. $D_{\infty h}$ is the spatial symmetry of a right circular cylinder or a homonuclear diatomic or linear molecule. [See Figure 5.2.1(b)]. The irreps of $D_{\infty h}$ follow directly from the products of $C_{\infty v}$ and C_i irreps. The standard subscript notation is used to tell whether a given irrep base is even (g) or odd (u) under the inversion operation I. The $D_{\infty h}$ irrep characters are given for the archetypical operations which are shown above the table in Figure 5.2.2. The parametric notation $R(\alpha, \beta, \gamma)$ is explained in the following section.

5.3 PARAMETERS OF R_3

Equation (5.1.12) shows that R_3 has three parameters. There are many ways to choose these parameters. The following is a discussion of two different choices which indicates the advantages of each.

A. Euler Angles ($\alpha\beta\gamma$)

Probably the most common choices for parameters are the EULER ANGLES α, β, and γ. The goniometer in Figure 5.3.1 defines the rotational position state $|\alpha\beta\gamma\rangle$ of a ball and its $\{\bar{x}, \bar{y}, \bar{z}\}$ axes by angles α, β, and γ on three dials. The α dial and β dial define the azimuth and polar angles, respectively, of the $\bar{z}$ axis. The α and β Euler angles can serve as polar coordinates $\phi = \alpha$ and $\theta = \beta$ for a radius vector $\hat{r} = \bar{z}$ in the $\bar{z}$ direction. However, the similarity between Euler angles and spatial coordinates ends there. The third (γ) Euler angle gives the twist of the $\{\bar{x}\bar{y}\bar{z}\}$ system about the $\bar{z}$ axis.

It is important to note that generally each rotational position state $|\alpha\beta\gamma\rangle$ of the ball in Figure 5.3.1 has two possible Euler angle settings; i.e.,

$$|\alpha\beta\gamma\rangle = |\alpha \pm 180°, -\beta, \gamma \pm 180°\rangle \tag{5.3.1}$$

The settings $\{\alpha = 50°, \beta = 60°, \gamma = 70°\}$ and $\{\alpha = -130°, \beta = -60°, \gamma = -110°\}$ are shown in Figures 5.3.1(b) and 5.3.1(c), respectively. They put the $\{\bar{x}, \bar{y}, \bar{z}\}$ axes in the same position relative to the lab $\{xyz\}$ system. One may choose to ignore this double-valuedness by restricting β by the relation

$$0° \leq \beta < 180° \tag{5.3.2}$$

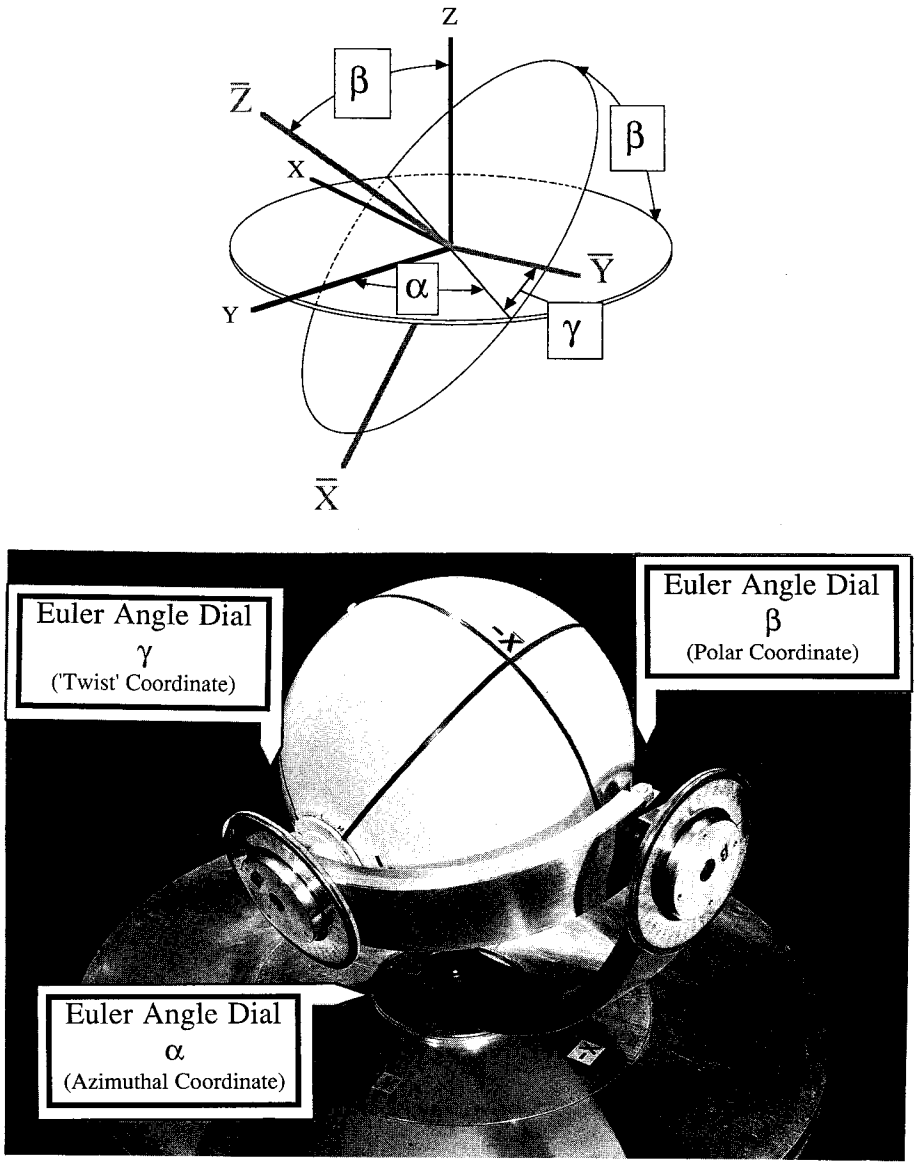

Figure 5.3.1 Definition of Euler angles as rotation position coordinates (*Photos by Vincent Malette and Joanie Geiser.*)

(b) Position State $|\alpha\beta\gamma\rangle = |\ 50°\ 60°\ 70°\rangle$

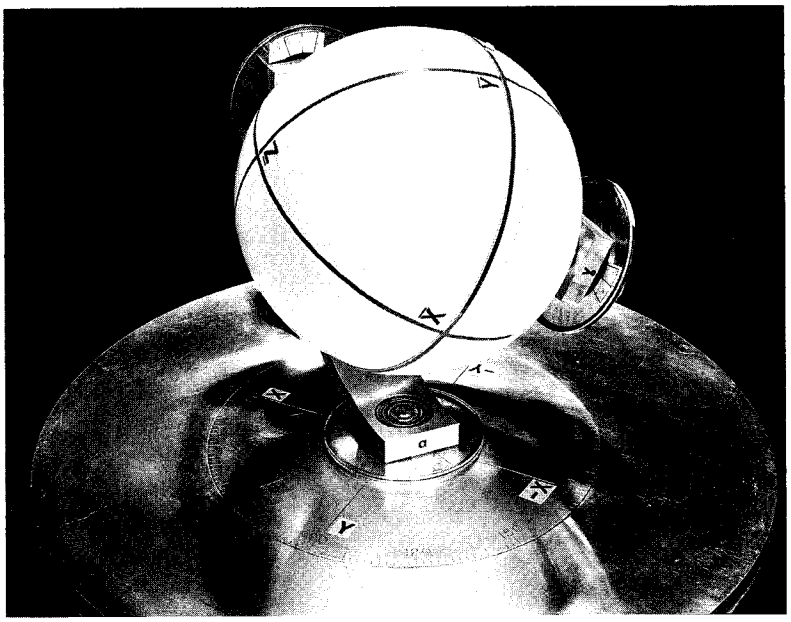

(c) Position State $|\alpha\beta\gamma\rangle = |\ -130°\ -60°\ -110°\rangle$

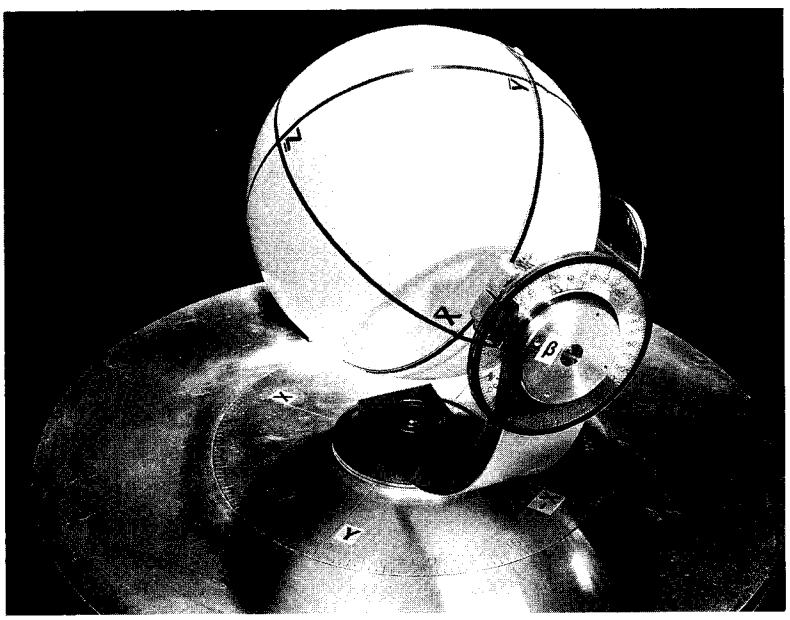

Figure 5.3.1 *(Continued).*

(d) Original State $|\alpha\beta\gamma\rangle = |\ 0°\ 0°\ 0°\rangle \equiv |\ 1\ \rangle$

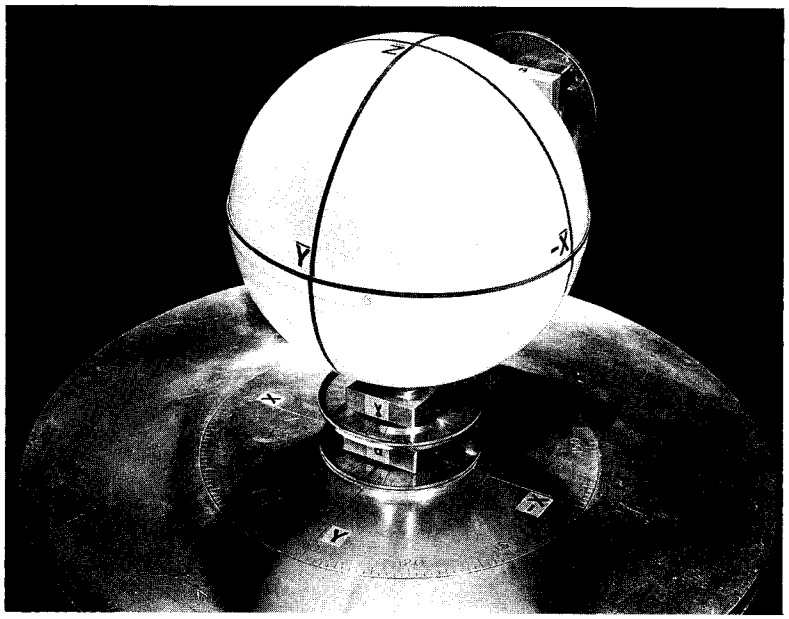

Figure 5.3.1 *(Continued).*

to positive angles. However, we shall see that the double-valuedness is an unavoidable part of any rotational coordinate system. It will turn out that an electron spin polarization state changes phase when the angles $\{\alpha, \beta, \gamma\}$ change from the values in Figure 5.3.1(b) to those in Figure 5.3.1(c). So in some sense the two positions really are different even if they look the same to the classically trained eye.

As in Chapters 2–4, it is necessary to define how a rotational position state $|\alpha\beta\gamma\rangle$ is obtained by *group operations* $R(\alpha\beta\gamma)$ acting upon an initial unrotated state $|1\rangle = |000\rangle$; i.e.,

$$|\alpha\beta\gamma\rangle = R(\alpha\beta\gamma)|1\rangle.$$

To do this, imagine that the $[\bar{x}, \bar{y}, \bar{z}]$ axes and ball are suspended at the center of a transparent shell as indicated in Figure 5.3.2. Suppose this shell supports two sliding cranks, which are fitted with suction cups, and capable of being moved parallel to the laboratory y and z axes, respectively.

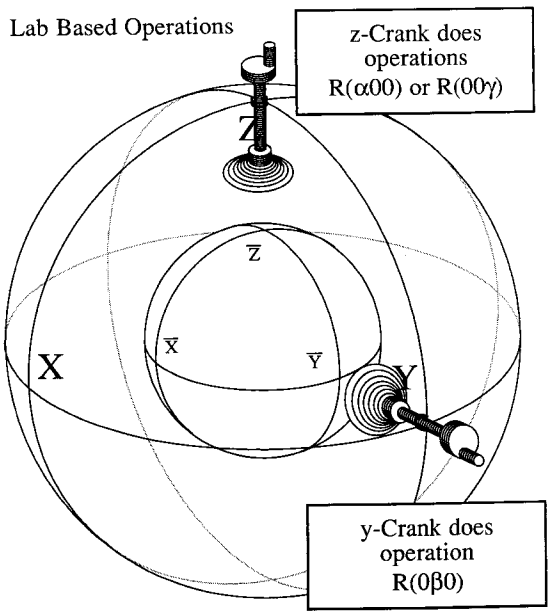

Figure 5.3.2 Laboratory definition of rotation operators $R(\alpha 00)$ and $R(0\beta 0)$. All rotations of the body can be achieved by successively working two cranks attached to a shell fixed in the laboratory. The z crank performs rotations $R(\alpha 00)$ or $R(00\gamma)$. The y crank performs rotations $R(0\beta 0)$.

One way to obtain the rotational position defined by α, β, and γ is through the following operational steps

First step: [This is labeled $R(00\gamma)$]: Attach $\bar{z}$ crank, turn it counterclockwise by angle γ, and then detach it.
Second step: [This is labeled $R(0\beta 0)$]: Attach $\bar{y}$ crank, turn it counterclockwise by angle β, and then detach it.
Third step: [This is labeled $R(\alpha 00)$]: Attach $\bar{z}$ crank, turn it counterclockwise by angle α, and then detach it.

It is conventional to write this sequence of rotations in the following way:

$$R(\alpha\beta\gamma) = R(\alpha 00)R(0\beta 0)R(00\gamma). \tag{5.3.3}$$

Then there is the following relation:

$$|\alpha\beta\gamma\rangle = R(\alpha\beta\gamma)|000\rangle = R(\alpha 00)R(0\beta 0)R(00\gamma)|000\rangle \tag{5.3.4}$$

between states and operators. As usual, the rightmost operator in a group product acts first. This sequence of rotations is shown in Figure 5.5.11 on

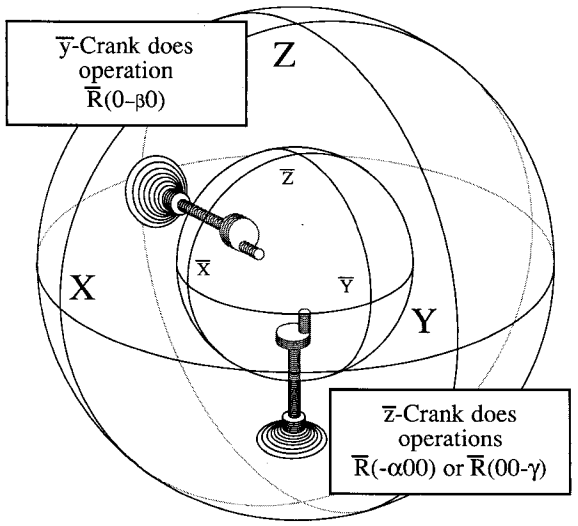

Figure 5.3.3 Body definition of rotation operators $\bar{R}(\alpha 00)$ and $\bar{R}(0\beta 0)$. All rotations of the outer (lab) shell can be achieved by working successively two cranks attached to the body. The $\bar{z}$ crank performs rotations $\bar{R}(\alpha 00)$ or $\bar{R}(00\gamma)$. The $\bar{y}$ crank performs rotations $\bar{R}(0\beta 0)$.

page 379. Note that the α and γ angles are redundant when $\beta = 0$. In the initial orientation state $|1\rangle = |000\rangle$ of Figure 5.3.1(d) the α and γ dials are parallel and coaxial. Hence, one may write

$$R(\alpha 00) = R(00\alpha) = R(\alpha + \gamma, 0, \alpha - \gamma)$$

for arbitrary α and γ.

Consider another way to define the relative orientation of the $[\overline{xyz}]$ and $[xyz]$ axes. Suppose someone on the rotating object can attach cranks to the inside of the spherical shell as indicated in Figure 5.3.3. Using the internal cranks according to the following steps also yields the $|\alpha\beta\gamma\rangle$ orientation state such as was shown first in Figure 5.3.1(a).

First step: [Labeled $\bar{R}(-\alpha 00)$]: Attach $\bar{z}$ crank, turn it *clockwise* by angle α, and then detach it.

Second step: [Labeled $\bar{R}(0 - \beta 0)$]: Attach $\bar{y}$ crank, turn it clockwise by angle β, and then detach it.

Third step: [Labeled $\bar{R}(00 - \gamma)$]: Attach $\bar{z}$ crank, turn it clockwise by angle γ, and then detach it.

Let us denote this sequence of operations as follows:

$$\begin{aligned}\left(\bar{R}(\alpha\beta\gamma)\right)^{-1} &= \bar{R}(00-\gamma)\bar{R}(0-\beta 0)\bar{R}(-\alpha 00)\\ &= \left(\bar{R}(00\gamma)\right)^{-1}\left(\bar{R}(0\beta 0)\right)^{-1}\left(\bar{R}(\alpha 00)\right)^{-1}\\ &= \left(\bar{R}(\alpha 00)\bar{R}(0\beta 0)\bar{R}(00\gamma)\right)^{-1},\end{aligned}$$

or, more simply, as

$$\bar{R}(\alpha\beta\gamma) = \bar{R}(\alpha 00)\bar{R}(0\beta 0)\bar{R}(00\gamma). \tag{5.3.5}$$

This defines another set of rotation operators $\bar{R}(\alpha\beta\gamma)$ with the same group structure as the $R(\alpha\beta\gamma)$ in Eq. (5.3.3). However, the $\bar{R}$ and R are *not* the same operators by any means. In fact, any pair $\bar{R}(\alpha\beta\gamma)$ and $R(\alpha'\beta'\gamma')$ will always commute; i.e.,

$$\bar{R}(\alpha\beta\gamma)R(\alpha'\beta'\gamma') = R(\alpha'\beta'\gamma')\bar{R}(\alpha\beta\gamma). \tag{5.3.6}$$

(Remember, pairs of different R do not commute, neither do different $\bar{R}$ unless the angles α, β, and γ equal 180° or 0°.)

One may imagine that the operators $R(\alpha\beta\gamma)$ move the laboratory system. If you like to be dramatic you could say the $\bar{R}(\alpha\beta\gamma)$ move the entire surrounding universe. However, let us assume that the only thing that counts here is the relative state of orientation of the object relative to the lab axes. Then we must accept the relation

$$|\alpha\beta\gamma\rangle = R(\alpha\beta\gamma)|000\rangle = \bar{R}^{-1}(\alpha\beta\gamma)|000\rangle. \tag{5.3.7}$$

This says that the effect of moving the object one way must be indistinguishable from that of moving the rest of the universe the opposite or inverse way.

The application of lab- and body-defined rotation operators to the theory of quantum rotors is introduced in Section 5.5.C. The explicit matrix representation and operator construction of the rotations and their generators is discussed in Section 5.5.E. Here we are giving their abstract definitions and properties.

B. Darboux or ω-Axis Angles [φθω]

No matter how many rotations are applied, there will always be a line of points in a rotated object that end up exactly where they were initially. In other words, any rotation can be done by just one crank axis provided it can be properly positioned. The geometer Darboux developed the idea of a movable axial or rotation vector $\boldsymbol{\omega}$. Therefore it is appropriate to name the angles involved in the related parametrization accordingly.

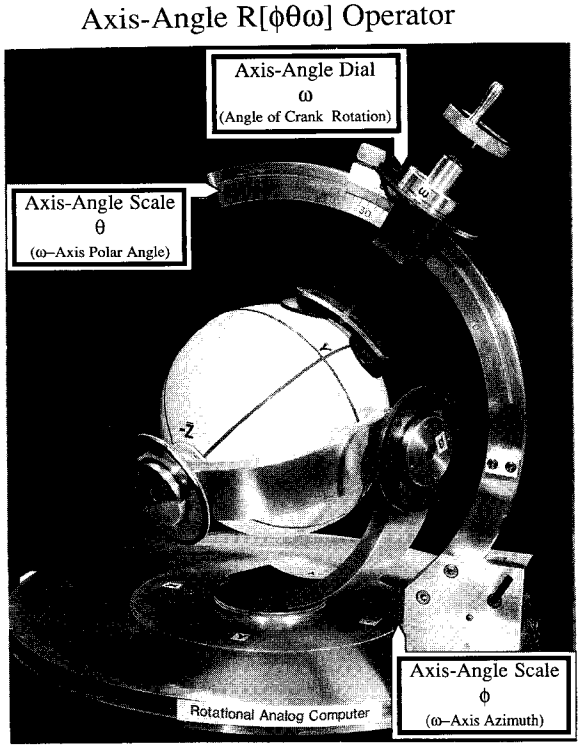

Figure 5.3.4 Defining axis or Darboux angles $R[\phi\theta\omega]$. Rotation operation $R[\phi\theta\omega]$ is defined by the angle ω of rotation and the direction of the axis of rotation given by angles ϕ and θ of azimuth and polar declination, respectively. (*Photo by Vincent Malette and Joanie Geiser.*)

Darboux angles $[\phi\theta\omega]$ are defined operationally using the device pictured in Figure 5.3.4. First one sets the rotation axis or ω crank according to polar angle θ and azimuth angle ϕ. Then one attaches the ω crank to the object, turns it counterclockwise by rotation angle ω, and detaches the crank. The setting $[\phi = 80°,\ \theta = 33.69°]$ of the axis angles followed by a rotation by $\omega = 128.68° \cong 129°$ corresponds to the rotation operator $R[\phi\theta\omega] = R[80°, 34°, 129°]$. (Note that we shall use square brackets $[\boldsymbol{\omega}]$ to distinguish Darboux angles from Euler angles.) Application of this operator to the initial state $|1\rangle = |000\rangle$ happens to yield the position state

$$|\alpha = 50°, \beta = 60°, \gamma = 70°\rangle = R[80°, 34°, 129°]|0, 0, 0\rangle, \qquad (5.3.8)$$

of Figure 5.3.1(a). This is shown in the sequence of Figures 5.3.5(a)–5.3.5(c). We shall derive later the algebraic relations which exist between the Darboux

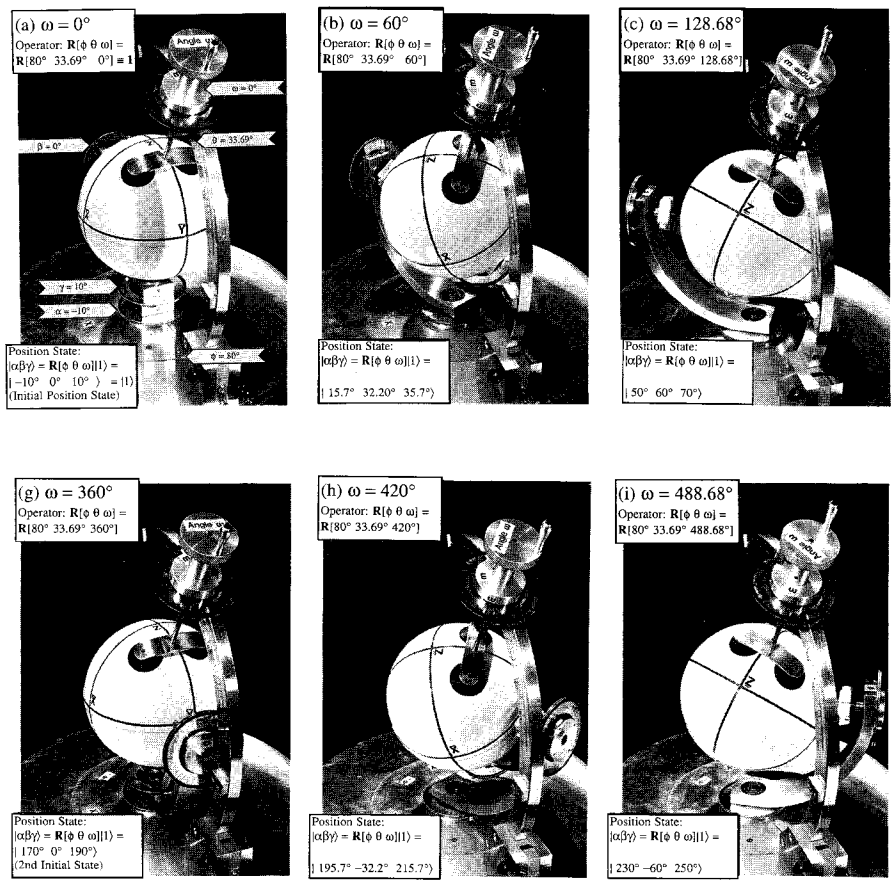

Figure 5.3.5 Sequence of rotations $R[\phi\theta\omega] = R[80°\ 33.69°\ \omega]$. Sequence repeats only after $\omega = 4\pi$ or 720°. Postion state $|\alpha\beta\gamma\rangle = |50°\ 50°\ 70°\rangle$ is obtained after rotating by angle $\omega = 128.68°$ as shown in part (*c*). Continued rotation through another 360° [as shown in parts (*d*) through (*i*)] yields another position state $|-130°\ -60°\ -110°\rangle$ with different Euler Angles but the same orientation of coordinates. Note that the difference $(\gamma - \alpha)$ is a constant (20°) throughout. (*Photos by Vincent Malette and Joanie Geiser.*)

or axis angles $[\phi\theta\omega]$ and the Euler angles $(\alpha\beta\gamma)$. In the meantime note that the sequence in Figures 5.3.5(d)–5.3.5(i) shows a continuation of the ω rotation by another 360°. This yields the alternative Euler-angle settings of state

$$|\alpha = -130°, \beta = -60°, \gamma = -110°\rangle = R[80°, 34°, 489°]|000\rangle, \quad (5.3.9)$$

which was first shown in Figure 5.3.1(c). The goniometer and crank demon-

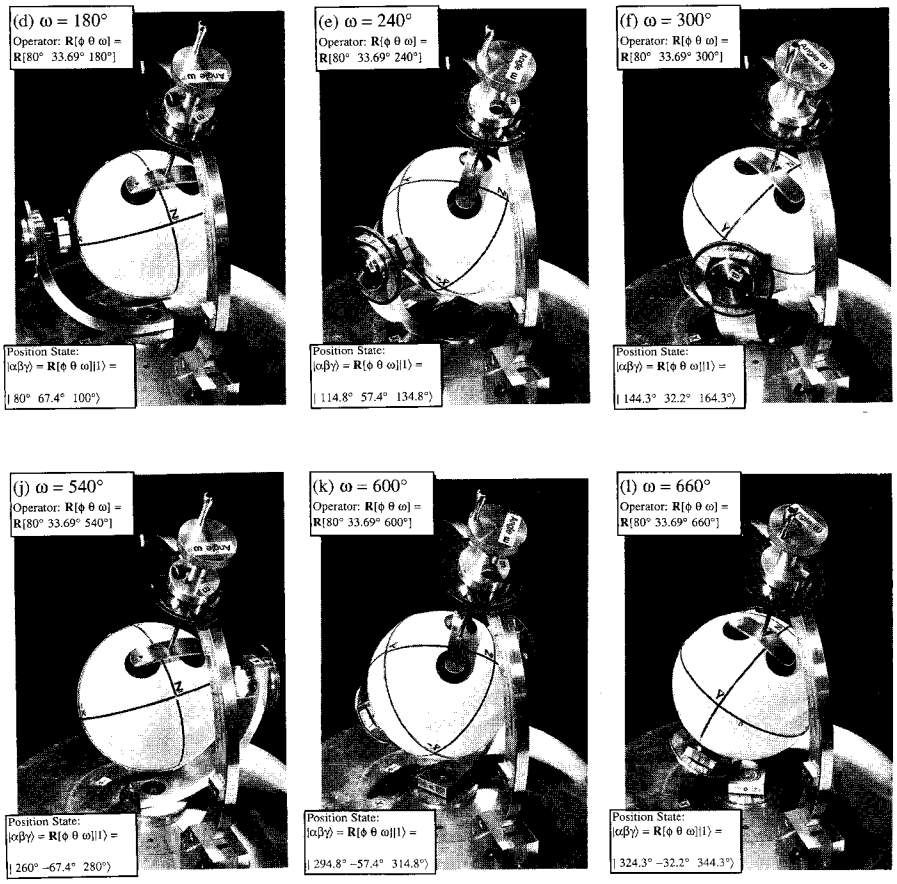

Figure 5.3.5 *(Continued).*

strate the double-valued nature of three-dimensional rotations. It also shows the complimentary relation between Euler angles and Darboux angles. Euler angles are convenient for labeling rotational *states*, while Darboux angles are more convenient for labeling rotational *operators*. Indeed, all the operators in Chapters 2–4 were defined by direction of axis and angle of rotation.

Therefore it is important to derive the mathematical relations between the two types of parameters. First we shall study a geometrical relation based upon Hamilton's rules in Section 5.3.C. Then in Section 5.5 an algebraic relation based upon representations of spin-$\frac{1}{2}$ will be given.

C. Hamilton's Rules and the Rotational Slide Rule

Hamilton's rules, as derived in the Section 3.1.B are used to find the product of two rotations $R[\boldsymbol{\omega}]$ and $R[\boldsymbol{\omega}']$ according to the following steps. First one

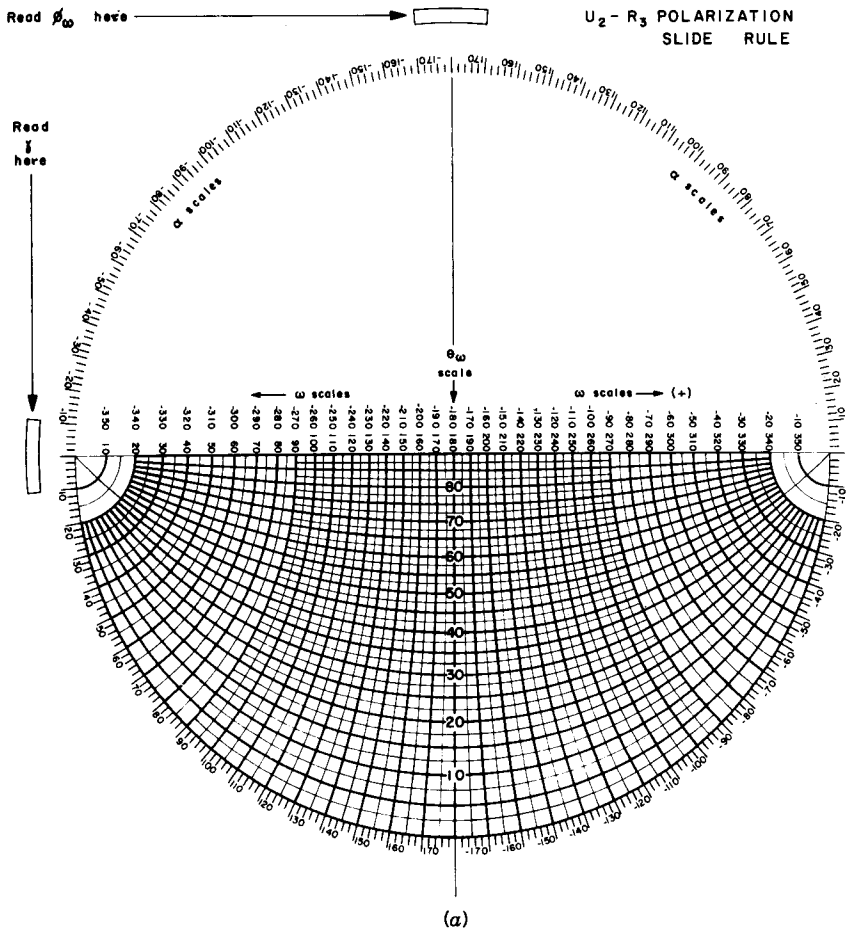

Figure 5.3.6 Rotational slide rule. (a) Lower scale, (b) upper scale.

constructs the great circle arcs perpendicular to $\boldsymbol{\omega}$ and $\boldsymbol{\omega}'$, respectively, on the unit sphere. Then one draws circle vectors along each arc of length $\omega/2$ and $\omega'/2$, respectively, and pointed in the directions of rotation so that the head of the arrow of the first rotation touches the tail of the arrow of the second rotation. Finally, one finds the great circle arc between the tail of the first arrow and the head of the second. The resulting vector-sum arrow defines the desired product rotation.

Figure 5.3.6 shows the slide rule that permits one to carry out the spherical vector addition accurately. The upper scale should be printed on a transparent plastic and fastened so its center rotates over the center of the lower scale. The scales are designed to facilitate group products and Euler $(\alpha\beta\gamma)$ to Darboux $[\phi\theta\omega]$ conversion.

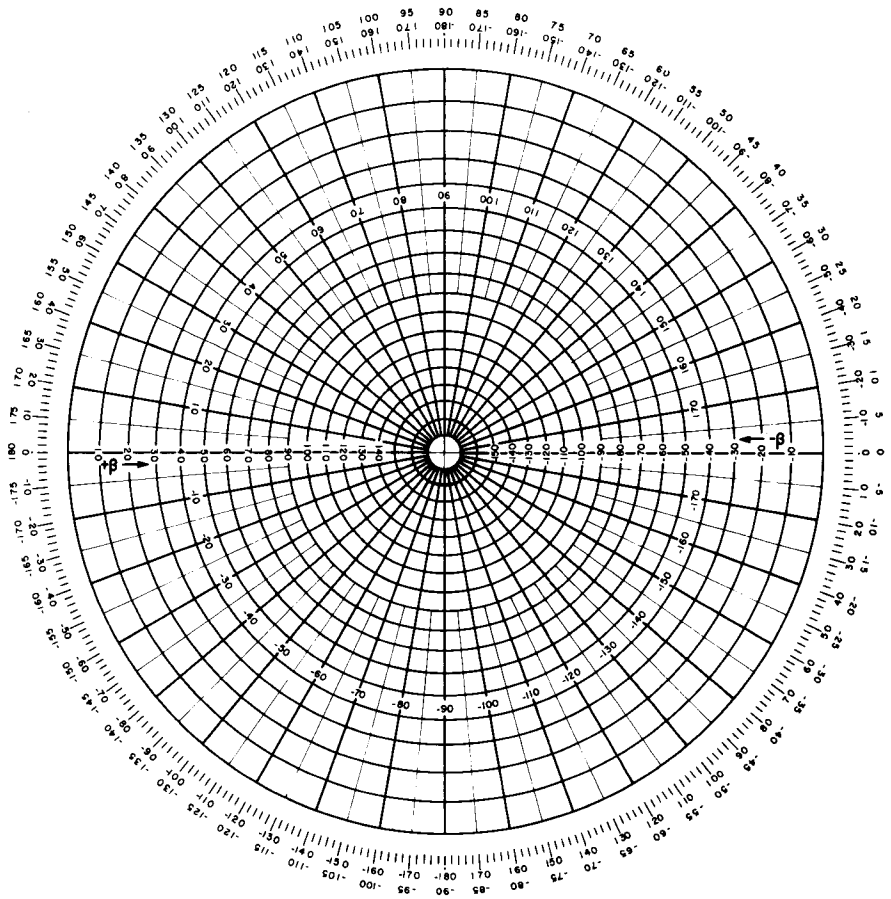

(*b*)

Figure 5.3.6 *(Continued).*

To compute a product of two rotations $R[\phi\theta\omega]$ and $R[\phi'\theta'\omega']$ one first draws the arcs of the respective rotations onto the upper scale. An arc is drawn by setting the desired ϕ in the "ϕ window" (see top of lower scale) and tracing the desired (θ, ω) arc onto the upper scale using the θ and ω scales of the lower scale. It is necessary to first find the intersection of the $[\phi\theta]$ arc with the $[\phi'\theta']$ arc. Then one counts back ω degrees along the $[\phi\theta]$ arc to mark the tail of the first vector, and counts forward ω' degrees along the $[\phi'\theta']$ arc to mark the head of the second vector. The ω scale is used for each counting. Finally the slide rule is turned until the head and tail points lie along a θ line. (Interpolation may be necessary.) Then the desired answer ϕ'' in the product $R[\phi''\theta''\omega''] = R[\phi'\theta'\omega']R[\phi\theta\omega]$ is read in the ϕ window, while θ'' and ω'' are shown by their respective scales.

The upper slide-rule scale is a stereographic projection of the northern hemisphere of a globe, while the lower scale is the same projection of half of the western hemisphere. The structure of rotations as described by Hamilton makes it possible to do all products on just half of a sphere. A rotation for which ω is less than 180° corresponds to an arc of less than 90°. Any rotation with ω between 180° and 360° can be replaced by a rotation that goes the other way by angle $-(360° - \omega)$ and has an arc of $-(180° - \omega/2)$, which again is less then 90°. Whenever this conversion is made while operating on electron wave functions, it is necessary to multiply the result by (-1), as we will prove later:

$$R[\omega \cdot \cdot] = \begin{cases} R[\omega - 2\pi \cdot \cdot], & \text{for integral spin,} \\ -R[\omega - 2\pi \cdot \cdot], & \text{for half-integral spin.} \end{cases} \tag{5.3.10}$$

So anytime there appears an arc vector that extends over the edge of the

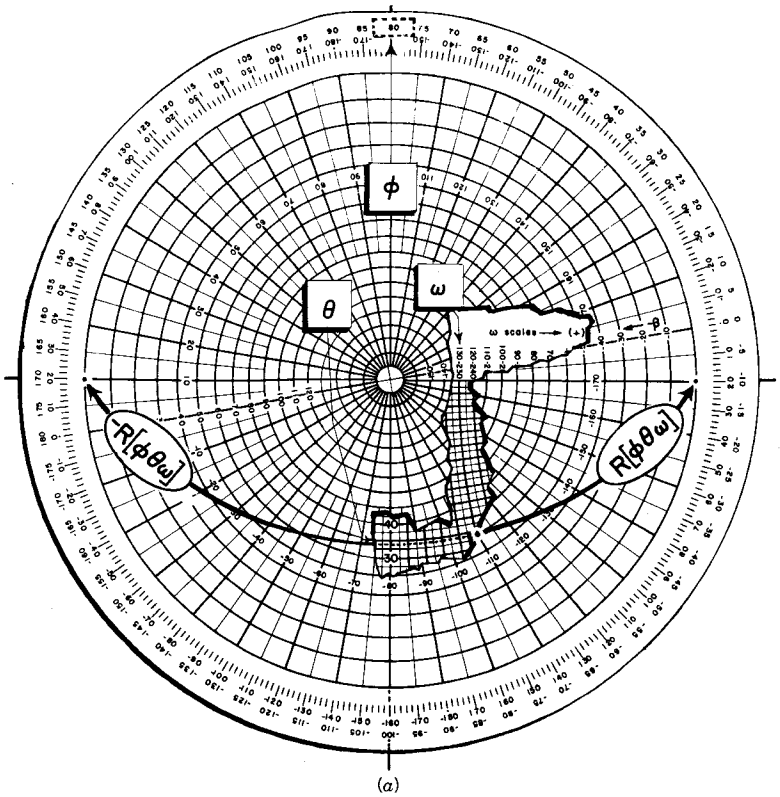

(a)

Figure 5.3.7 Setting the rotational slide rule. (a) Darboux or axis angles. (b) Euler angles.

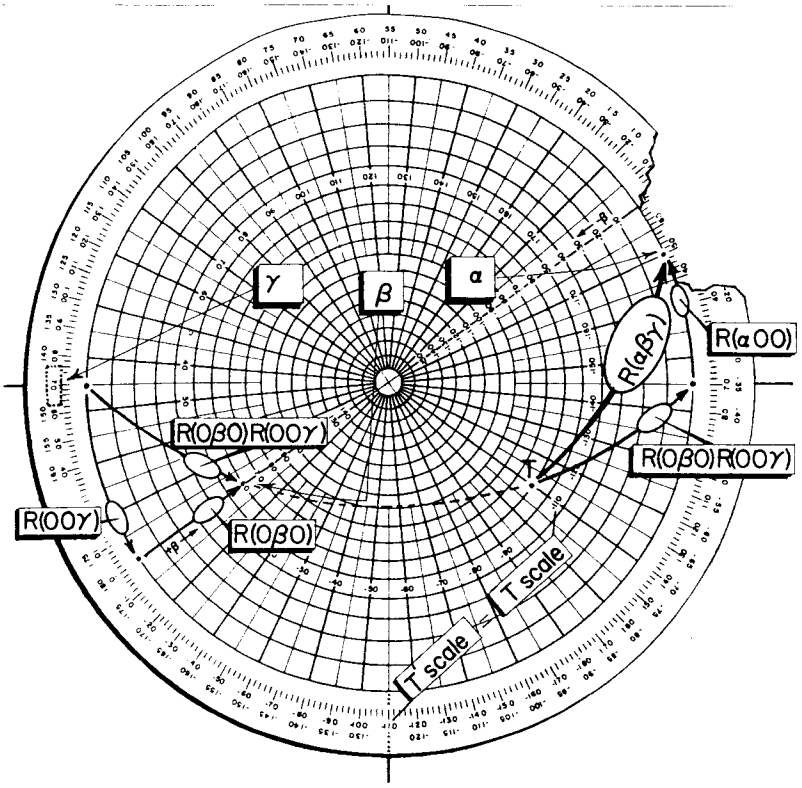

(b)

Figure 5.3.7 *(Continued).*

slide rule, we simply replace it by one of length $(360° - \omega)/2$ going the other way.

Figure (5.3.7) shows how the slide rule may be used to convert back and forth between Euler angles $(\alpha\beta\gamma)$ and axis angles $[\phi\theta\omega]$ in the equation

$$R(\alpha\beta\gamma) = R[\phi\theta\omega] \equiv R[\boldsymbol{\omega}].$$

Figure 5.3.7(b) shows a given rotation $R[\omega]$ reduced by two vector sums into the product $R(\alpha 00)R(0\beta 0)R(00\gamma) = R(\alpha\beta\gamma)$ given by Eq. (5.3.3). The scales of the slide rule have been designed so that these products can be done without drawing arrows. To obtain the position shown in Figure 5.3.7(b) one must move the upper scale so that the angle between the meridian passing through the tail of $R[\omega]$ and the $+\beta$ scale is bisected by the center (θ) line of the lower scale. The "tail scales" or T scales indicated in Figure 5.3.7(b) make this easy. One simply reads the angle of $R[\omega]$'s tail using the T scale. Then one finds this number on the T' scale, and sets it over the center line as shown in Figure 5.3.7(b). This converts an $R[\phi\theta\omega]$ operator to the equal $R(\alpha\beta\gamma)$ operator. The inverse is done by reversing the procedure. Different choices for three inputs from the six angles α, β, γ, ϕ, θ, and ω can be used to calculate the three remaining unknown angles.

Algebraic relations between the Euler and Darboux angles will be derived in Section 5.5.A. These are used in Chapter 7 to help analyze optical polarization and two-dimensional oscillator mechanics.

Then one finds this number on the T' scale, and sets it over the center line as shown in Figure 5.3.7(b). This converts an $R[\phi\theta\omega]$ operator to the equal $R(\alpha\beta\gamma)$ operator. The inverse is done by reversing the procedure. Different choices for three inputs from the six angles α, β, γ, ϕ, θ, and ω can be used to calculate the three remaining unknown angles.

Algebraic relations between the Euler and Darboux angles will be derived in Section 5.5.A. These are used in Chapter 7 to help analyze optical polarization and two-dimensional oscillator mechanics.

5.4 IRREDUCIBLE REPRESENTATIONS OF R_3 AND O_3

This section contains derivations of the all-important $\mathscr{D}^j$ matrices or irreducible representations of R_3. Starting with simple rotation vector algebra we will introduce matrix operators which generate rotation matrices. The connection with the quantum theory of angular momentum will be made. (The elementary angular-momentum relations are reviewed in Appendix E.) Finally, a formula for the irrep $\mathscr{D}^j$ is given.

A. Generators and Infinitesimal Rotations

Consider a rotation $R \cdot \mathbf{u}$ of a vector $\mathbf{u}$ by a very small (preferably infinitesimal) angle $\delta\omega$ around some axis defined by vector $\delta\boldsymbol{\omega} = \delta\omega\hat{\boldsymbol{\omega}}$. This is shown by Figure 5.4.1. In vector notation one may write this transformation as

$$R[\phi\theta\delta\omega] \cdot \mathbf{u} = \mathbf{u} + \delta\boldsymbol{\omega} \times \mathbf{u}. \tag{5.4.1}$$

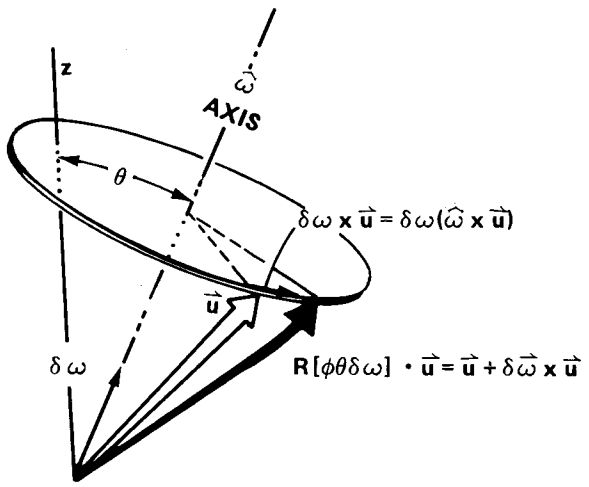

Figure 5.4.1 Small or infinitesimal rotation $R[\phi\theta\omega]$. The rotation moves vector $\mathbf{u}$ into vector $R[\phi\theta\omega]\mathbf{u}$.

This is represented in Cartesian coordinates by

$$\mathscr{R}[\phi\theta\delta\omega]\begin{pmatrix} u_x \\ u_y \\ u_z \end{pmatrix} = \begin{pmatrix} u_x \\ u_y \\ u_z \end{pmatrix} + \begin{pmatrix} \delta\omega_y u_z - \delta\omega_z u_y \\ \delta\omega_z u_x - \delta\omega_x u_z \\ \delta\omega_x u_y - \delta\omega_y u_x \end{pmatrix}, \tag{5.4.2}$$

where the components of $\boldsymbol{\delta\omega}$ are

$$\delta\omega_x = \delta\omega \cos\phi \sin\theta, \quad \delta\omega_y = \delta\omega \sin\phi \sin\theta, \quad \text{and} \quad \delta\omega_z = \delta\omega \cos\theta. \tag{5.4.3}$$

We may expand Eq. (5.4.2) into matrix form:

$$\mathscr{R}[\phi\theta\delta\omega]\begin{pmatrix} u_x \\ u_y \\ u_z \end{pmatrix} = \left[\begin{pmatrix} 1 & \cdot & \cdot \\ \cdot & 1 & \cdot \\ \cdot & \cdot & 1 \end{pmatrix} + \delta\omega_x \begin{pmatrix} \cdot & \cdot & \cdot \\ \cdot & \cdot & -1 \\ \cdot & 1 & \cdot \end{pmatrix} + \delta\omega_y \begin{pmatrix} \cdot & \cdot & 1 \\ \cdot & \cdot & \cdot \\ -1 & \cdot & \cdot \end{pmatrix} + \delta\omega_z \begin{pmatrix} \cdot & -1 & \cdot \\ 1 & \cdot & \cdot \\ \cdot & \cdot & \cdot \end{pmatrix}\right]\begin{pmatrix} u_x \\ u_y \\ u_z \end{pmatrix}. \tag{5.4.4}$$

The preceding equation is independent of the u_j. Hence a matrix equation holds:

$$\mathscr{R}[\phi\theta\delta\omega] = \mathbf{1} + \delta\omega_x \mathscr{G}_x + \delta\omega_y \mathscr{G}_y + \delta\omega_z \mathscr{G}_z. \tag{5.4.5a}$$

Here the matrices

$$\mathscr{G}_x \equiv \begin{pmatrix} \cdot & \cdot & \cdot \\ \cdot & \cdot & -1 \\ \cdot & 1 & \cdot \end{pmatrix}, \quad \mathscr{G}_y \equiv \begin{pmatrix} \cdot & \cdot & 1 \\ \cdot & \cdot & \cdot \\ -1 & \cdot & \cdot \end{pmatrix}, \quad \text{and} \quad \mathscr{G}_z \equiv \begin{pmatrix} \cdot & -1 & \cdot \\ 1 & \cdot & \cdot \\ \cdot & \cdot & \cdot \end{pmatrix} \tag{5.4.5b}$$

are the representations of the R_3 GENERATORS. The idea of this name is that you may generate any rotation in R_3 from them.

For example, in order to perform a z-axis rotation by a finite angle ω_z you may take the following limit as $\delta\omega = \omega_z/n \to 0$:

$$\mathscr{R}[00\omega_z] = \lim_{n\to\infty} \left(\mathscr{R}[00\omega_z/n]\right)^n = \lim_{n\to\infty} \left(\mathbf{1} + \frac{\omega_z}{n}\mathscr{G}_z\right)^n = e^{\omega_z \mathscr{G}_z}. \tag{5.4.6}$$

It is then an easy matter to evaluate $e^{\omega_z \mathscr{G}_z}$ using the spectral decomposition methods derived in Section 1.2. First the eigenvalues ε_l of G_z are found by

solving the secular equation:

$$\det|\mathscr{G}_z - \varepsilon 1| = \det\begin{vmatrix} -\varepsilon & -1 & \cdot \\ 1 & -\varepsilon & \cdot \\ \cdot & \cdot & -\varepsilon \end{vmatrix} = \varepsilon^3 + \varepsilon = 0.$$

Substitution of the eigenvalues $\{\varepsilon_1 = i,\ \varepsilon_2 = -i,\ \varepsilon_3 = 0\}$ into the spectral decomposition give $\mathscr{R}[00\omega_z]$.

$$\mathscr{R}[00\omega_z] = e^{\omega_z \mathscr{G}_z} = \sum_{l=1}^{3} e^{\omega_z \varepsilon_l} \prod_{k \neq l} (\mathscr{G}_z - \varepsilon_k \mathbf{1}) \Big/ \prod_{k \neq l} (\varepsilon_l - \varepsilon_k),$$

$$\mathscr{R}[000_z] = e^{i\omega_z} \frac{\begin{pmatrix} 0 & -1 & 0 \\ 1 & 0 & 0 \\ 0 & 0 & 0 \end{pmatrix}\begin{pmatrix} i & -1 & 0 \\ 1 & i & 0 \\ 0 & 0 & i \end{pmatrix}}{(i-0)\qquad (i+i)}$$

$$+ e^{-i\omega_z} \frac{\begin{pmatrix} -i & -1 & 0 \\ 1 & -i & 0 \\ 0 & 0 & i \end{pmatrix}\begin{pmatrix} 0 & -1 & 0 \\ 1 & 0 & 0 \\ 0 & 0 & 0 \end{pmatrix}}{(-i-i)\qquad (-i-0)}$$

$$+ e^{0} \frac{\begin{pmatrix} -i & -1 & 0 \\ 1 & -i & 0 \\ 0 & 0 & -i \end{pmatrix}\begin{pmatrix} i & -1 & 0 \\ 1 & i & 0 \\ 0 & 0 & i \end{pmatrix}}{(0-i)\qquad (0+i)}$$

$$= e^{i\omega_z}\begin{pmatrix} 1/2 & i/2 & 0 \\ -i/2 & 1/2 & 0 \\ 0 & 0 & 0 \end{pmatrix} + e^{-i\omega_z}\begin{pmatrix} 1/2 & -i/2 & 0 \\ i/2 & 1/2 & 0 \\ 0 & 0 & 0 \end{pmatrix} + \begin{pmatrix} 0 & 0 & 0 \\ 0 & 0 & 0 \\ 0 & 0 & 1 \end{pmatrix}$$

$$= \begin{pmatrix} \cos\omega_z & -\sin\omega_z & 0 \\ \sin\omega_z & \cos\omega_z & 0 \\ 0 & 0 & 1 \end{pmatrix} \tag{5.4.7}$$

This is the standard z-rotation matrix represented in a Cartesian $\{xyz\}$ basis. The spectral decomposition used to derive it will be used again in Section 5.4.D to find more general types of R_3 representations. The idea is to use a representation of the generators to make the corresponding representation of any rotation in R_3.

There are some important properties of the generators which are useful in the construction of their representations. Note first that even rotations by

very small angles do not commute. Consider the following rotation:

$$R = \underset{\left(\begin{array}{l}\text{rotation by } (-\varepsilon)\\ \text{around } y \text{ axis}\end{array}\right)}{e^{-\varepsilon \mathcal{G}_y}} \cdot \underset{\left(\begin{array}{l}\text{rotation by } (-\varepsilon)\\ \text{around } x \text{ axis}\end{array}\right)}{e^{-\varepsilon \mathcal{G}_x}} \cdot \underset{\left(\begin{array}{l}\text{rotation by } (\varepsilon)\\ \text{around } y \text{ axis}\end{array}\right)}{e^{-\varepsilon \mathcal{G}_y}} \cdot \underset{\left(\begin{array}{l}\text{rotation by } (\varepsilon)\\ \text{around } x \text{ axis}\end{array}\right)}{e^{\varepsilon \mathcal{G}_x}} . \tag{5.4.8}$$

Let us expand this by assuming $\varepsilon \sim \frac{1}{3}$ radian and keeping only the lowest-order terms.

$$\begin{aligned} R = &\left(\mathbf{1} - \varepsilon\mathcal{G}_y + \frac{\varepsilon^2}{2}\mathcal{G}_y^2 \cdots\right)\left(\mathbf{1} - \varepsilon\mathcal{G}_x + \frac{\varepsilon^2}{2}\mathcal{G}_x^2 \cdots\right)\left(\mathbf{1} + \varepsilon\mathcal{G}_y + \frac{\varepsilon^2}{2}\mathcal{G}_y^2 \cdots\right) \\ &\times\left(\mathbf{1} + \varepsilon\mathcal{G}_x + \frac{\varepsilon^2}{2}\mathcal{G}_x^2 \cdots\right) \\ = &\ \mathbf{1} + \varepsilon\mathcal{G}_x + \varepsilon^2\mathcal{G}_y\mathcal{G}_x - \varepsilon^2\mathcal{G}_x^2 - \varepsilon^2\mathcal{G}_y\mathcal{G}_x + \frac{\varepsilon^2}{2}\mathcal{G}_x^2 \\ &+ \varepsilon\mathcal{G}_y - \varepsilon^2\mathcal{G}_x\mathcal{G}_y - \varepsilon^2\mathcal{G}_y^2 + \frac{\varepsilon^2}{2}\mathcal{G}_y^2 \\ &- \varepsilon\mathcal{G}_x + \varepsilon^2\mathcal{G}_y\mathcal{G}_x + \frac{\varepsilon^2}{2}\mathcal{G}_x^2 \\ &- \varepsilon\mathcal{G}_y + \frac{\varepsilon^2}{2}\mathcal{G}_y^2 + \cdots . \end{aligned}$$

Cancellation of ε terms leaves only ε^2-and-higher order terms:

$$\mathcal{R} = \mathbf{1} - \varepsilon^2\left(\mathcal{G}_x\mathcal{G}_y - \mathcal{G}_y\mathcal{G}_x\right) + \cdots = \mathbf{1} - \varepsilon^2\left[\mathcal{G}_x, \mathcal{G}_y\right] + \cdots . \tag{5.4.9}$$

From the generator matrices given by Eq. (5.4.5b) we evaluate the commutator

$$\left[\mathcal{G}_x, \mathcal{G}_y\right] = \mathcal{G}_z . \tag{5.4.10}$$

This shows that R given by Eq. (5.4.8) is a small clockwise (negative) rotation by angle $\varepsilon^2 \sim \frac{1}{9}$ around the z axis. (This neglects an error of order ε^3.) The rotation (5.4.8) is shown graphically in Figure 5.4.2.

The other commutation relations are cyclic permutations of the first one, and can be interpreted equivalently:

$$\left[\mathcal{G}_y, \mathcal{G}_z\right] = \mathcal{G}_x, \qquad \left[\mathcal{G}_z, \mathcal{G}_x\right] = \mathcal{G}_y . \tag{5.4.11}$$

These relations define what is called the LIE ALGEBRA of R_3. They are a

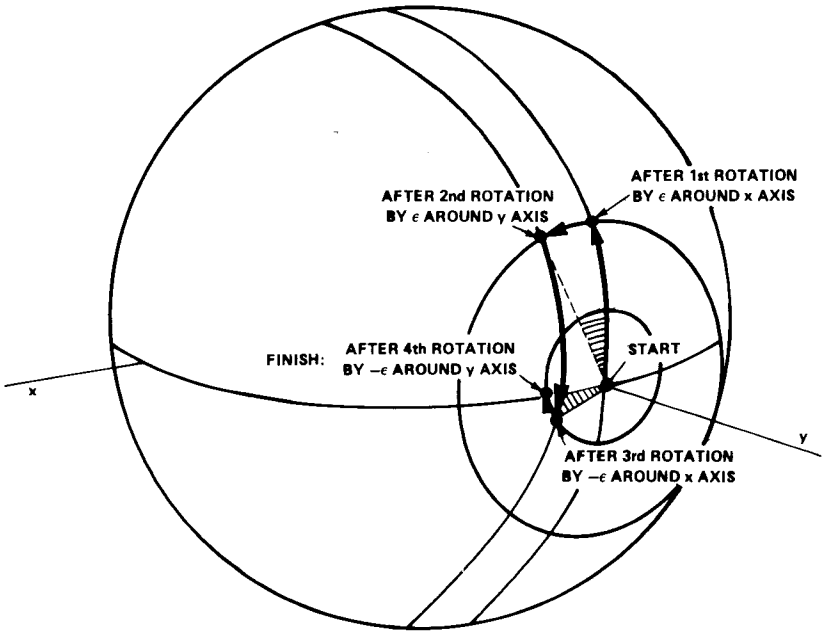

Figure 5.4.2 Effect of commutator operator $R = e^{-\varepsilon G_y} e^{-\varepsilon G_x} e^{\varepsilon G_y} e^{\varepsilon G_x}$ for $\varepsilon \approx 1/3$. Path of a vector which starts along the y axis is traced. (Note: The paths indicated by arrows are not Hamilton arcs.)

finite code for the structure of the infinite group R_3. The relations will be used to generate the irreducible representations, coupling coefficients, and other things connected with R_3.

B. Physical Interpretation of Generators

For rotations around the z axis Eq. (5.4.5) gives

$$\mathscr{R}(\delta\alpha 00) = \mathbf{1} + \delta\alpha \mathscr{G}_z \tag{5.4.12}$$

for a rotation by infinitesimal angle $\delta\alpha$. We use Euler parameters from now on unless otherwise stated. Rewriting this equation in terms of corresponding abstract quantum operators R, $\mathbf{1}$, and G_z gives

$$R(\delta\alpha 00) = \mathbf{1} + \delta\alpha G_z. \tag{5.4.13}$$

Let us consider the effect of this rotation on an abstract position state $|xyz\rangle$ of a particle located at point (xyz). We want the particle to be rotated to the

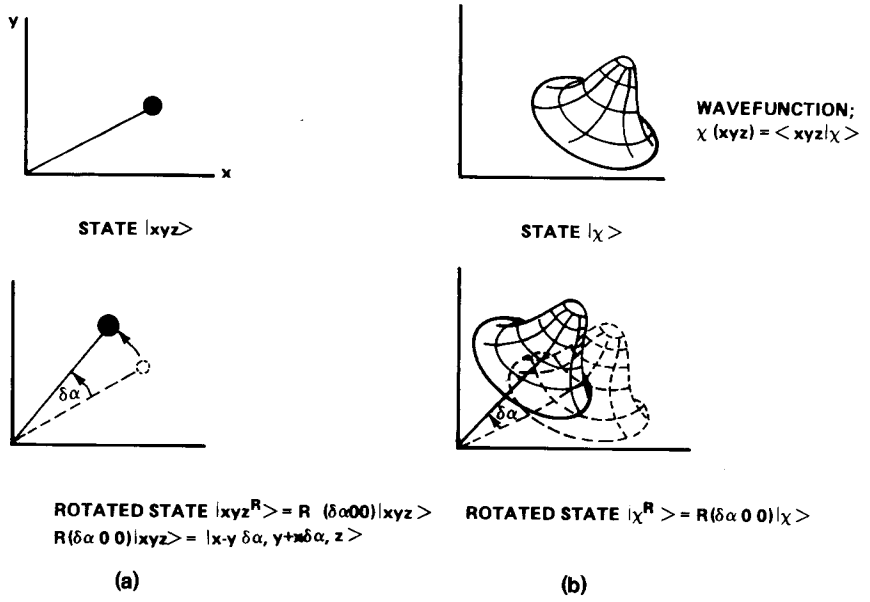

Figure 5.4.3 Effect of infinitesimal rotation operator $R(\alpha 00)$ on quantum states. (a) Localized state has Dirac-delta wave function centered at one point. (b) General state has arbitrary wave function $\chi(xyz) = \langle xyz|\chi\rangle$.

new point $(x - y\delta\alpha, y + x\delta\alpha, z)$ as shown in Figure 5.4.3(a):

$$R(\delta\alpha 00)|xyz\rangle = |x - y\delta\alpha, y + x\delta\alpha, z\rangle. \tag{5.4.14}$$

We also want the rotation operator to be unitary so that $R^\dagger(\delta\alpha 00) = R(-\delta\alpha 00)$, or

$$\begin{aligned}(R(\delta\alpha 00)|xyz\rangle)^\dagger &= (|x - y\delta\alpha, y + x\delta\alpha, z\rangle)^\dagger \\ \langle xyz|R(-\delta\alpha 00) &= \langle x - y\delta\alpha, y + x\delta\alpha, z|.\end{aligned} \tag{5.4.15}$$

This in turn implies that the wave function $\psi(xyz) = \langle xyz|\psi\rangle$ of a general quantum state $|\psi\rangle$ transforms into the following wave function:

$$\begin{aligned}\psi'(xyz) &\equiv \langle xyz|R(\delta\alpha 00)|\psi\rangle \\ &= \langle x + y\delta\alpha, y - x\delta\alpha, z|\psi\rangle \\ &= \psi(x + y\delta\alpha, y - x\delta\alpha, z).\end{aligned} \tag{5.4.16}$$

The rotated point and the rotated wave function are sketched in Figure 5.4.3.

One may expand the rotated wave function into a Taylor series:

$$\psi'(xyz) = \psi(xyz) + y\frac{\partial\psi}{\partial x}\delta\alpha - x\frac{\partial\psi}{\partial y}\delta\alpha \cdots$$

$$= \left[\mathbf{1} - \delta\alpha\left(x\frac{\partial}{\partial y} - y\frac{\partial}{\partial x}\right)\right]\psi(xyz) + \cdots . \qquad (5.4.17)$$

Now from elementary quantum mechanics the coordinate representation of the quantum operators for x and y components of momentum are given by $p_x \to (\hbar/i)\partial/\partial x$ and $p_y \to (\hbar/i)\partial/\partial y$; i.e.,

$$\langle xyz|p_x|\psi\rangle = (\hbar/i)\frac{\partial}{\partial x}\langle xyz|\psi\rangle, \qquad \langle xyz|p_y|\psi\rangle = (\hbar/i)\frac{\partial}{\partial y}\langle xyz|\psi\rangle.$$

This in turn gives the following representation of the z component of angular momentum $\mathbf{J} = \mathbf{r} \times \mathbf{p}$:

$$\langle xyz|J_z|\psi\rangle = \langle xyz|xp_y - yp_x|\psi\rangle = \hbar/i\left(x\frac{\partial}{\partial y} - y\frac{\partial}{\partial x}\right)\psi(xyz). \quad (5.4.18)$$

Comparison of Eqs. (5.4.13), (5.4.17), and (5.4.18) shows that the R_3 generators must be the angular-momentum operators divided by the constant $(i\hbar)$:

$$\langle xyz|R(\delta\alpha 00)|\psi\rangle = \langle xyz|1 + \delta\alpha G_z|\psi\rangle = \langle xyz|1 + \frac{\delta\alpha\, J_z}{i\hbar}|\psi\rangle.$$

This holds for all components:

$$G_x = J_x/i\hbar, \qquad G_y = J_y/i\hbar, \qquad G_z = J_z/i\hbar. \qquad (5.4.19)$$

The following commutation relations:

$$[J_x, J_y] = i\hbar J_z, \qquad [J_y, J_z] = i\hbar J_x, \qquad [J_z, J_x] = i\hbar J_y \quad (5.4.20)$$

follow from Eqs. (5.4.10) and (5.4.11). They also follow directly from the commutation relations of $\mathbf{x}$ and $\mathbf{p}$. ($[x_a, p_b] = i\hbar\delta_{ab}$.)

If rotations are symmetry operators for a Hamiltonian H then the generators must commute with H, too. This implies that each angular-momentum operator may be diagonalized simultaneously with H. A very important consequence of rotational symmetry is the CONSERVATION OF ANGULAR MOMENTUM. The relation between conservation and symmetry can be understood physically. If an object has no "lumps" which ruin its spherical symmetry, then there can be no "bumps" which alter the angular momentum.

C. Irreps of Angular-Momentum and Generator Operators

The following abstract relations hold between angular-momentum operators and their eigenstates $\left|\begin{matrix} j \\ m \end{matrix}\right\rangle$ for $j = 0, \frac{1}{2}, 1, \ldots$ and $|m| \leq j$.

$$J_z\left|\begin{matrix} j \\ m \end{matrix}\right\rangle = m\hbar\left|\begin{matrix} j \\ m \end{matrix}\right\rangle \tag{5.4.21}$$

$$J^2\left|\begin{matrix} j \\ m \end{matrix}\right\rangle \equiv \left(J_x^2 + J_y^2 + J_z^2\right)\left|\begin{matrix} j \\ m \end{matrix}\right\rangle = j(j+1)\hbar^2\left|\begin{matrix} j \\ m \end{matrix}\right\rangle, \tag{5.4.22}$$

$$J_+\left|\begin{matrix} j \\ m \end{matrix}\right\rangle \equiv (J_x + iJ_y)\left|\begin{matrix} j \\ m \end{matrix}\right\rangle = \sqrt{(j-m)(j+m+1)}\,\hbar\left|\begin{matrix} j \\ m+1 \end{matrix}\right\rangle, \tag{5.4.23a}$$

$$J_-\left|\begin{matrix} j \\ m \end{matrix}\right\rangle \equiv (J_x - iJ_y)\left|\begin{matrix} j \\ m \end{matrix}\right\rangle = \sqrt{(j+m)(j-m+1)}\,\hbar\left|\begin{matrix} j \\ m-1 \end{matrix}\right\rangle. \tag{5.4.23b}$$

These are derived in Appendix E and later in this section.

The quantum numbers m and j define the z component and total angular momentum, respectively, of the eigenstates. For each allowed value of j there are $2j + 1$ partner states

$$\left\{\left|\begin{matrix} j \\ j \end{matrix}\right\rangle, \left|\begin{matrix} j \\ j-1 \end{matrix}\right\rangle, \left|\begin{matrix} j \\ j-2 \end{matrix}\right\rangle, \ldots, \left|\begin{matrix} j \\ -j \end{matrix}\right\rangle\right\},$$

which are a basis of an irreducible representation $\mathscr{D}^j$ of the Lie algebra of generators. By rewriting Eqs. (5.4.23) we obtain representations of the angular-momentum operators:

$$J_x = (J_+ + J_-)/2, \qquad J_y = (J_+ - J_-)/2i. \tag{5.4.24}$$

The angular-momentum representations are given here:

$$\mathscr{D}^j_{m'm}(J_x) = \left\langle\begin{matrix} j \\ m' \end{matrix}\right|J_x\left|\begin{matrix} j \\ m \end{matrix}\right\rangle = \frac{\delta_{m'm+1}}{2}\hbar\sqrt{(j-m)(j+m+1)} + \frac{\delta_{m'm-1}}{2}\hbar\sqrt{(j+m)(j-m+1)}, \tag{5.4.25a}$$

$$\mathscr{D}^j_{m'm}(J_y) = \left\langle\begin{matrix} j \\ m' \end{matrix}\right|J_y\left|\begin{matrix} j \\ m \end{matrix}\right\rangle = \frac{\delta_{m'm+1}}{2i}\hbar\sqrt{(j-m)(j+m+1)} - \frac{\delta_{m'm-1}}{2i}\hbar\sqrt{(j+m)(j-m+1)}, \tag{5.4.25b}$$

$$\mathscr{D}^j_{m'm}(J_z) = \left\langle\begin{matrix} j \\ m' \end{matrix}\right|J_z\left|\begin{matrix} j \\ m \end{matrix}\right\rangle = \delta_{m'm}m\hbar. \tag{5.4.25c}$$

The following are some numerical examples of the irreps (in units of $\hbar$).

$$
\begin{array}{lccccc}
\left|\begin{matrix} j \\ m \end{matrix}\right\rangle = & \left|\begin{matrix} 0 \\ 0 \end{matrix}\right\rangle & \left|\begin{matrix} 1/2 \\ 1/2 \end{matrix}\right\rangle\left|\begin{matrix} 1/2 \\ 1/2 \end{matrix}\right\rangle & \left|\begin{matrix} 1 \\ 1 \end{matrix}\right\rangle\left|\begin{matrix} 1 \\ 0 \end{matrix}\right\rangle\left|\begin{matrix} 1 \\ -1 \end{matrix}\right\rangle & \left|\begin{matrix} 3/2 \\ 3/2 \end{matrix}\right\rangle\left|\begin{matrix} 3/2 \\ 1/2 \end{matrix}\right\rangle\left|\begin{matrix} 3/2 \\ -1/2 \end{matrix}\right\rangle\left|\begin{matrix} 3/2 \\ -3/2 \end{matrix}\right\rangle & \left|\begin{matrix} 2 \\ 2 \end{matrix}\right\rangle\left|\begin{matrix} 2 \\ 1 \end{matrix}\right\rangle\left|\begin{matrix} 2 \\ 0 \end{matrix}\right\rangle\left|\begin{matrix} 2 \\ -1 \end{matrix}\right\rangle\left|\begin{matrix} 2 \\ -2 \end{matrix}\right\rangle \\
\mathscr{D}^j(J_x) = & (0) & \begin{pmatrix} \cdot & \frac{1}{2} \\ \frac{1}{2} & \cdot \end{pmatrix} & \begin{pmatrix} \cdot & \frac{\sqrt{2}}{2} & \cdot \\ \frac{\sqrt{2}}{2} & \cdot & \frac{\sqrt{2}}{2} \\ \cdot & \frac{\sqrt{2}}{2} & \cdot \end{pmatrix} & \begin{pmatrix} \cdot & \frac{\sqrt{3}}{2} & \cdot & \cdot \\ \frac{\sqrt{3}}{2} & \cdot & 1 & \cdot \\ \cdot & 1 & \cdot & \frac{\sqrt{3}}{2} \\ \cdot & \cdot & \frac{\sqrt{3}}{2} & \cdot \end{pmatrix} & \begin{pmatrix} \cdot & 1 & \cdot & \cdot & \cdot \\ 1 & \cdot & \frac{\sqrt{3}}{2} & \cdot & \cdot \\ \cdot & \frac{\sqrt{3}}{2} & \cdot & \frac{\sqrt{3}}{2} & \cdot \\ \cdot & \cdot & \frac{\sqrt{3}}{2} & \cdot & 1 \\ \cdot & \cdot & \cdot & 1 & \cdot \end{pmatrix} \ldots, \quad (5.4.25a)_x \\
\mathscr{D}^j(J_y) = & (0) & \begin{pmatrix} \cdot & \frac{-1}{2}i \\ \frac{1}{2}i & \cdot \end{pmatrix} & \begin{pmatrix} \cdot & -\frac{\sqrt{2}}{2}i & \cdot \\ \frac{\sqrt{2}}{2}i & \cdot & -\frac{\sqrt{2}}{2}i \\ \cdot & \frac{\sqrt{2}}{2}i & \cdot \end{pmatrix} & \begin{pmatrix} \cdot & -\frac{\sqrt{3}}{2}i & \cdot & \cdot \\ \frac{\sqrt{3}}{2}i & \cdot & -i & \cdot \\ \cdot & i & \cdot & -\frac{\sqrt{3}}{2}i \\ \cdot & \cdot & \frac{\sqrt{3}}{2}i & \cdot \end{pmatrix} & \begin{pmatrix} \cdot & -i & \cdot & \cdot & \cdot \\ i & \cdot & -\frac{\sqrt{3}}{2}i & \cdot & \cdot \\ \cdot & \frac{\sqrt{3}}{2}i & \cdot & -\frac{\sqrt{3}}{2}i & \cdot \\ \cdot & \cdot & \frac{\sqrt{3}}{2}i & \cdot & -i \\ \cdot & \cdot & \cdot & i & \cdot \end{pmatrix} \ldots, \quad (5.4.25b)_x \\
\mathscr{D}^j(J_z) = & (0) & \begin{pmatrix} \frac{1}{2} & \cdot \\ \cdot & \frac{-1}{2} \end{pmatrix} & \begin{pmatrix} 1 & \cdot & \cdot \\ \cdot & 0 & \cdot \\ \cdot & \cdot & -1 \end{pmatrix} & \begin{pmatrix} \frac{3}{2} & \cdot & \cdot & \cdot \\ \cdot & \frac{1}{2} & \cdot & \cdot \\ \cdot & \cdot & \frac{-1}{2} & \cdot \\ \cdot & \cdot & \cdot & \frac{-3}{2} \end{pmatrix} & \begin{pmatrix} 2 & \cdot & \cdot & \cdot & \cdot \\ \cdot & 1 & \cdot & \cdot & \cdot \\ \cdot & \cdot & 0 & \cdot & \cdot \\ \cdot & \cdot & \cdot & -1 & \cdot \\ \cdot & \cdot & \cdot & \cdot & -2 \end{pmatrix} \ldots. \quad (5.4.25c)_x
\end{array}
$$

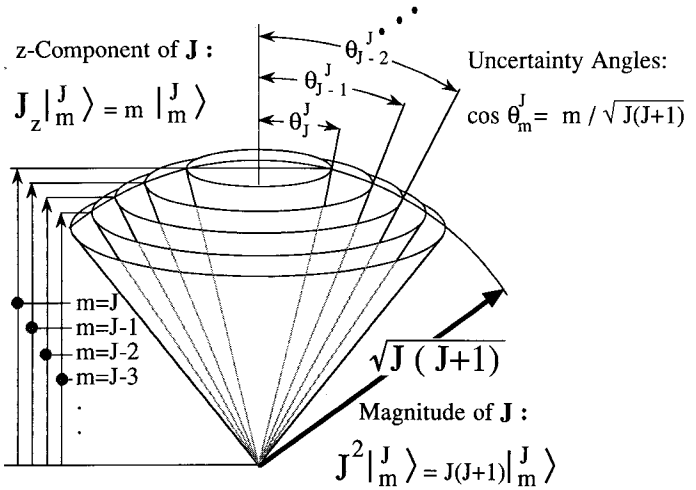

Figure 5.4.4 Angular-momentum vector cones for quantum states $\left|{}^{J}_{J}\right\rangle$, $\left|{}^{J}_{J-1}\right\rangle$, $\left|{}^{J}_{J-2}\right\rangle$, ... Note that uncertainty angle θ_m increases $\langle J_z\rangle = m$ decreases. States with the lowest $|m|$ have the highest uncertainty in the J_x and J_y components.

In order to gain a physical interpretation of Eqs. (5.4.21)–(5.4.25) one may imagine that the classical picture of an angular-momentum vector is replaced by a cone as shown in Figure 5.4.4. One represents the angular momentum of each state $\left|{}^{j}_{m}\right\rangle$ by a cone centered on the z axis with altitude $m\hbar$ according to Eq. (5.4.21) and a slant height of $\sqrt{j(j+1)}\,\hbar$ according to Eq. (5.4.22).

Since neither J_x nor J_y commute with J_z or with each other, one cannot find a state which is an eigenvector of more than one of these operators. Having chosen J_z to be diagonal one expects some uncertainty in the values of J_y and J_x. This uncertainty is indicated roughly by the cone base in Figure 5.4.4. A more quantitative description of the uncertainty in the transverse J_x and J_y components is contained in Section 5.5.B.

It was necessary to choose one J generator to be diagonal in order to complete the irrep derivation. The choice is analogous to that which we encountered in the derivation of C_{3v} irreps. There a particular generator of an Abelian subgroup (viz., σ_3 of C_v, or else r of C_3) was chosen to be diagonal. Such choices are needed to provide a subgroup labeling chain as explained in Chapter 4. For the rotation group R_3 the most commonly chosen labeling chain is simply $R_3 \supset R_2$, where R_2 is generated by J_z. Then the quantum numbers j and m in the bases $\left|{}^{j}_{m}\right\rangle$ serve as irrep labels for R_3 and R_2, respectively. Together, they label each base vector of the rotation group representations.

D. Irreducible Representations of Rotation Operators

Let us represent rotated states $R(\alpha\beta\gamma)\left|\begin{smallmatrix} j \\ m \end{smallmatrix}\right\rangle$ by cone drawings such as the one of $R(0\beta0)\left|\begin{smallmatrix} j \\ m \end{smallmatrix}\right\rangle$ in Figure 5.4.4. A rotated state can be written as a combination of the original $2j + 1$ unrotated partner states:

$$R(\alpha\beta\gamma)\left|\begin{matrix} j \\ m \end{matrix}\right\rangle = \sum_{m'} \left|\begin{matrix} j \\ m' \end{matrix}\right\rangle \left\langle\begin{matrix} j \\ m' \end{matrix}\right| R(\alpha\beta\gamma) \left|\begin{matrix} j \\ m \end{matrix}\right\rangle. \tag{5.4.26}$$

The coefficients

$$\mathscr{D}^j_{m'm}(R(\alpha\beta\gamma)) \equiv \left\langle\begin{matrix} j \\ m' \end{matrix}\right| R(\alpha\beta\gamma) \left|\begin{matrix} j \\ m \end{matrix}\right\rangle \equiv \mathscr{D}^j_{m'm}(\alpha\beta\gamma) \tag{5.4.27}$$

are the irreducible representations (irreps) which will be derived now. The derivation uses the irreps $\mathscr{D}^j(J)$ of the generators and Eq. (5.3.3), (5.4.6), and (5.4.19). The latter are summarized as follows:

$$R(\alpha\beta\gamma) = R(\alpha00)R(0\beta0)R(00\gamma) = e^{\alpha J_z/i\hbar} e^{\beta J_y/i\hbar} e^{\gamma J_z/i\hbar}. \tag{5.4.28}$$

The ($j = 0$) irrep is trivial since the generators are represented by zero on the left-hand side of Eq. (5.4.28):

$$\mathscr{D}^0(\alpha\beta\gamma) = 1. \tag{5.4.29}$$

This is called the SCALAR or INVARIANT irrep of R_3.

The ($j = \frac{1}{2}$) irrep involves two diagonal matrices for the α and γ angles and one nondiagonal matrix for the β rotation around the y axis. The latter can be evaluated by spectral decomposition as was done in Eq. (5.4.7):

$$\begin{aligned} \mathscr{D}^{1/2}(\alpha\beta\gamma) &= e^{\frac{\alpha}{i}\begin{pmatrix} 1/2 & 0 \\ 0 & -1/2 \end{pmatrix}} e^{\frac{\beta}{i}\begin{pmatrix} 0 & -i/2 \\ i/2 & 0 \end{pmatrix}} e^{\frac{\gamma}{i}\begin{pmatrix} 1/2 & 0 \\ 0 & -1/2 \end{pmatrix}} \\ &= \begin{pmatrix} e^{-i\alpha/2} & 0 \\ 0 & e^{i\alpha/2} \end{pmatrix} \begin{pmatrix} \cos\beta/2 & -\sin\beta/2 \\ \sin\beta/2 & \cos\beta/2 \end{pmatrix} \begin{pmatrix} e^{-i\gamma/2} & 0 \\ 0 & e^{i\gamma/2} \end{pmatrix} \\ &= \begin{pmatrix} e^{-i(\alpha+\gamma)/2}\cos\beta/2 & -e^{-i(\alpha-\gamma)/2}\sin\beta/2 \\ e^{i(\alpha-\gamma)/2}\sin\beta/2 & e^{i(\alpha+\gamma)/2}\cos\beta/2 \end{pmatrix}. \end{aligned} \tag{5.4.30}$$

This is called the SPINOR or FUNDAMENTAL irrep of R_3. Strictly speaking, however, $\mathscr{D}^{1/2}$ is not a representation of R_3. Note that the product of 180° rotations is represented by

$$\mathscr{D}^{1/2}(\pi00)\mathscr{D}^{1/2}(\pi00) = \begin{pmatrix} e^{-i\pi/2} & 0 \\ 0 & e^{i\pi/2} \end{pmatrix} \begin{pmatrix} e^{-i\pi/2} & 0 \\ 0 & e^{i\pi/2} \end{pmatrix} = \begin{pmatrix} -1 & 0 \\ 0 & -1 \end{pmatrix}. \tag{5.4.31}$$

In other words, if you walk completely around, or rotate by 360° any spin state, its phase will come out negative! For half-integral j one has the following:

$$\mathscr{D}^j(R)\mathscr{D}^j(R') = \omega_{RR'}\mathscr{D}^j(RR'), \tag{5.4.32}$$

where

$$\omega_{RR'} = \pm 1.$$

Such representations of are called PROJECTIVE or RAY REPRESENTATIONS of R_3. More details of these will be discussed in Section 5.7.

The $(j = 1)$ irrep may be calculated in the same manner:

$$\mathscr{D}^1(\alpha\beta\gamma) = \begin{pmatrix} e^{-i\alpha} & \cdot & \cdot \\ \cdot & 1 & \cdot \\ \cdot & \cdot & e^{i\alpha} \end{pmatrix} \begin{pmatrix} \frac{1+\cos\beta}{2} & \frac{-\sin\beta}{\sqrt{2}} & \frac{1-\cos\beta}{2} \\ \frac{\sin\beta}{\sqrt{2}} & \cos\beta & \frac{-\sin\beta}{\sqrt{2}} \\ \frac{1-\cos\beta}{2} & \frac{\sin\beta}{\sqrt{2}} & \frac{1+\cos\beta}{2} \end{pmatrix} \begin{pmatrix} e^{-i\gamma} & \cdot & \cdot \\ \cdot & 1 & \cdot \\ \cdot & \cdot & e^{i\gamma} \end{pmatrix}. \tag{5.4.33}$$

This is called the VECTOR or DIPOLE representation. It is equivalent to the $\mathscr{R}$ representation of Eq. (5.4.7). If $R[00\omega_z]$ is diagonalized then $\mathscr{D}^1(\omega_z 00)$ results. The bases for $\mathscr{R}$ are the vector components $\{x, y, z\}$, but the bases for $\mathscr{D}^1$ are the circular vector components $\{-(x + iy), z, (x - iy)\}$ by inspecting the columns (or rows) of the projection matrices in Eq. (5.4.7).

The $(j = \frac{3}{2})$ and $(j = 2)$ irreps for the nondiagonal $\mathscr{R}(0\beta 0)$ rotation are

$$\mathscr{D}^{3/2}(0\beta 0) = \begin{pmatrix} \cos^3\frac{\beta}{2} & -\sqrt{3}\cos^2\frac{\beta}{2}\sin\frac{\beta}{2} & \sqrt{3}\cos\frac{\beta}{2}\sin^2\frac{\beta}{2} & -\sin^3\frac{\beta}{2} \\ \sqrt{3}\cos^2\frac{\beta}{2}\sin\frac{\beta}{2} & \cos^3\frac{\beta}{2} - 2\cos\frac{\beta}{2}\sin^2\frac{\beta}{2} & \sin^3\frac{\beta}{2} 2\cos^2\frac{\beta}{2}\sin\frac{\beta}{2} & \sqrt{3}\cos\frac{\beta}{2}\sin^2\frac{\beta}{2} \\ \sqrt{3}\cos\frac{\beta}{2}\sin^2\frac{\beta}{2} & -\sin^3\frac{\beta}{2} + 2\cos^2\frac{\beta}{2}\sin\frac{\beta}{2} & \cos^3\frac{\beta}{2} - 2\cos\frac{\beta}{2}\sin^2\frac{\beta}{2} & -\sqrt{3}\cos^2\frac{\beta}{2}\sin\frac{\beta}{2} \\ \sin^3\frac{\beta}{2} & \sqrt{3}\cos\frac{\beta}{2}\sin^2\frac{\beta}{2} & \sqrt{3}\cos^2\frac{\beta}{2}\sin\frac{\beta}{2} & \cos^3\frac{\beta}{2} \end{pmatrix} \tag{5.4.34}$$

$$\mathscr{D}^2(0\beta 0) = \begin{vmatrix} \left(\frac{1+\cos\beta}{2}\right)^2 & \left(\frac{1+\cos\beta}{2}\right)\sin\beta & \sqrt{\frac{3}{8}}\sin^2\beta & \left(\frac{1+\cos\beta}{2}\right)\sin\beta & \left(\frac{1-\cos\beta}{2}\right)^2 \\ \left(\frac{1+\cos\beta}{2}\right)\sin\beta & \left(\frac{1+\cos\beta}{2}\right)(2\cos\beta - 1) & -\sqrt{\frac{3}{2}}\sin\beta\cos\beta & \left(\frac{1-\cos\beta}{2}\right)(2\cos\beta + 1) & -\left(\frac{1-\cos\beta}{2}\right)\sin\beta \\ \sqrt{\frac{3}{8}}\sin^2\beta & \sqrt{\frac{3}{2}}\sin\beta\cos\beta & \frac{3\cos^2\beta - 1}{2} & \sqrt{\frac{3}{2}}\sin\beta\cos\beta & \sqrt{\frac{3}{8}}\sin^2\beta \\ \left(\frac{1+\cos\beta}{2}\right)\sin\beta & \left(\frac{1-\cos\beta}{2}\right)(2\cos\beta + 1) & \sqrt{\frac{3}{2}}\sin\beta\cos\beta & \left(\frac{1+\cos\beta}{2}\right)(2\cos\beta - 1) & -\left(\frac{1+\cos\beta}{2}\right)\sin\beta \\ \left(\frac{1-\cos\beta}{2}\right)^2 & \left(\frac{1-\cos\beta}{2}\right)\sin\beta & \sqrt{\frac{3}{8}}\sin^2\beta & \left(\frac{1+\cos\beta}{2}\right)\sin\beta & \left(\frac{1+\cos\beta}{2}\right)^2 \end{vmatrix} \tag{5.4.35}$$

Irrep $\mathscr{D}^2$ is called the TENSOR or QUADRUPOLE representations. These names will be explained in later sections.

For the $j = \frac{3}{2}, 2$, or higher it is convenient to derive a general formula for the irreps. An elegant construction due to Schwinger gives the general formula. Schwinger's construction identifies the angular-momentum states with creation operators of a two-dimensional oscillator. The spin-$\frac{1}{2}$ states are defined by

$$a_\uparrow^\dagger|00\rangle = \left|\begin{matrix} j = 1/2 \\ m = 1/2 \end{matrix}\right\rangle, \qquad a_\downarrow^\dagger|00\rangle = \left|\begin{matrix} 1/2 \\ -1/2 \end{matrix}\right\rangle, \tag{5.4.36}$$

where the a operators satisfy the oscillator commutation relations

$$\left[a_i, a_j^\dagger\right] = \delta_{ij}1,$$

which were given in Eqs. (4.4.51). The angular-momentum operators defined by

$$J_- \equiv a_\downarrow^\dagger a_\uparrow, \qquad J_z \equiv \left(a_\uparrow^\dagger a_\uparrow - a_\downarrow^\dagger a_\downarrow\right)/2, \qquad J_+ = a_\uparrow^\dagger a_\downarrow \tag{5.4.37}$$

then satisfy their commutation relations as well:

$$[J_z, J_\pm] = \pm J_\pm.$$

(Here we are using units for which $\hbar = 1$.) The general angular-momentum state is defined by

$$\begin{aligned} \left|\begin{matrix} j \\ m \end{matrix}\right\rangle &= \left(a_\uparrow^\dagger\right)^{n_\uparrow}\left(a_\downarrow^\dagger\right)^{n_\downarrow}|00\rangle/(n_\uparrow! n_\downarrow!)^{1/2} \\ &= |n_\uparrow n_\downarrow\rangle, \end{aligned} \tag{5.4.38a}$$

where

$$\begin{aligned} n_\uparrow &= j + m, \qquad j = (n_\uparrow + n_\downarrow)/2, \\ n_\downarrow &= j - m, \qquad m = (n_\uparrow - n_\downarrow)/2. \end{aligned} \tag{5.4.38b}$$

According to Eq. (4.4.62) the angular-momentum lowering operator has the following effect on $\left|\begin{matrix} j \\ m \end{matrix}\right\rangle$:

$$J_-\left|\begin{matrix} j \\ m \end{matrix}\right\rangle = a_\downarrow^\dagger a_\uparrow |n_\uparrow n_\downarrow\rangle = \left[(n_\uparrow)(n_\downarrow + 1)\right]^{1/2}|n_\uparrow - 1, n_\downarrow + 1\rangle. \tag{5.4.39}$$

This is an elegant rederivation of the familiar result in Eq. (5.4.23b).

$$J_-\left|\begin{matrix} j \\ m \end{matrix}\right\rangle = \left[(j + m)(j - m + 1)\right]^{1/2}\left|\begin{matrix} j \\ m - 1 \end{matrix}\right\rangle$$

Similarly, a formula for D^j can be derived from $\mathscr{D}^{1/2}$. Let us rewrite Eq. (5.4.30) as

$$\begin{aligned} R(0\beta 0)\left|\begin{matrix}1/2\\1/2\end{matrix}\right\rangle &= \cos\beta/2\left|\begin{matrix}1/2\\1/2\end{matrix}\right\rangle + \sin\beta/2\left|\begin{matrix}1/2\\-1/2\end{matrix}\right\rangle,\\ R(0\beta 0)\left|\begin{matrix}1/2\\-1/2\end{matrix}\right\rangle &= -\sin\beta/2\left|\begin{matrix}1/2\\1/2\end{matrix}\right\rangle + \cos\beta/2\left|\begin{matrix}1/2\\-1/2\end{matrix}\right\rangle, \end{aligned} \tag{5.4.40}$$

then as an operator equation.

$$\begin{aligned} R(0\beta 0)a^\dagger_\uparrow &\equiv a^{\dagger\prime}_\uparrow = \cos\beta/2a^\dagger_\uparrow + \sin\beta/2a^\dagger_\downarrow,\\ R(0\beta 0)a^\dagger_\downarrow &\equiv a^{\dagger\prime}_\downarrow = -\sin\beta/2a^\dagger_\uparrow + \cos\beta/2a^\dagger_\downarrow. \end{aligned} \tag{5.4.41}$$

This will yield the transformation properties of the general state:

$$\begin{aligned} R(0\beta 0)\left|\begin{matrix}j\\n\end{matrix}\right\rangle &= \frac{\left(a^{\dagger\prime}_\uparrow\right)^{j+n}}{\sqrt{(j+n)!}}\frac{\left(a^{\dagger\prime}_\downarrow\right)^{j-n}}{\sqrt{(j-n)!}}|00\rangle\\ &= \frac{1}{\sqrt{(j+n)!(j-n)!}}\left(\cos\beta/2a^\dagger_\uparrow + \sin\beta/2a^\dagger_\downarrow\right)^{j+n}\\ &\quad\times\left(-\sin\beta/2a^\dagger_\uparrow + \cos\beta/2a^\dagger_\downarrow\right)^{j-n}|00\rangle. \end{aligned} \tag{5.4.42}$$

Expanding the binomials yields a polynomial in creation operators:

$$\begin{aligned} &R(0\beta 0)\left|\begin{matrix}j\\n\end{matrix}\right\rangle\\ &= \left[\frac{1}{(j+n)!(j-n)!}\right]^{1/2}\\ &\quad\times\left[\sum_l \frac{(j+n)!}{l!(j+n-l)!}\left(\cos\frac{\beta}{2}a^\dagger_\uparrow\right)^l\left(\sin\frac{\beta}{2}a^\dagger_\downarrow\right)^{j+n-l}\right]\\ &\quad\times\left[\sum_k \frac{(j-n)!}{k!(j-n-k)!}\left(-\sin\frac{\beta}{2}a^\dagger_\uparrow\right)^k\left(\cos\frac{\beta}{2}a^\dagger_\downarrow\right)^{j-n-k}\right]|00\rangle\\ &= \left[\frac{1}{(j+n)!(j-n)!}\right]^{1/2}\\ &\quad\times\left[\sum_l\sum_k(-1)^k\frac{\left(\cos\frac{\beta}{2}\right)^{j-n-k+l}\left(\sin\frac{\beta}{2}\right)^{j+n-l+k}\left(a^\dagger_\uparrow\right)^{l+k}\left(a^\dagger_\downarrow\right)^{2j-l-k}}{l!(j+n-l)!k!(j-n-k)!}\right]|00\rangle. \end{aligned} \tag{5.4.43}$$

By making the substitutions

$$j+m \equiv l+k, \qquad j-m \equiv 2j-l-k, \qquad l=j+m-k,$$

one recovers the recognizable form of Eq. (5.4.24).

$$R(0\beta 0)\left|\begin{matrix} j \\ n \end{matrix}\right\rangle = \left[\frac{1}{(j+n)!(j-n)!}\right]^{1/2}$$

$$\times\left[\sum_m \sum_k (-1)^k \frac{\left(\cos\frac{\beta}{2}\right)^{2j+m-n-2k}\left(\sin\frac{\beta}{2}\right)^{n-m+2k}\left(a_\uparrow^\dagger\right)^{j+m}\left(a_\downarrow^\dagger\right)^{j-m}}{(j+m-k)!(n-m+k)!k!(j-n-k)!}\right]|00\rangle$$

$$= \sum_m \left[\sum_k (-1)^k \frac{\sqrt{(j+n)!(j-n)!(j+m)!(j-m)!}\left(\cos\frac{\beta}{2}\right)^{2j+m-n-2k}\left(\sin\frac{\beta}{2}\right)^{n-m+2k}}{(j+m-k)!(n-m+k)!k!(j-n-k)!}\right]$$

$$\times\frac{\left(a_\uparrow^\dagger\right)^{j+m}\left(a_\downarrow^\dagger\right)^{j-m}}{\sqrt{(j+m)!}\sqrt{(j-m)!}}|00\rangle. \tag{5.4.44}$$

Identification of the factor in brackets in the foregoing with the transformation matrix $\mathscr{D}^j$ in the following completes its derivation:

$$R(0\beta 0)\left|\begin{matrix} j \\ n \end{matrix}\right\rangle = \sum_m \mathscr{D}^j_{mn}(0\beta 0)\left|\begin{matrix} j \\ m \end{matrix}\right\rangle.$$

Addition of the factors $e^{-i\alpha m}$ and $e^{-i\gamma n}$ gives the complete formula for all R_3 representations in the $\left|\begin{matrix} j \\ m \end{matrix}\right\rangle$ bases:

$$\mathscr{D}^j_{mn}(\alpha\beta\gamma) = \sum_{k=0} (-1)^k \frac{\sqrt{(j+m)!(j-m)!(j+n)!(j-n)!}}{(j+m-k)!k!(j-n-k)!(n-m+k)!}$$

$$\times e^{-i(m\alpha+n\gamma)}\left(\cos\frac{\beta}{2}\right)^{2j+m-n-2k}\left(\sin\frac{\beta}{2}\right)^{n-m+2k}. \tag{5.4.45}$$

Since the orthogonal group O_3 is the outer product $R_3 \times C_i$ it is a simple matter to obtain its irreps from those of its factor groups R_3 and C_i. Two classes of irreps arise; an even-parity class $\mathscr{D}^{j+}$ and an odd-parity class $\mathscr{D}^{j-}$.

They are defined as follows:

$$\mathscr{D}^{j+}(R) = \mathscr{D}^{j}(R), \qquad \mathscr{D}^{j+}(IR) = \mathscr{D}^{j}(R),$$
$$\mathscr{D}^{j-}(R) = \mathscr{D}^{j}(R), \qquad \mathscr{D}^{j-}(IR) = -\mathscr{D}^{j}(R). \tag{5.4.46}$$

All group irreps defined so far are unitary matrices by construction. The $\mathscr{D}^{j}(\alpha\beta\gamma)$ matrices are unitary since the operators $R(\alpha\beta\gamma)$ are unitary:

$$R^{\dagger}(\alpha\beta\gamma) = (e^{\alpha J_z/ih}e^{\beta J_y/ih}e^{\gamma J_z/ih})^{\dagger} = e^{-\alpha J_z/ih}e^{-\beta J_y/ih}e^{-\gamma J_z/ih}$$
$$= R(-\alpha-\beta-\gamma) = R^{-1}(\alpha\beta\gamma).$$

In the preceding we use the fact that the J operators are self-conjugate or Hermitian ($J_i = J_i^{\dagger}$) operators. Finally, we have

$$\mathscr{D}^{j*}_{mn}(\alpha\beta\gamma) = \mathscr{D}^{j}_{nm}(-\alpha-\beta-\gamma).$$

5.5 SOME APPLICATIONS OF R_3 REPRESENTATIONS

Much of the remainder of this book will be devoted to applications of the $\mathscr{D}^{j}$-matrix representations of the rotation group R_3. However, there are some important elementary applications which are useful for familiarizing oneself with the properties of the $\mathscr{D}^{j}$ matrices. These will be discussed now.

A. $\mathscr{D}^{1/2}$-Spinor Representations and Hamilton's Turns

Hamilton's rules for spherical vector addition of rotations were introduced in Section 3.1.B and again in Section 5.3.C. It is instructive to see how they are derived from spinor representations. Indeed, the spinor representations are closely related to Hamilton's quarternion or "hypercomplex" numbers.

In order to rederive Hamilton's rules using spinors we shall need the spinor representation in terms of Darboux or axis angles $[\phi\theta\omega]$. We already have irreps of z rotations $R(\alpha 00)$ and y rotations $R(0\beta 0)$ in Eq. (5.4.30) for the Euler parametrization. Therefore, all that is needed is to express the $\boldsymbol{\omega}$ rotation $R[\phi\theta\omega]$ around axis $[\phi\theta]$ in terms of $R(\phi 00)$, $R(0\theta 0)$, and $R(\omega 00)$. In other words, we need to find how the $\boldsymbol{\omega}$ rotation can be done using just y and z cranks in Figure 5.3.2.

The $R[\phi\theta\omega]$ rotation may be done using only the y and z cranks by performing the following steps. First, one moves the $\boldsymbol{\omega}$ contact point so it lies under the z crank. This is accomplished by zeroing the azimuth ϕ with z crank $R(-\phi 00)$, and then zeroing the polar angle θ with y crank $R(0-\theta 0)$. Then the ω rotation can be done by z crank $R(0\omega 0)$. Finally, one returns the ω-contact point to its original position using the reverse and inverse operator sequence $R(\phi 00)R(0\theta 0)$. The desired product of the five operations is

$$R[\phi\theta\omega] = R(\phi 00)R(0\theta 0)R(\omega 00)R(0-\theta 0)R(-\phi 00).$$

The spinor representation of this product is

$$\mathscr{D}^{1/2}[\phi\theta\omega] =$$

$$\times \begin{pmatrix} e^{-i\phi/2} & 0 \\ 0 & e^{i\phi/2} \end{pmatrix} \begin{pmatrix} \cos\frac{\theta}{2} & -\sin\frac{\theta}{2} \\ \sin\frac{\theta}{2} & \cos\frac{\theta}{2} \end{pmatrix} \begin{pmatrix} e^{-i\omega/2} & \\ & e^{i\omega/2} \end{pmatrix} \begin{pmatrix} \cos\frac{\theta}{2} & \sin\frac{\theta}{2} \\ -\sin\frac{\theta}{2} & \cos\frac{\theta}{2} \end{pmatrix} \begin{pmatrix} e^{i\phi/2} & \\ & e^{-i\phi/2} \end{pmatrix}$$

$$= \begin{pmatrix} \cos\frac{\omega}{2} - i\cos\theta\sin\frac{\omega}{2} & -\sin\phi\sin\theta\sin\frac{\omega}{2} - i\cos\phi\sin\theta\sin\frac{\omega}{2} \\ \sin\phi\sin\theta\sin\frac{\omega}{2} - i\cos\phi\sin\theta\sin\frac{\omega}{2} & \cos\frac{\omega}{2} + i\cos\theta\sin\frac{\omega}{2} \end{pmatrix}. \tag{5.5.1}$$

By equating the components of $\mathscr{D}^{1/2}[\phi\theta\omega]$ to those of $\mathscr{D}^{1/2}(\alpha\beta\gamma)$ in Eq. (5.4.30) one obtains relations between Euler and Darboux angles:

$$\cos[(\alpha+\gamma)/2]\cos\beta/2 = \cos\omega/2, \tag{5.5.2a}$$

$$\sin[(\alpha+\gamma)/2]\cos\beta/2 = \sin\omega/2\cos\theta, \tag{5.5.2b}$$

$$\cos[(\gamma-\alpha)/2]\sin\beta/2 = \sin\omega/2\sin\theta\sin\phi, \tag{5.5.2c}$$

$$\sin[(\gamma-\alpha)/2]\sin\beta/2 = \sin\omega/2\sin\theta\cos\phi. \tag{5.5.2d}$$

Hamilton, and more recently, Cayley and Klein showed how to expand $\mathscr{D}^{1/2}[\phi\theta\omega]$ into QUATERNIONS q_α or PAULI SPINORS σ_α defined by

$$q_x \equiv i\sigma_x \equiv i\begin{pmatrix} 0 & 1 \\ 1 & 0 \end{pmatrix}, \qquad q_y \equiv i\sigma_y \equiv i\begin{pmatrix} 0 & -i \\ i & 0 \end{pmatrix}, \qquad q_z \equiv i\sigma_z \equiv i\begin{pmatrix} 1 & 0 \\ 0 & -1 \end{pmatrix},$$
$$= 2i\mathscr{D}^{1/2}(J_x), \qquad = 2i\mathscr{D}^{1/2}(J_y), \qquad = 2i\mathscr{D}^{1/2}(J_z). \tag{5.5.3}$$

[Note that quaternion q_α is proportional to the irrep $\mathscr{D}^{1/2}(J_\alpha)$ in Eqs. (5.5.12).] The desired expansion is

$$\mathscr{D}^{1/2}[\phi\theta\omega] = \cos\frac{\omega}{2}\begin{pmatrix} 1 & 0 \\ 0 & 1 \end{pmatrix} - i\sin\frac{\omega}{2}\left[\cos\phi\sin\theta\begin{pmatrix} 0 & 1 \\ 1 & 0 \end{pmatrix}\right.$$
$$\left. + \sin\phi\sin\theta\begin{pmatrix} 0 & -i \\ i & 0 \end{pmatrix} + \cos\theta\begin{pmatrix} 1 & 0 \\ 0 & -1 \end{pmatrix}\right]. \tag{5.5.4}$$

In operator notation this is

$$R[\phi\theta\omega] = \cos\frac{\omega}{2}\mathbf{1} - i\sin\frac{\omega}{2}\left[\hat{\boldsymbol{\omega}}_x\sigma_x + \hat{\boldsymbol{\omega}}_y\sigma_y + \hat{\boldsymbol{\omega}}_z\sigma_z\right] \tag{5.5.5a}$$

$$= \cos\frac{\omega}{2}\mathbf{1} - i\sin\frac{\omega}{2}[\boldsymbol{\omega}\cdot\boldsymbol{\sigma}], \tag{5.5.5b}$$

where

$$\omega_x = \cos\phi \sin\theta, \qquad \omega_y = \sin\phi \sin\theta, \qquad \omega_z = \cos\theta \tag{5.5.5c}$$

are the Cartesian components of the unit vector along the $\boldsymbol{\omega}$-crank axis. This expansion allows one to write a closed-form expression for group products such as

$$\begin{aligned} R[\phi'\theta'\omega']R[\phi\theta\omega] &= \left(\cos\frac{\omega'}{2}\mathbf{1} - i\sin\frac{\omega'}{2}\hat{\boldsymbol{\omega}}'\cdot\boldsymbol{\sigma}\right)\left(\cos\frac{\omega}{2}\mathbf{1} - i\sin\frac{\omega}{2}\hat{\boldsymbol{\omega}}\cdot\boldsymbol{\sigma}\right) \\ &= \cos\frac{\omega'}{2}\cos\frac{\omega}{2}\mathbf{1} - i\left[\cos\frac{\omega'}{2}\sin\frac{\omega}{2}\hat{\boldsymbol{\omega}} + \cos\frac{\omega}{2}\sin\frac{\omega'}{2}\hat{\boldsymbol{\omega}}'\right]\cdot\boldsymbol{\sigma} \\ &\quad - \sin\frac{\omega'}{2}\sin\frac{\omega}{2}(\hat{\boldsymbol{\omega}}\cdot\boldsymbol{\sigma})(\hat{\boldsymbol{\omega}}\cdot\boldsymbol{\sigma}). \end{aligned} \tag{5.5.6}$$

The third term in the foregoing can be reduced by the Pauli identity

$$(\mathbf{A}\cdot\boldsymbol{\sigma})(B\cdot\boldsymbol{\sigma}) \equiv \mathbf{A}\cdot\mathbf{B} + i(\mathbf{A}\times\mathbf{B})\cdot\boldsymbol{\sigma}. \tag{5.5.7}$$

The identity is easily proved by writing out each Pauli spinor component σ_x, σ_y, and σ_z as defined in Eq. (5.5.3). The result is the desired product

$$R[\phi'\theta'\omega']R[\phi\theta\omega] = R[\phi''\theta''\omega''], \tag{5.5.8}$$

where

$$R[\phi''\theta''\omega''] \equiv \cos\frac{\omega''}{2}1 - i\sin\frac{\omega''}{2}\hat{\boldsymbol{\omega}}''\cdot\boldsymbol{\sigma} \tag{5.5.9}$$

and

$$\cos\frac{\omega''}{2} = \cos\frac{\omega'}{2}\cos\frac{\omega}{2} - \sin\frac{\omega'}{2}\sin\frac{\omega}{2}\hat{\boldsymbol{\omega}}'\cdot\hat{\boldsymbol{\omega}}, \tag{5.5.10a}$$

$$\hat{\boldsymbol{\omega}}''\sin\frac{\omega''}{2} = \cos\frac{\omega'}{2}\sin\frac{\omega}{2}\hat{\boldsymbol{\omega}} + \cos\frac{\omega}{2}\sin\frac{\omega'}{2}\hat{\boldsymbol{\omega}}' + \sin\frac{\omega'}{2}\sin\frac{\omega}{2}\hat{\boldsymbol{\omega}}'\times\hat{\boldsymbol{\omega}}. \tag{5.5.10b}$$

This can be regarded as the principal structure equation for the two-dimensional UNIMODULAR UNITARY group SU_2 as well as R_3. The group of all matrices of the form given in Eq. (5.4.16) or (5.5.1) is the same as that of all unitary ($U^\dagger = U^{-1}$) and unimodular (det $U = 1$) two-by-two matrices. The structure equations are the ones which the slide rule described in Section 5.3.C is designed to solve using Hamilton's construction.

To show that Hamilton's construction is the same as the structure equations (5.5.10) one needs to analyze the spherical trigonometry. Consider a

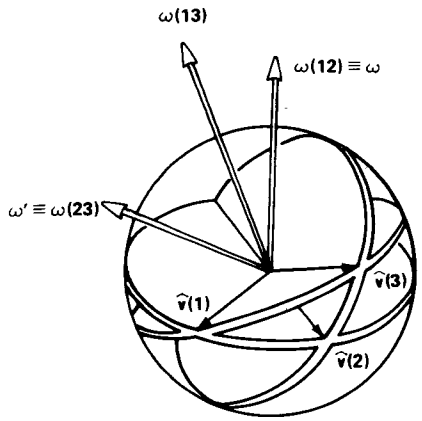

Figure 5.5.1 Hamilton arcs associated with rotation axes $\omega \equiv \omega(12)$, $\omega' \equiv \omega(23)$, and $\omega'' \equiv \omega(13)$.

spherical triangle defined by three unit normal vectors $\hat{\mathbf{v}}(1)$, $\hat{\mathbf{v}}(2)$, and $\hat{\mathbf{v}}(3)$, as shown in Figure 5.5.1. Let rotation axes $\omega \equiv \omega(12)$ and $\omega' \equiv \omega(23)$ have their directions defined by

$$\hat{\mathbf{v}}(1) \times \hat{\mathbf{v}}(2) = \sin(12)\hat{\boldsymbol{\omega}}, \qquad \hat{\mathbf{v}}(2) \times \hat{\mathbf{v}}(3) = \sin(23)\hat{\boldsymbol{\omega}}',$$

where (ij) is the arc length or angle between $\hat{\mathbf{v}}(i)$ and $\hat{\mathbf{v}}(j)$. By definition we can write $\hat{\mathbf{v}}(2)$ as

$$\hat{\mathbf{v}}(2) = \cos(12)\hat{\mathbf{v}}(1) + \sin(12)\hat{\boldsymbol{\omega}} \times \hat{\mathbf{v}}(1), \tag{5.5.11}$$

and similarly for $\hat{\mathbf{v}}(3)$:

$$\hat{\mathbf{v}}(3) = \cos(23)\hat{\mathbf{v}}(2) + \sin(23)\hat{\boldsymbol{\omega}}' \times \hat{\mathbf{v}}(2). \tag{5.5.12}$$

Substituting the expression for $\hat{\mathbf{v}}(2)$ gives

$$\begin{aligned}\hat{\mathbf{v}}(3) = {} & \cos(23)\cos(12)\hat{\mathbf{v}}(1) + [\cos(23)\sin(12)\hat{\boldsymbol{\omega}} + \sin(23)\cos(12)\hat{\boldsymbol{\omega}}'] \times \hat{\mathbf{v}}(1) \\ & + \sin(23)\sin(12)\hat{\boldsymbol{\omega}}' \times (\hat{\boldsymbol{\omega}} \times \hat{\mathbf{v}}(1)).\end{aligned} \tag{5.5.13}$$

The third term above can be reduced by using cross-product identities:

$$\begin{aligned}\hat{\boldsymbol{\omega}}' \times (\hat{\boldsymbol{\omega}} \times \hat{\mathbf{v}}(1)) &\equiv (\hat{\boldsymbol{\omega}}' \cdot \hat{\mathbf{v}}(1))\hat{\boldsymbol{\omega}} - (\hat{\boldsymbol{\omega}}' \cdot \hat{\boldsymbol{\omega}})\hat{\mathbf{v}}(1), \\ (\hat{\boldsymbol{\omega}}' \times \hat{\boldsymbol{\omega}}) \times \hat{\mathbf{v}}(1) &\equiv (\hat{\boldsymbol{\omega}}' \cdot \hat{\mathbf{v}}(1))\hat{\boldsymbol{\omega}} - (\hat{\boldsymbol{\omega}} \cdot \hat{\mathbf{v}}(1))\hat{\boldsymbol{\omega}}' \\ &= (\hat{\boldsymbol{\omega}}' \cdot \hat{\mathbf{v}}(1))\hat{\boldsymbol{\omega}}.\end{aligned}$$

Subtracting the identities gives

$$\hat{\boldsymbol{\omega}}' \times (\hat{\boldsymbol{\omega}} \times \hat{\mathbf{v}}(1)) - (\hat{\boldsymbol{\omega}}' \times \hat{\boldsymbol{\omega}}) \times \hat{\mathbf{v}}(1) = -(\hat{\boldsymbol{\omega}}' \cdot \hat{\boldsymbol{\omega}})\hat{\mathbf{v}}(1).$$

The resulting expression for $\hat{\omega}' \times (\hat{\omega} \times \hat{v}(1))$ can be substituted into the one for $\hat{v}(3)$. There results an equation

$$\hat{v}(3) = \cos(13)\hat{v}(1) + \sin(13)\hat{\omega}'' \times \hat{v}(1), \tag{5.5.14}$$

where

$$\cos(13) = \cos(23)\cos(12) - \sin(23)\sin(12)\hat{\omega}' \cdot \hat{\omega}, \tag{5.5.15a}$$

and

$$\hat{\omega}'' \sin(13) = \cos(23)\sin(12)\hat{\omega} + \cos(12)\sin(23)\hat{\omega}' + \sin(23)\sin(12)\hat{\omega}' \times \hat{\omega}. \tag{5.5.15b}$$

The form of the vector equations matches the principal structure equations (5.5.10) provided one makes the half-angle identifications

$$(12) = \omega/2, \qquad (23) = \omega'/2, \qquad (13) = \omega''/2. \tag{5.5.16}$$

This completes the vector-based proof of Hamilton's construction.

B. Spin-j Polarization Experiments

The matrix $\mathscr{D}^{1/2}(\alpha = \pi/2, \beta = \theta, \gamma = 0)$ is the example of transformation matrix $\mathscr{T}$ which was introduced in Eq. (1.1.3). In general, $\mathscr{D}^{j}_{m'm}(\alpha\beta\gamma)$ gives the amplitude for a particle or system in a rotated state $R(\alpha\beta\gamma)|^j_m\rangle$, to choose the state $\left|{}^{j}_{m'}\right\rangle$ if it is somehow forced to make a choice between all the $|^j_m\rangle$. In Chapter 1 thought experiments involving ($j = \frac{1}{2}$) states were sketched. The amplitudes $\mathscr{D}_{m'm} = \langle m'|m\rangle$ between states

$$\left\{\left|{}^{1/2}_{1/2}\right\rangle = |1\rangle = |\text{“up”}\rangle, \left|{}^{1/2}_{-1/2}\right\rangle = |2\rangle = |\text{“down”}\rangle\right\}$$

and rotated states $\{R(\pi/2, \theta, 0)|1\rangle = |1'\rangle,\ R(\pi/2, \theta, 0)|2\rangle = |2'\rangle\}$ were introduced.

Figure 5.5.2 depicts a similar thought experiment involving ($j = 2$) states or particles. It begins with states $R(\alpha\beta\gamma)|^2_1\rangle$ represented by tipped cones emerging from a β-tipped analyzer drawn on the left. We suppose that these are all forced by an untipped analyzer to choose one of the untipped states $|^2_2\rangle$, $|^2_1\rangle$, $|^2_0\rangle$, $|^2_{-1}\rangle$, or $|^2_{-2}\rangle$. The amplitude for choosing channel m' or state $|^2_{m'}\rangle$ is then $\mathscr{D}^2_{m'1}(0\beta 0)$. The $\mathscr{D}$ functions from Eq. (5.4.35) are plotted with a broken line at the right of Figure. 5.5.2 for each m'. The intensity or probability $|\mathscr{D}^2_{m'1}|^2$ is the solid curve. Note that 100% of the particles would choose the $|^2_{-1}\rangle$ channel when $\beta = \pi$. This is right, since $|^2_1\rangle$ turned upside down must be the same as $|^2_{-1}\rangle$ to within a phase factor.

It is interesting to try to get some feeling for the behavior $\mathscr{D}$ functions. Consider a ($j = 6$) basis. The cone pictures of all the base states are drawn in Figure 5.5.3(a).

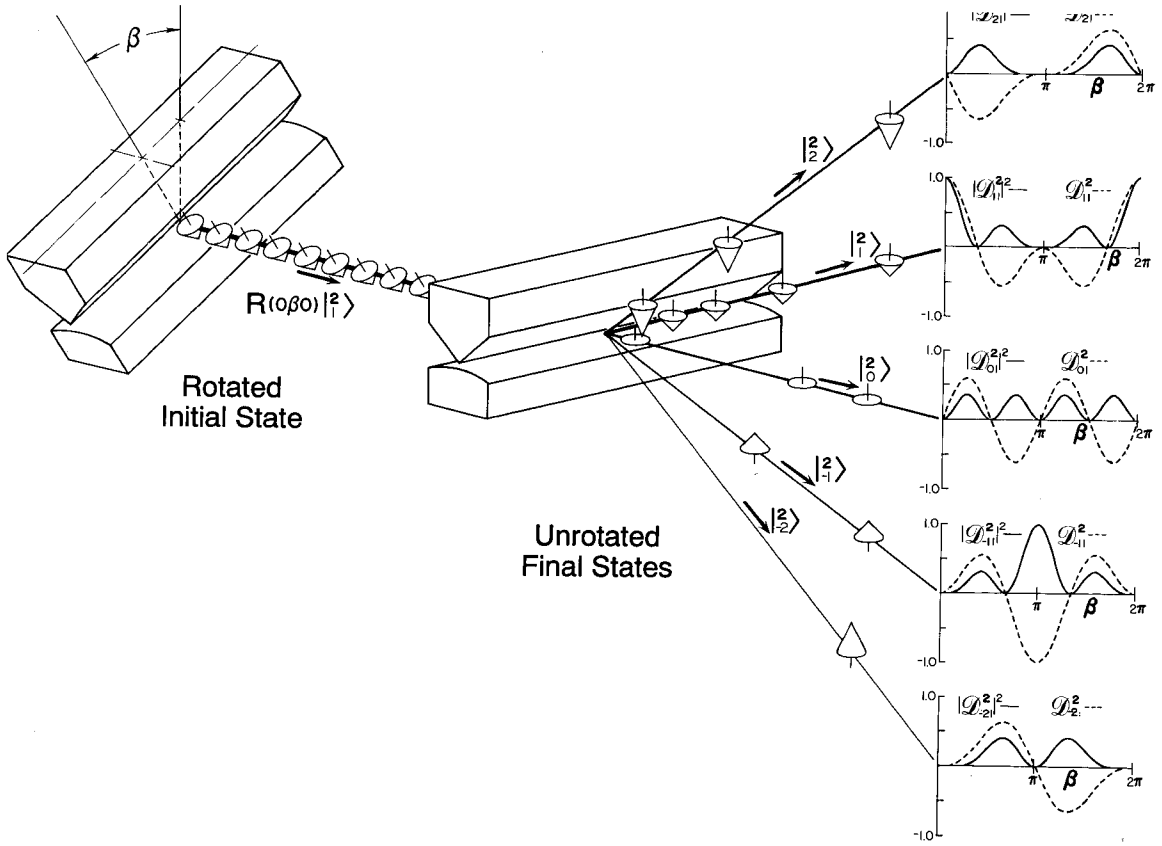

Figure 5.5.2 Representation of ideal Stern-Gerlach-like experiments. Polarized beam of spin-2 particles emerges from a rotated analyzer on the left. The particles emerge in a rotated state $R(0\beta 0)\left|\begin{smallmatrix}2\\1\end{smallmatrix}\right\rangle$ and are then forced to choose from unrotated states $\left\{\left|\begin{smallmatrix}2\\2\end{smallmatrix}\right\rangle, \left|\begin{smallmatrix}2\\1\end{smallmatrix}\right\rangle, \left|\begin{smallmatrix}2\\0\end{smallmatrix}\right\rangle, \left|\begin{smallmatrix}2\\-1\end{smallmatrix}\right\rangle, \left|\begin{smallmatrix}2\\-2\end{smallmatrix}\right\rangle\right\}$ by the analyzer on the right. The amplitudes (dashed lines) and probabilities (solid lines) are plotted as a function of rotation angle β for each choice.

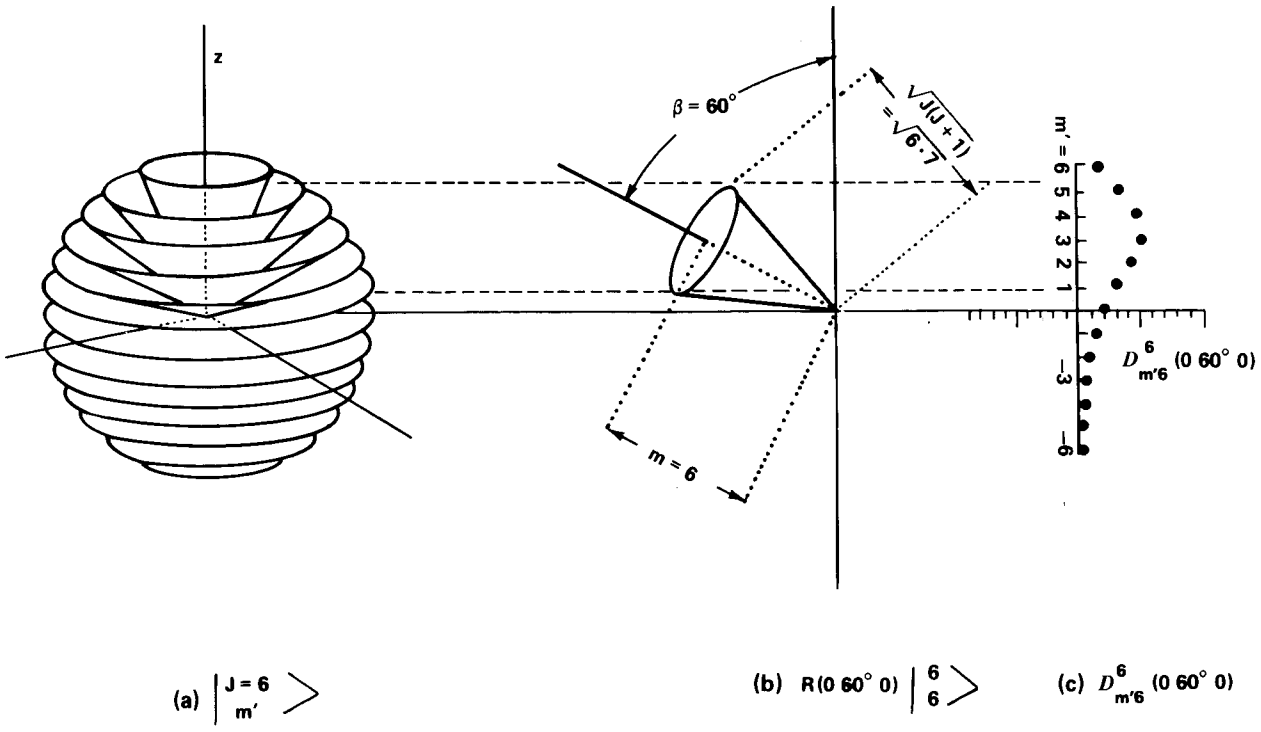

Figure 5.5.3 Angular-momentum vector-cone geometry and rotation amplitudes for $J = 6$. (a) Vector cones for all the states $\left\{\left|\begin{matrix}6\\6\end{matrix}\right\rangle, \left|\begin{matrix}6\\5\end{matrix}\right\rangle, \left|\begin{matrix}6\\4\end{matrix}\right\rangle, \ldots, \left|\begin{matrix}6\\-6\end{matrix}\right\rangle\right\}$ belonging to $J = 6$. (b) Vector cone for rotated state $R(0\ 60^\circ\ 0)\left|\begin{matrix}6\\6\end{matrix}\right\rangle$. Dashed lines indicate projection of uncertainty of rotated cone. (c) Greatest amplitudes $D^6_{m'6}$ (0 60° 0) occur for the m' values which lie inside the projection of uncertainty.

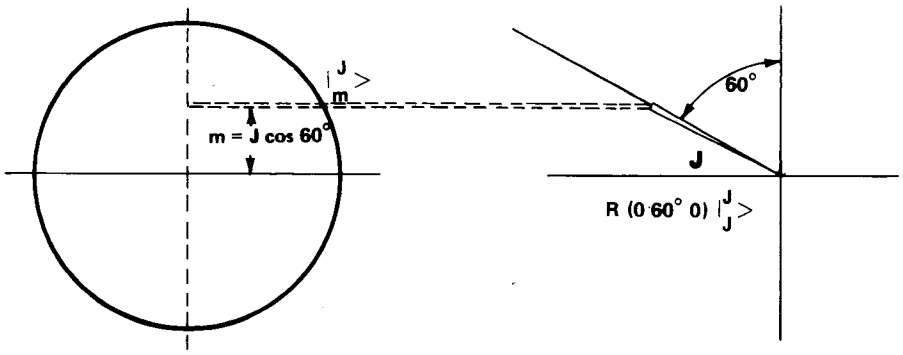

Figure 5.5.4 Vector geometry in classical limit for large $J > 10^4$. Uncertainty of $\left|{}^{J}_{J}\right\rangle$ state is negligible in the classical limit.

Consider the rotated state $R(0\ 60°\ 0)|^6_6\rangle$ shown in Figure 5.5.3(b). Let us compare the amplitudes for it to choose the unrotated states belonging to cones that lie inside the projection of its cone, namely, $|^6_5\rangle$ to $|^6_1\rangle$, to those that lie outside. For classical angular momentum the z component of a 60° rotated angular-momentum vector of length j is $m' = j\cos 60°$ as shown in Figure 5.5.4, simple classical vector rules apply for angular-momentum states for which the $|^j_j\rangle$-cone apex angle

$$\theta_{\text{cone}} = 2\cos^{-1}\left[j/\sqrt{(j(j+1)}\right] \sim \cos^{-1}[j/(j+1/2)] \quad (5.5.17)$$

is small enough to consider the cone as a vector. Even the high value of $j = 10^4$ gives $\theta_{\text{cone}} = 1.15°$. For $j = 10^6$ we have $\theta_{\text{cone}} = 0.115°$. This should be regarded as an approximate lower bound to classical angular-momentum theory.

For lesser j one must settle for a series of quantum amplitudes given by $\mathscr{D}$ functions in Eq. (5.4.45). The exact values of $\mathscr{D}^6_{m'6}(0\ 60°\ 0)$ are plotted in Figure 5.5.3(c). Note that the amplitudes seem to form a smooth lump around the inside components. However, the amplitudes are nonzero outside the projection of the $R(0\ 60°\ 0)|^6_6\rangle$ cone.

Figure 5.5.5 shows a whole series of plots of $\mathscr{D}^{20}_{m'm}(0\beta 0)$ as a function of m' for various fixed constants β and m. In the first column each plot has $m' = 20 = j$. This gives a Gaussian-like lump similar to Figure 5.5.3(c) for $\beta \neq 0$. (For $\beta = 0$ the lump collapses into a single spike since $\left\langle {}^{j}_{m'} \middle| {}^{j}_{m} \right\rangle = \delta_{m'm}$.)

For the other columns we set $m' = (j-1)$, $(j-2)$, and $(j-3)$. One observes a lump with one, two, and three nodes, respectively. For $\beta > 30°$ these lumps resemble oscillator wave functions. Their "classical turning points" or points of inflection occur at the projections of the cone edges.

This curious discrete wave behavior occurs for other angular-moment quantities such as coupling and recoupling coefficients. Ponzano and Regge [1968] and Shulten and Gordon [1975] have given a theory for this behavior in

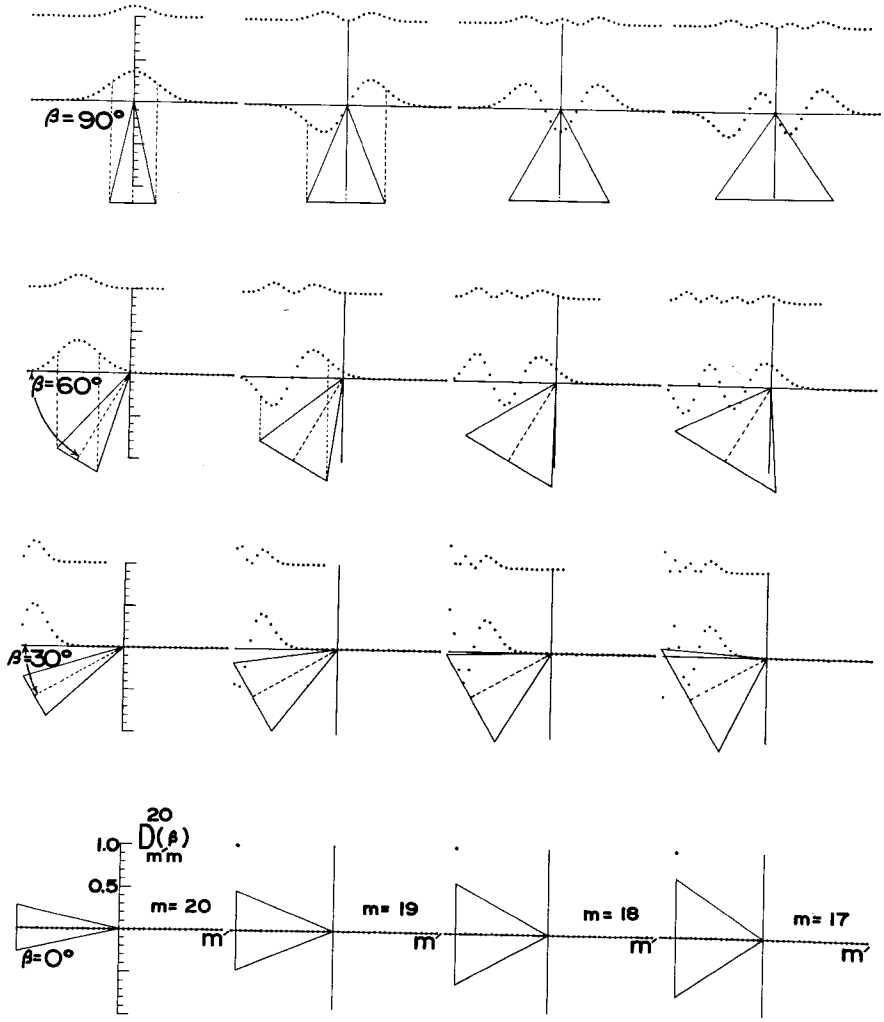

Figure 5.5.5 Rotation amplitudes, probabilities, and cone geometry for $J = 20$. In each subdiagram the amplitudes $D^{20}_{m'm}(0\beta 0)$ are plotted as a function of m' for fixed $\beta = 0°$, 30°, 60°, and 90° and fixed $m = 20$, 19, 18, and 17. The squared amplitudes or probabilities are plotted above each subdiagram.

coupling coefficients. They have derived one-dimensional potential wells which give wavelike solutions which approximate the discrete waves closely.

Finally it is interesting to note that the first moment or the J_z expectation value,

$$M' = \langle {}^{j}_{m}|R^{\dagger}(0\beta 0)J_z R(0\beta 0)|{}^{j}_{m}\rangle$$
$$= \sum_{m'=-j}^{j} m' \left|\mathscr{D}^{j}_{m'm}(0\beta 0)\right|^2, \tag{5.5.18}$$

of the probability distribution $|\mathscr{D}^j|^2$ gives the classical value $M' = m\cos\beta$. (This will be proved in Chapter 7.) The squares $|\mathscr{D}^j|^2$ of the $\mathscr{D}$ amplitudes are plotted above each $\mathscr{D}$ graph in Figure 5.5.5.

C. Symmetry Analysis of Quantum Rotors

Chapters 1–3 contained a development the basic ideas of symmetry analysis. The mathematics is summarized by the following. A group $\mathscr{G} = \{\cdots R \cdots R' \cdots\}$ of operators can have each element written

$$R = \sum_j \sum_m \sum_n \mathscr{D}^j_{mn}(R) P^j_{mn} \tag{5.5.19}$$

in terms of irrep components $\mathscr{D}^j_{mn}$ and a complete set of elementary projection operators

$$P^j_{mn} = \frac{l^j}{{}^o\mathscr{G}} \sum_R \mathscr{D}^{j*}_{mn}(R) R, \tag{5.5.20}$$

where l^j is the dimension of irrep $\mathscr{D}^j$, and the sum is over all group operators. ${}^o\mathscr{G}$ is the number of operators in $\mathscr{G}$. Elementary projectors satisfy orthonormality relations

$$P^j_{mn} P^{j'}_{m'n'} = \delta^{jj'} \delta_{nm'} P^j_{mn'}, \tag{5.5.21}$$

and a completeness relation,

$$1 = \sum_j \sum_m^{l^j} P^j_{mm}. \tag{5.5.22}$$

For the groups R_3, O_3, and SU_2 the formulas are the same except that the group sum $(1/{}^o\mathscr{G})\Sigma_R$ is replaced by an integral over Euler angles:

$$(1/{}^o\mathscr{G})\sum = 1 \to (1/8\pi^2)\int_0^{2\pi} d\alpha \int_{0 \text{ or } -\pi}^{\pi} \sin\beta\, d\beta \int_0^{2\pi} d\gamma = 1 \equiv \int d(\alpha\beta\gamma).$$

The integral over α and β (or γ and β) is analogous to a spherical polar area integral over ϕ and θ, respectively. As explained in Section 5.3.A, Euler angles α and β play the roles of azimuthal and polar angles in the laboratory coordinate frame while γ and β play the same roles in the body frame. For R_3 the range of β is 0 to π, for SU_2 it is $-\pi$ to π. A rigorous derivation of the Euler integral involves the theory of invariant group measure which is beyond the scope of this text. The integral formula for the R_3 $(0 \le \beta < \pi)$ or

SU_2 ($-\pi \leq \beta\pi$) projection operator is

$$P^j_{mn} = (2j + 1)\int d(\alpha\beta\gamma)\, \mathscr{D}^{j*}_{mn}(\alpha\beta\gamma) R(\alpha\beta\gamma), \qquad (5.5.23)$$

where $l^j = (2j + 1)$ is the dimension of the irreps $\mathscr{D}^j$. (See Appendix G.)

The application of P operators in the quantum theory of molecular rotation is analogous to the applications discussed in Chapters 1–4. One begins with a starting position state $|1\rangle = |000\rangle$ in which a rigid molecular body has its body coordinates $\{\bar{x}\bar{y}\bar{z}\}$ lined up with the lab coordinates $\{xyz\}$. Then the P operators are applied to this state to give symmetry-defined states

$$|^j_{mn}\rangle = P^j_{mn}|000\rangle/(2j + 1)^{1/2}$$

$$= \int d(\alpha\beta\gamma)\, \mathscr{D}^{j*}_{mn}(\alpha\beta\gamma)(2j + 1)^{1/2} R(\alpha\beta\gamma)|000\rangle. \qquad (5.5.24)$$

The states $|^j_{mn}\rangle$ have definite R_3 transformation properties as well as some simple physical properties which will be discussed shortly. Each $|^j_{mn}\rangle$ state is a linear combination of rotational position states

$$|\alpha\beta\gamma\rangle = R(\alpha\beta\gamma)|000\rangle$$

multiplied by amplitudes

$$r^j_{mn}(\alpha\beta\gamma) = \mathscr{D}^{j*}_{mn}(\alpha\beta\gamma)\sqrt{2l + 1}\,. \qquad (5.5.25)$$

The amplitude $r^j_{mn}(\alpha\beta\gamma)$ is called the QUANTUM ROTOR WAVE FUNCTION. Its absolute square $|r^j_{mn}(\alpha\beta\gamma)|^2$ gives the probability that a molecular rotor in state $|^j_{mn}\rangle$ would end up in rotational position state $|\alpha\beta\gamma\rangle$ if it was somehow forced to choose from all Euler angles. We shall sometimes write the r amplitude as

$$r^j_{mn}(\alpha\beta\gamma) = \langle\alpha\beta\gamma|^j_{mn}\rangle = \langle 000|R^\dagger(\alpha\beta\gamma)|^j_{mn}\rangle. \qquad (5.5.26)$$

The orthogonality of the r and $\mathscr{D}$ functions follows from that of the P operators. Rewriting Eq. (3.4.18) gives

$$\mathscr{D}^{j'}_{m'n'}(P^j_{mn}) = \delta^{jj'}\delta_{mm'}\delta_{nn'}. \qquad (5.5.27)$$

Inserting Eq. (5.5.23) gives $\mathscr{D}$ orthogonality relations

$$(2j + 1)\int d(\alpha\beta\gamma)\mathscr{D}^{j*}_{mn}(\alpha\beta\gamma)\mathscr{D}^{j'}_{m'n'}(\alpha\beta\gamma) = \delta^{jj'}\delta_{mm'}\delta_{nn'}, \qquad (5.5.28)$$

as well as r orthogonality. ($\mathscr{D}$ orthogonality is discussed in Appendix G.)

$$\int d(\alpha\beta\gamma) r^{j*}_{mn}(\alpha\beta\gamma) r^{j'}_{m'n'}(\alpha\beta\gamma) = \delta^{jj'}\delta_{mm'}\delta_{nn'}. \tag{5.5.29}$$

Let us consider now the transformation properties of the $|^j_{mn}\rangle$ states under the laboratory-based rotation operators $R(\alpha\beta\gamma)$ or body-based rotation operators $\bar{R}(\alpha\beta\gamma)$. This will include discussion of the corresponding generators $\{J_x J_y J_z\}$ and $\{\bar{J}_{\bar{x}} \bar{J}_{\bar{y}} \bar{J}_{\bar{z}}\}$, respectively. The transformation rules will follow more or less directly from the elementary left- and right-hand multiplication formulas:

$$R(\alpha\beta\gamma) P^j_{mn} = \sum_{m'} \mathscr{D}^j_{m'm}(\alpha\beta\gamma) P^j_{m'n}, \tag{5.5.30a}$$

$$P^j_{mn} R(\alpha\beta\gamma) = \sum_{n'} \mathscr{D}^j_{nn'}(\alpha\beta\gamma) P^j_{mn'}. \tag{5.5.30b}$$

The left- and right-handed formulas are verified by replacing R using Eq. (5.5.19) and then using orthogonality relations (5.5.21). Recall a similar derivation of Eq. (3.3.14).

The left-handed formula gives the standard laboratory transformation of state $|^j_{mn}\rangle$ in Eq. (5.5.24):

$$\begin{aligned} R(\alpha\beta\gamma)|^j_{mn}\rangle &= R(\alpha\beta\gamma) P^j_{mn} |000\rangle / \sqrt{2j+1} \\ &= \sum_{m'} \mathscr{D}^j_{m'm}(\alpha\beta\gamma) P^j_{m'n} |000\rangle / \sqrt{2j+1}\,, \\ R(\alpha\beta\gamma)|^j_{mn}\rangle &= \sum_{m'} \mathscr{D}^j_{m'm}(\alpha\beta\gamma) |^j_{m'n}\rangle. \end{aligned} \tag{5.5.31}$$

Note that only the left m subindices of the state are involved. Using the lab-based rotation-generator relations

$$\begin{aligned} R(\alpha\beta\gamma) &= R(\alpha 00) R(0\beta 0) R(00\gamma) \\ &= e^{\alpha J_z / i\hbar} e^{\beta J_y / i\hbar} e^{\gamma J_z / i\hbar} \end{aligned} \tag{5.5.32}$$

one can rederive the effect of lab J operators from infinitesimal rotations such as

$$R(\delta\alpha 00) = 1 - i\delta\alpha J_z/\hbar, \tag{5.5.33a}$$

$$R(0\delta\beta 0) = 1 - i\delta\beta J_y/\hbar. \tag{5.5.33b}$$

For example, one obtains

$$(1 - i\delta\alpha J_z)|^j_{mn}\rangle = \sum_{m'} \mathscr{D}^j_{m'm}(1 - i\delta\alpha J_z)|^j_{m'n}\rangle$$
$$= \sum_{m'} \left[\mathscr{D}^j_{m'm}(1) - i\delta\alpha \mathscr{D}^j_{m'm}(J_z)\right]|^j_{m'n}\rangle. \quad (5.5.34)$$

Using the representations $\mathscr{D}_{m'm}(1) = \delta_{m'm}$ and $\mathscr{D}_{m'm}(J_z) = \delta_{m'm} m\hbar$ from Eq. (5.5.12c) one obtains

$$J_z \left| \begin{matrix} j \\ mn \end{matrix} \right\rangle = \hbar m \left| \begin{matrix} j \\ mn \end{matrix} \right\rangle. \quad (5.5.35a)$$

The lab operators J_x and J_y are treated similarly:

$$J_x \left| \begin{matrix} j \\ mn \end{matrix} \right\rangle = \frac{\hbar}{2}(j(j+1) - m(m+1))^{1/2} \left| \begin{matrix} j \\ m+1\, n \end{matrix} \right\rangle$$
$$+ \frac{\hbar}{2}(j(j+1) - m(m-1))^{1/2} \left| \begin{matrix} j \\ m-1\, n \end{matrix} \right\rangle, \quad (5.5.35b)$$
$$J_y \left| \begin{matrix} j \\ mn \end{matrix} \right\rangle = \frac{-i\hbar}{2}(j(j+1) - m(m+1))^{1/2} \left| \begin{matrix} j \\ m-1\, n \end{matrix} \right\rangle$$
$$+ \frac{i\hbar}{2}(j(j+1) - m(m-1))^{1/2} \left| \begin{matrix} j \\ m-1\, n \end{matrix} \right\rangle. \quad (5.5.35c)$$

The transformation derivations for the body operators $\overline{R}(\alpha\beta\gamma)$ and their generators are only slightly more complicated:

$$\overline{R}(\alpha\beta\gamma)|^j_{mn}\rangle = \overline{R}(\alpha\beta\gamma) P^j_{mn}|000\rangle/\sqrt{2j+1} \quad (5.5.36)$$
$$= P^j_{mn}\overline{R}(\alpha\beta\gamma)|000\rangle/\sqrt{2j+1} \quad (5.5.37)$$
$$= P^j_{mn} R^\dagger(\alpha\beta\gamma)|000\rangle/\sqrt{2j+1}\,. \quad (5.5.38)$$

Here the commutation (5.3.6) between a body operator $\overline{R}$ and the lab-based P operator is used to give Eq. (5.5.37). Then we use initial state relation (5.3.7) between $\overline{R}$ and inverse $R^{-1} = R^\dagger$ of lab rotations. Finally, the right multiplication formula (5.5.30b) gives the body-operator transformation rules:

$$\overline{R}(\alpha\beta\gamma)|^j_{mn}\rangle = \sum_{n'} \mathscr{D}^{j\dagger}_{nn'}(\alpha\beta\gamma) P^j_{mn'}|000\rangle/\sqrt{2j+1}\,, \quad (5.5.39)$$
$$\overline{R}(\alpha\beta\gamma)|^j_{mn}\rangle = \sum_{n'} \mathscr{D}^{j\dagger}_{nn'}(\alpha\beta\gamma)|^j_{mn'}\rangle. \quad (5.5.40)$$

Note that the right-hand n indices are involved in the body-based transformation. The n index is analogous to the local symmetry index discussed in Section 3.4.A. Indeed, one can think of the general quantum rotor states as bases of the regular representation of R_3.

The body-based angular-momentum operators $\bar{J}_{\bar{z}}$ and $\bar{J}_{\bar{y}}$ are related to $\bar{R}$ through relations such as

$$\begin{aligned}\bar{R}(\alpha\beta\gamma) &= \bar{R}(\alpha 00)\,\bar{R}(0\beta 0)\,\bar{R}(00\gamma)\\ &= e^{\alpha\bar{J}_{\bar{z}}/\hbar}e^{\beta\bar{J}_{\bar{y}}/i\hbar}e^{\gamma\bar{J}_{\bar{z}}/i\hbar}.\end{aligned} \tag{5.5.41}$$

In particular, an infinitesimal $\bar{z}$ rotation is

$$\bar{R}(00\delta\gamma) = 1 - i\delta\gamma\bar{J}_{\bar{z}}/\hbar.$$

Substituting this into Eq. (5.3.35) and (5.5.40) gives

$$\begin{aligned}\bar{R}(00\delta\gamma)|^j_{mn}\rangle &= \sum_n \mathscr{D}^{j\dagger}_{nn'}(R(00\delta\gamma))|^j_{mn'}\rangle,\\ (1 - i\delta\gamma J_z/\hbar)|^j_{mn}\rangle &= \sum_{n'} \mathscr{D}^{j\dagger}_{nn'}(1 - i\delta\gamma J_z/\hbar)|^j_{mn'}\rangle.\end{aligned}$$

Using the definitions of unitarity ($\mathscr{D}^{j\dagger}_{nn'} = \mathscr{D}^{j*}_{n'n}$) and identity $\mathscr{D}^j_{nn'}(1) = \delta_{nn'}$, we obtain

$$\bar{J}_{\bar{z}}\left|\begin{matrix}j\\ mn\end{matrix}\right\rangle = -\sum_{n'}\left|\begin{matrix}j\\ mn'\end{matrix}\right\rangle \mathscr{D}^j_{n'n}(J^*_z). \tag{5.5.42}$$

The minus sign arises from the conjugation ($*$):

$$\mathscr{D}^{j*}(i\delta\gamma J_z) = -i\mathscr{D}^j(\delta\gamma J^*_z).$$

The irrep formula (5.4.25c) gives the result

$$\bar{J}_{\bar{z}}\left|\begin{matrix}j\\ mn\end{matrix}\right\rangle = -n\hbar\left|\begin{matrix}j\\ mn\end{matrix}\right\rangle. \tag{5.5.43}$$

The minus sign for the body-based angular-momentum components is regarded as a nuisance. It can be traced right back to the lab-body relation (5.3.7). Obviously, any body residents would report that the laboratory was whirling around with a rotational sense opposite to the sense of rotation of the body measured in the lab. Jahn [1938] chose to eliminate the minus sign by introducing REVERSED angular momentum operators

$$J_{\bar{x}} = -\bar{J}_{\bar{x}}, \qquad J_{\bar{y}} = -\bar{J}_{\bar{y}}, \qquad J_{\bar{z}} = -\bar{J}_{\bar{z}}. \tag{5.5.44}$$

This definition leads to the following body-based equations:

$$J_{\bar{z}}\left|\begin{matrix} j \\ mn \end{matrix}\right\rangle = n\hbar\left|\begin{matrix} j \\ mn \end{matrix}\right\rangle, \tag{5.5.45a}$$

$$J_{\bar{y}}\left|\begin{matrix} j \\ mn \end{matrix}\right\rangle = \frac{i\hbar}{2}\left(j(j+1) - n(n+1)\right)^{1/2}\left|\begin{matrix} j \\ m\,n+1 \end{matrix}\right\rangle - \frac{i\hbar}{2}\left(j(j+1) - n(n-1)\right)^{1/2}\left|\begin{matrix} j \\ m\,n-1 \end{matrix}\right\rangle, \tag{5.5.45b}$$

$$J_{\bar{x}}\left|\begin{matrix} j \\ mn \end{matrix}\right\rangle = \frac{\hbar}{2}\left(j(j+1) - n(n+1)\right)^{1/2}\left|\begin{matrix} j \\ m\,n+1 \end{matrix}\right\rangle + \frac{\hbar}{2}\left(j(j+1) - n(n-1)\right)^{1/2}\left|\begin{matrix} j \\ m\,n-1 \end{matrix}\right\rangle. \tag{5.5.45c}$$

These results complement the lab-based equations (5.5.35).

A physical interpretation of the $J_{\bar{z}}$ equation is shown partly by Figure 5.5.6. One may regard the $\langle J_{\bar{z}}\rangle = n\hbar$ as the $\bar{z}$ component of lab-based angular momentum on the body $\bar{z}$ axis. Note that the same $\left|\begin{matrix} j \\ mn \end{matrix}\right\rangle$ state will also have a definite z component $\langle J_z\rangle = m\hbar$ of angular momentum on the

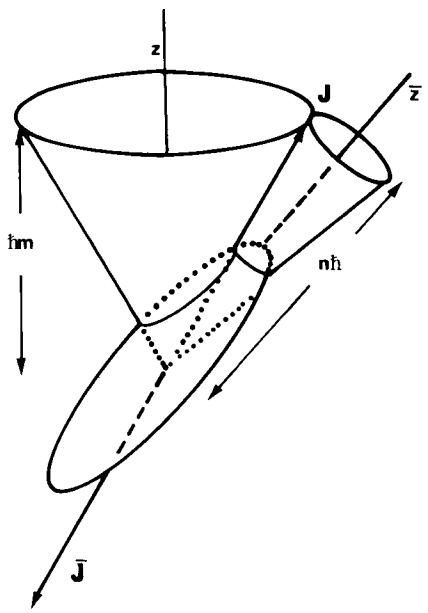

Figure 5.5.6 Laboratory and body components of rotational momentum.

laboratory z axis. Since J_z and $J_{\bar{z}}$ commute they may share the eigenstate $\left|\begin{matrix} j \\ mn \end{matrix}\right\rangle$.

The price one pays for reversing the momenta comes in the form of negative commutation relations:

$$\left[J_{\bar{x}}, J_{\bar{y}}\right] = -i\hbar J_{\bar{z}} \tag{5.5.46}$$

between body-component operators. The raising and lowering operators are interchanged, also:

$$\left(J_{\bar{x}} + iJ_{\bar{y}}\right)\left|\begin{matrix} j \\ mn \end{matrix}\right\rangle = \hbar\left(j(j+1) - n(n-1)\right)^{1/2}\left|\begin{matrix} j \\ m\,n-1 \end{matrix}\right\rangle, \tag{5.5.47a}$$

$$\left(J_{\bar{x}} - iJ_{\bar{y}}\right)\left|\begin{matrix} j \\ mn \end{matrix}\right\rangle = \hbar\left(j(j+1) - n(n+1)\right)^{1/2}\left|\begin{matrix} j \\ m\,n+1 \end{matrix}\right\rangle. \tag{5.5.47b}$$

This follows from the body-based equations (5.5.45b) and (5.5.45c) for the $\left|\begin{matrix} j \\ mn \end{matrix}\right\rangle$ states.

Using the same equations it is easy to show that the states $\left|\begin{matrix} j \\ mn \end{matrix}\right\rangle$ are eigenstates of the spherical quantum rotor Hamiltonian,

$$\begin{aligned} H_{\text{sphere}} &= (J)^2/2I = B(J)^2 \\ &= B\left(J_{\bar{x}}^2 + J_{\bar{y}}^2 + J_{\bar{z}}^2\right), \end{aligned} \tag{5.5.48}$$

where I is the rotational inertia, and

$$B = 1/2I$$

is called the rotational constant. The energy-level spectrum of the spherical rotor is given by the eigenvalues

$$E^j = \left\langle\begin{matrix} j \\ mn \end{matrix}\right|H_{\text{sphere}}\left|\begin{matrix} j \\ mn \end{matrix}\right\rangle = j(j+1)\hbar^2 B. \tag{5.5.49}$$

The spectrum consists of j levels with a spacing of

$$E_j - E_{j-1} = 2\hbar^2 Bj, \tag{5.5.50}$$

as shown on the left-hand side of Figure 5.5.7.

$1, 9, 25, 49, \ldots$ for $j = 0, 1, 2, 3, \ldots$, respectively, in the spherical quantum rotor level spectrum.

The states $\left|{}^{j}_{mn}\right\rangle$ are also eigenvectors of the cylindrical or symmetric quantum rotor Hamiltonian:

$$\begin{aligned} H_{\text{sym.}} &= \left(J_{\bar{x}}^2 + J_{\bar{y}}^2\right)/2I_{\bar{x},\bar{y}} + J_{\bar{z}}^2/2I_{\bar{z}} \\ &= \left(J_{\bar{x}}^2 + J_{\bar{y}}^2 + J_{\bar{z}}^2\right)/2I_{\bar{x},\bar{y}} + J_{\bar{z}}^2\left[(1/2I_{\bar{z}}) - (1/2I_{\bar{x},\bar{y}})\right] \\ &= B(J)^2 + J_{\bar{z}}^2[C - B]. \end{aligned} \tag{5.5.51a}$$

Here the constant

$$I_{\bar{x},\bar{y}} = I_{\bar{x}} = I_{\bar{y}} = 1/2B \tag{5.5.51b}$$

is the transverse moment of inertia for a cylindrical object, and $I_{\bar{z}} = 1/2C$ is the axial inertia. If the rotor is a PROLATE symmetric or football-shaped object, then $I_{\bar{z}} < I_{\bar{x},\bar{y}}$. We shall consider this case. In the opposite case ($I_{\bar{z}} > I_{\bar{x}\bar{y}}$) one has an OBLATE symmetric or discus-shaped rotor.

The prolate symmetric rotor spectrum depends on total momentum quantum number j, the body component n, and the molecular constants B and C:

$$E_n^j = \left\langle {}^{j}_{mn} \middle| H_{\text{sym.}} \middle| {}^{j}_{mn} \right\rangle = j(j+1)\hbar^2 B + n^2\hbar^2(C - B). \tag{5.5.52}$$

For the prolate rotor the constant $(C - B)$ is positive and so the high-$|n|$ levels have higher energy, as shown in the left-hand central column of Figure 5.5.7. The levels for $|n| = 0, 1, 2, 3, 4$ are labeled $\Sigma, \Pi, \Delta, \Phi, \Gamma, \ldots$ according to a tradition that grew out of atomic spectroscopy. In atomic spectroscopy, transitions to $j = 0, 1, 2, 3, 4$, are labeled $s, p, d, f, g, \ldots$, which stand for "sharp," "principal," "diffuse," "fine," "goodness-knows-what," etc. (Thereafter the labeling is alphabetical except that the letter j is deleted so as not to confuse it with the quantum number j.)

Note that the letters $\Sigma, \Pi, \Delta, \ldots$ appear as an alternative labeling for irreps of $C_{\infty v}$ symmetry in Eq. (5.2.4) and $D_{\infty h}$ symmetry in Figure 5.2.1. A prolate rotor has $D_{\infty h} \supset C_{\infty v}$ body symmetry and so it is appropriate to label its energy levels with the $C_{\infty v}$ irreps. In later discussions we will consider the inversion and reflection symmetry labels as well. For now we note that a rotor which is invariant to reflections through any plane containing its $\bar{z}$ axis must have degenerate $+n$ and $-n$ levels for $n \geq 1$.

An asymmetric rotor has a Hamiltonian of the form

$$\begin{aligned} H_{\text{asym.}} &= J_{\bar{x}}^2/2I_{\bar{x}} + J_{\bar{y}}^2/2I_{\bar{x}} + J_{\bar{z}}^2/2I_{\bar{z}} \\ &= AJ_{\bar{x}}^2 + BJ_{\bar{y}}^2 + CJ_{\bar{z}}^2. \end{aligned} \tag{5.5.53}$$

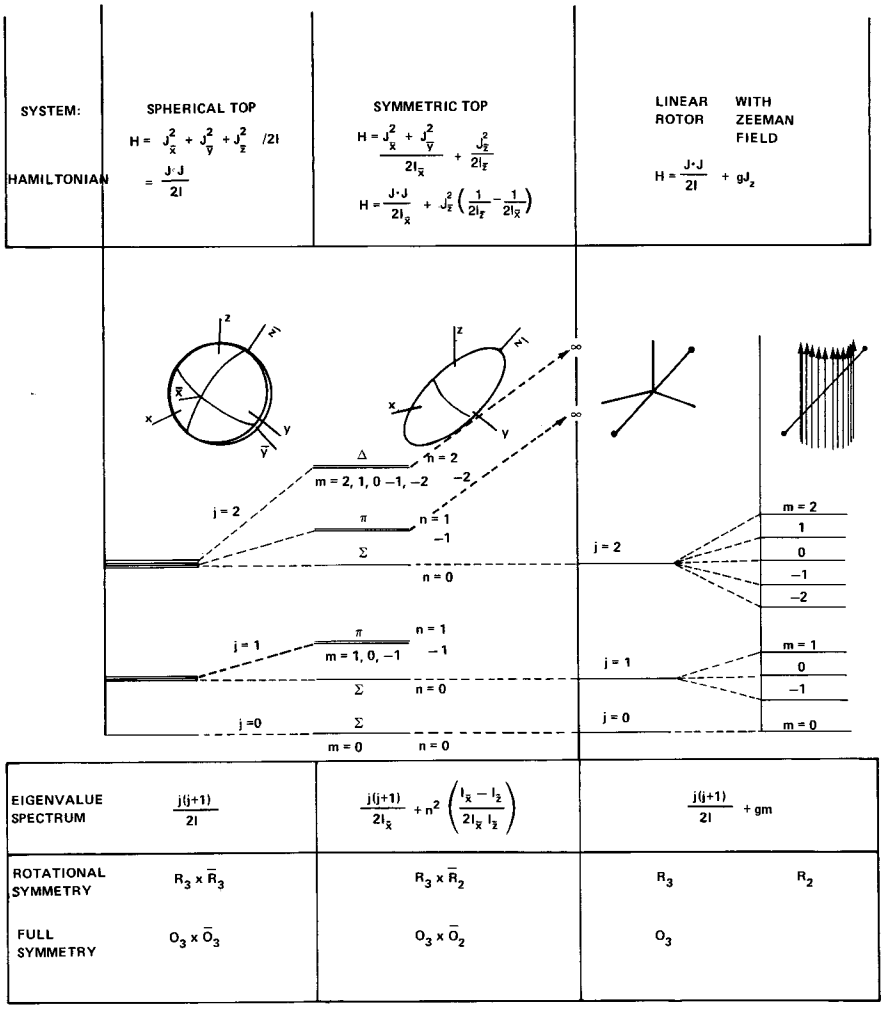

Figure 5.5.7 Hamiltonians, energy levels, and symmetry groups of various quantum rotor systems.

Each j level of the spherical rotor for $j > 0$ is degenerate with a degeneracy of $(2j + 1)^2$. In elementary quantum theory one learns that atomic levels of angular momentum j have degeneracy $(2j + 1)$ corresponding to $(2j + 1)$ states $\left|\begin{matrix} j \\ m \end{matrix}\right\rangle$ for each magnetic quantum number $m = j, j - 1, \ldots, -j + 1$, and $-j$. For the quantum rotor the z component m ranges over the same values. However, for each m value there are $(2j + 1)$ more n values $n = j, j - 1, \ldots, -j$ of the body $\bar{z}$ component. This gives a total degeneracy of

For this the body symmetry is reduced to D_2 or D_{2h}, i.e., 180° rotation reflections around the $\bar{x}$, $\bar{y}$, and $\bar{z}$ body axes. This symmetry is Abelian and has only one-dimensional irreps. Therefore no degeneracy between states belonging to different body labeling can be expected. The representations of $H_{\text{asym.}}$ in the $\left|\begin{matrix} j \\ mn \end{matrix}\right\rangle$ basis is found using Eq. (5.5.45):

$$\begin{aligned} H_{\text{asym.}}&\left|\begin{matrix} j \\ mn \end{matrix}\right\rangle \\ &= \hbar^2\left[\left(\frac{A+B}{2}\right)(j(j+1)-n^2)+Cn^2\right]\left|\begin{matrix} j \\ mn \end{matrix}\right\rangle \\ &\quad + \hbar^2\left(\frac{A-B}{4}\right)[(j+n+1)(j+n+2)(j-n)(j-n-1)]^{1/2}\left|\begin{matrix} j \\ m\,n+2 \end{matrix}\right\rangle \\ &\quad + \hbar^2\left(\frac{A-B}{4}\right)[(j+n)(j+n-1)(j-n+1)(j-n+2)]^{1/2}\left|\begin{matrix} j \\ m\,n-2 \end{matrix}\right\rangle. \end{aligned} \tag{5.5.54}$$

Clearly, eigenvector combinations of $\left|\begin{matrix} j \\ mn \end{matrix}\right\rangle$ for fixed m and various $n, n \pm 2$, $n \pm 4, \ldots$ are needed to diagonalize $\langle H_{\text{asym.}}\rangle$. This problem will be discussed in later chapters. Note, however, that the components of $\langle H_{\text{asym.}}\rangle$ reproduce those of $\langle H_{\text{sym.}}\rangle$ for $A = B$ and $\langle H_{\text{sph.}}\rangle$ for $A = B = C$.

So far we have seen what happens when the body symmetry is reduced from spherical R_3 symmetry to $R_2 = C_\infty$ symmetry of the cylindrical rotor (if we count reflections, then $H_{\text{sym.}}$ has $O_2 \sim C_{\infty v}$ symmetry), and finally to a finite D_2 symmetry. The n degeneracy becomes more and more split until finally there is none. However, we have not yet reduced the lab symmetry and until we do, the $(2j+1)$-fold m-degeneracy will remain for each (j, n) level. Body-based operators $J_{\bar{x}}$, $J_{\bar{y}}$, and $J_{\bar{z}}$ have no effect on the m labels. A simple example of the effect of a lab-based operator is the Hamiltonian

$$H_Z = B(J)^2 + gJ_z. \tag{5.5.55}$$

The perturbation gJ_z is a simplified model for the ZEEMAN effect on a rotor of an external uniform magnetic field along the z axis of the laboratory. The constant g is called the gyromagnetic ratio for the rotor. The level spectrum of the Zeeman Hamiltonian is given by

$$E_m^j = \left\langle \begin{matrix} j \\ mn \end{matrix}\middle| H_z \middle| \begin{matrix} j \\ mn \end{matrix}\right\rangle = Bj(j+1)\hbar^2 + gm\hbar. \tag{5.5.56}$$

Each j level gets split into $2j+1$ parts as shown in Figure 5.5.7 on the right-hand side. The magnetic field reduces the lab symmetry from spherical R_3 symmetry of a vacuum to $R_2 = C_\infty$ symmetry of the field axis. The magnetic quantum numbers m are R_2 irrep labels for the split levels.

A more symmetric example of a lab-based perturbation is given by

$$H_S + B(J)^2 + \mu J_z^2. \tag{5.5.57}$$

Here μJ_z^2 is a very simplified model for a STARK effect on a rotor of an external uniform electric field along the z axis. An electric field has a higher $C_{\infty v} \sim O_2$ symmetry since reflections through any plane parallel to the E field leaves it unchanged. Hence a degeneracy between $\pm m$ levels will exist in the level spectrum:

$$E^j_{|m|} = \left\langle \begin{matrix} j \\ mn \end{matrix} \middle| H_S \middle| \begin{matrix} j \\ mn \end{matrix} \right\rangle = Bj(j+1)\hbar^2 + \mu m^2 \hbar^2. \tag{5.5.58}$$

Hamiltonian H_S is the laboratory analogy for the body Hamiltonian $H_{\text{sym.}}$ of the symmetric rotor. H_S reduces the lab symmetry from R_3 to R_2, while the other reduces the body symmetry in the same way. You may realize now that there are two sides to any quantum rotor story: an inside and an outside. Two commuting sets of symmetry operators will exist for each rotor Hamiltonian H. The first set will be a subgroup $M^{\text{LAB}} \subset O_3^{\text{LAB}}$ of lab operators $\{\cdots R(\alpha\beta\gamma), \ldots, IR(\alpha\beta\gamma), \ldots\}$, which commute with H. The nature of subgroup M^{LAB} will depend on the laboratory situation and the symmetry or shape of the external fields being applied. The second set will be a subgroup $\overline{N}^{\text{BODY}} \subset \overline{O}_3^{\text{BODY}}$ of body operators $\{\ldots \overline{R}(\alpha\beta\gamma), \ldots, I\overline{R}(\alpha\beta\gamma), \ldots\}$, which commute with H. The nature of $\overline{N}^{\text{BODY}}$ depends on molecular structure and the internal symmetry or shape of the rotor. The whole rotor symmetry may be written

$$G^{\text{ROTOR}} = M^{\text{LAB}} \times \overline{N}^{\text{BODY}}, \tag{5.5.59}$$

since the two subgroups M and $\overline{N}$ are independent and mutually commuting. For example, a spherical rotor in a field-free laboratory environment is said to have $O_3 \times \overline{O}_3$ symmetry, while symmetric and asymmetric rotors have $O_3 \times \overline{O}_2$ and $O_3 \times \overline{D}_2$ symmetry, respectively, in the same environment. In the presence of a laboratory electric field the spherical rotor has $O_2 \times \overline{O}_3$ symmetry, while the symmetric and asymmetric rotors have $O_2 \times \overline{O}_2$ and $O_2 \times \overline{D}_2$ symmetry, respectively. In later chapters we will consider tetrahedral rotors in free space of symmetry $O_3 \times \overline{T}_d$ as well as rotors in various external fields with symmetry $O_2 \times \overline{T}_d$, $R_2 \times \overline{T}_d$, $D_2 \times \overline{T}_d$, and so forth. Any of some thousand combinations $(M \times \overline{N})$ of point groups are possible rotor symmetries which are subgroups of $O_3 \times \overline{O}_3$. (With just the crystal point symmetries there are $32^2 = 1024$ different combinations.) The problem of correlating R_3 and O_3 irreps with point symmetry subgroups is treated in Section 5.6.

D. Spherical Harmonics and Rotational Wave Functions

Some quantum rotors have a very simple internal structure. An orbiting electron is one example. A rotating diatomic molecule is another. For each of these examples a single vector $\bar{z}$ determines the orientation of the body. The radius vector $\mathbf{r}$ for the electron or the internuclear position vector $\mathbf{r}_1 - \mathbf{r}_2$ for a linear molecular rotor define the rotational position of these bodies. The position vectors have polar coordinates of azimuth (ϕ) and polar angle (θ) which can be identified with the first two Euler angles, respectively.

$$\alpha = \phi, \qquad \beta = \theta. \tag{5.5.60}$$

The third Euler angle (γ) is superfluous since a rotation $\bar{R}(00\gamma)$ of a vector around its own direction should have no effect. Here we ignore any internal structure of the nuclei or the electron whose positions are defined by a $\bar{z}$ vector. The particles are imagined to be points.

These arguments lead to a LOCAL SYMMETRY condition for pointlike rotors:

$$R(00\gamma)|000\rangle = |000\rangle \tag{5.5.61}$$

This condition is analogous to similar conditions discussed in Chapter 4. It leads to the conclusion that

$$\left|\begin{matrix} j \\ mn \end{matrix}\right\rangle = P^j_{mn}|000\rangle/(2j+1)^{1/2} \tag{5.5.62}$$

will vanish for linear rotors unless $n = 0$. By substituting the condition into the projection we derive

$$\begin{aligned}\left|\begin{matrix} j \\ mn \end{matrix}\right\rangle &= P^j_{mn}R(00\gamma)|000\rangle/(2j+1)^{1/2} \\ &= e^{-in\gamma}\left|\begin{matrix} j \\ mn \end{matrix}\right\rangle,\end{aligned} \tag{5.5.63}$$

which is true for all γ only if $n = 0$.

Note also that a linear rotor or orbiting electron has vanishing rotational inertia $I_{\bar{z}}$ around the radius $\bar{z}$ vector. The energy values (5.5.52) go to infinity for such a rotor for all nonzero n. On the right-hand side of Figure 5.5.7 only the $n = 0$ levels are drawn.

With $n = 0$ the $\mathscr{D}$ functions simplify considerably. Rewriting the central ($n = 0$) column of the $\mathscr{D}^{1*}$ and $\mathscr{D}^{2*}$ matrices using (5.4.33) and (5.4.35) yields the following:

$$\mathscr{D}^{1*}_{m,0}(\alpha\beta\gamma) = \begin{pmatrix} \cdot & -\dfrac{e^{+i\alpha}\sin\beta}{\sqrt{2}} & \cdot \\ \cdot & \cos\beta & \cdot \\ \cdot & \dfrac{e^{-i\alpha}\sin\beta}{\sqrt{2}} & \cdot \end{pmatrix} \begin{matrix} (m=1) \\ (m=0) \\ (m=-1) \end{matrix} \tag{5.5.64a}$$

$$\mathscr{D}^{2*}_{m,0}(\alpha\beta\gamma) = \begin{pmatrix} \cdot & \cdot & \sqrt{\dfrac{3}{8}}\,e^{+2i\alpha}\sin^2\beta & \cdot & \cdot \\ \cdot & \cdot & -\sqrt{\dfrac{3}{2}}\,e^{+i\alpha}\sin\beta\cos\beta & \cdot & \cdot \\ \cdot & \cdot & \dfrac{3\cos^2\beta - 1}{2} & \cdot & \cdot \\ \cdot & \cdot & \sqrt{\dfrac{3}{2}}\,e^{-i\alpha}\sin\beta\cos\beta & \cdot & \cdot \\ \cdot & \cdot & \sqrt{\dfrac{3}{8}}\,e^{-2i\alpha}\sin^2\beta & \cdot & \cdot \end{pmatrix} \begin{matrix} (m=2) \\ (m=1) \\ (m=0) \\ (m=-1) \\ (m=-2) \end{matrix} \tag{5.5.64b}$$

If you are familiar with the SPHERICAL HARMONICS Y^j_n from elementary quantum mechanics, then you will recognize them here. In fact they are special cases of the rotor wave functions for $n = 0$:

$$r^j_{m0}(\alpha\beta\gamma) = \mathscr{D}^{j*}_{m0}(\alpha\beta\gamma)(2j+1)^{1/2} = \sqrt{4\pi}\,Y^j_m(\beta\alpha). \tag{5.5.65}$$

Note that body quantum number n and the third Euler angle are not present in a linear rotor wave function.

It is important to summarize several of the roles which the $\mathscr{D}$ matrix functions play. For the physicist they are wave functions as stated in Eqs. (5.5.25) and (5.5.26):

$$\begin{aligned} r^j_{mn}(\alpha\beta\gamma) &= \mathscr{D}^{j*}_{mn}(\alpha\beta\gamma)(2j+1)^{1/2} = \langle 000|R^\dagger(\alpha\beta\gamma)\left|{}^{j}_{mn}\right\rangle \\ &= \langle \alpha\beta\gamma|^{j}_{mn}\rangle, \end{aligned} \tag{5.5.66}$$

but they are mainly rotation representations, i.e., the representation of a product $R^\dagger(\alpha\beta\gamma)R(\phi\theta\omega)$ is the product of the representations as stated here:

$$\mathscr{D}^j_{mn}(R^\dagger(\alpha\beta\gamma)R(\phi\theta\omega)) = \sum_{m'} \mathscr{D}^j_{mm'}(R^\dagger(\alpha\beta\gamma))\mathscr{D}^j_{m'n}(R(\phi\theta\omega)). \quad (5.5.67)$$

Taking the complex conjugate yields

$$\mathscr{D}^{j*}_{mn}(R^\dagger(\alpha\beta\gamma)R(\phi\theta\omega)) = \sum_{m'} \mathscr{D}^j_{m'm}(R(\alpha\beta\gamma))\mathscr{D}^{j*}_{m'n}(R(\phi\theta\omega)).$$

Using the notation of Eq. (5.5.66) one derives

$$\langle 000|R^\dagger(\phi\theta\omega)R(\alpha\beta\gamma)\Big|\begin{matrix} j \\ mn \end{matrix}\Big\rangle = \sum_{m'} \mathscr{D}^j_{m'm}(R(\alpha\beta\gamma))\langle 000|R^\dagger(\phi\theta\omega)\Big|\begin{matrix} j \\ m'n \end{matrix}\Big\rangle, \quad (5.5.68)$$

which simplifies to the following form:

$$\langle \phi\theta\omega|R(\alpha\beta\gamma)\Big|\begin{matrix} j \\ mn \end{matrix}\Big\rangle = \sum_{m'} \mathscr{D}^j_{m'm}(\alpha\beta\gamma)\Big\langle \phi\theta\omega\Big|\begin{matrix} j \\ m'n \end{matrix}\Big\rangle. \quad (5.5.69)$$

This agrees with the left transformation formula (5.5.31) if the bra $\langle\phi\theta\omega|$ is dropped.

A special case of this transformation formula for $n = 0$ involves the Y functions:

$$Y^{jR}_m(\theta\phi) = \sum_{m'} \mathscr{D}^j_{m'm}(\alpha\beta\gamma)Y^j_{m'}(\theta\phi). \quad (5.5.70a)$$

Here the function

$$Y^{jR}_m(\theta\phi) = \langle \phi\theta \cdot |R(\alpha\beta\gamma)\Big|\begin{matrix} j \\ m0 \end{matrix}\Big\rangle \quad (5.5.70b)$$

is a spherical harmonic wave function of a rotated state $R(\alpha\beta\gamma)\Big|\begin{matrix} j \\ m \end{matrix}\Big\rangle$. The rotated harmonic is schematically represented by lobes of a wave function centered on the $\{\bar{x}\bar{y}\bar{z}\}$ axes in Figure 5.5.8. The wave function Y^{jR}_m looks the same in the rotated $\{\bar{x}\bar{y}\bar{z}\}$ axes as Y^j_m looks in the lab axes $\{xyz\}$. Y^j_m is

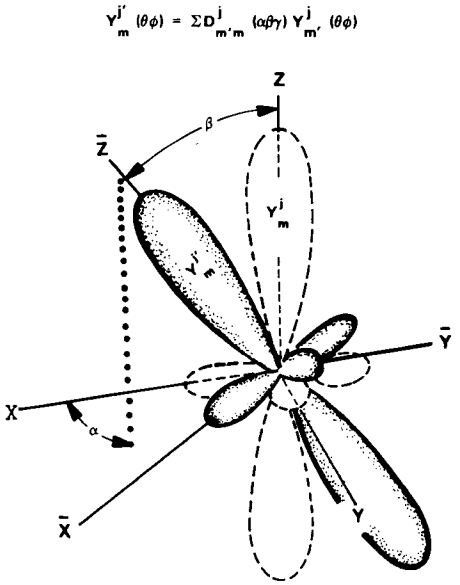

Figure 5.5.8 Transformation between rotated harmonic $Y^{j'}_m$ and unrotated wave functions. Lobes of the wave are represented by level surfaces: $Y^{j'}(\theta\phi)$ = constant.

sketched by dotted lines in the figure. The real or imaginary parts of $Y^j_m(\theta\phi)$ will have $2m$ lobes and $2m$ nodes in the interval $\{0 \leq \phi < 2\pi\}$. This can be derived from its z-rotation properties or by inspecting the standard formula:

$$Y^j_m(\theta\phi) = \left[\frac{(2j+1)(j-m)!}{4\pi(j+m)!}\right]^{1/2} (-1)^m e^{im\phi} P^m_j(\cos\theta). \quad (5.5.71)$$

The P^m_l are the well-known associated Legendre functions. The fact that $(2j+1)$ different functions $\{Y^j_j, Y^j_{j-1}, \ldots, Y^j_{-j}\}$ should combine in Eq. (5.5.70a) to make a rotated version is a wonderful thing indeed. The role of $\mathscr{D}$ functions as transformation coefficients for harmonics is important, and it is probably their best-known role.

If one sets $m = 0$ the resulting harmonic has no azimuthal dependence. Y^j_0 wave functions have cylindrical or azimuthal symmetry as schematized in Figure 5.5.9. Y^j_0 is a function only of its local polar angle θ,

$$Y^j_0(\theta\,\cdot) = \left(\frac{2j+1}{4\pi}\right)^{1/2} P^0_j(\cos\theta), \quad (5.5.72)$$

where $P^0_j(\cos\theta)$ is a standard Legendre function. The rotated harmonic Y^{jR} in Figure 5.5.9 is a function only of the polar angle Θ with respect to the

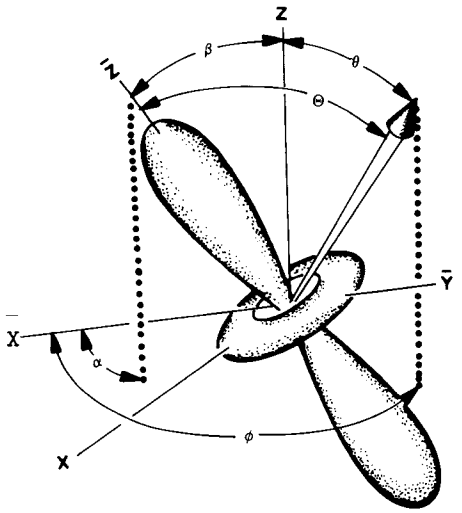

Figure 5.5.9 Azimuthally symmetric rotated harmonic $Y_0^{j'}$. Angles shown are used in the addition theorem.

tipped $\bar{z}$ axis. Substituting this into the Y transformation (5.5.70) yields

$$Y_0^{j^R}(\theta\phi) = \sum_m \mathscr{D}^j_{m0}(\alpha\beta\cdot)Y_m^j(\theta\phi), \tag{5.5.73}$$

$$\left(\frac{2j+1}{4\pi}\right)^{1/2} P_j^0(\cos\Theta) = \sum_m \left(\frac{4\pi}{2j+1}\right)^{1/2} Y_m^{j*}(\beta\alpha)Y_m^j(\theta\phi), \tag{5.5.74}$$

where Eq. (5.5.65) was used, also. This yields the very important ADDITION THEOREM

$$P_j(\cos\Theta) = \left(\frac{4\pi}{2j+1}\right) \sum_{m=-j}^{j} Y_m^{j*}(\beta\alpha)Y_m^j(\theta\phi) \tag{5.5.75}$$

for spherical harmonics. However, a better name for this might have been the *multiplication* theorem, since it follows directly from the R_3 group multiplication relation (5.5.67).

E. Explicit Relations for Rotation Operators and Generators

(a) Laboratory- and Body-Defined Polar Coordinates The Euler-angle device introduced in Figure 5.3.1 is redrawn in Figure 5.5.10 to include labeling which will aid in the discussion of explicit representations of coordinate rotations. The device consists of four rigid parts or frames, and each

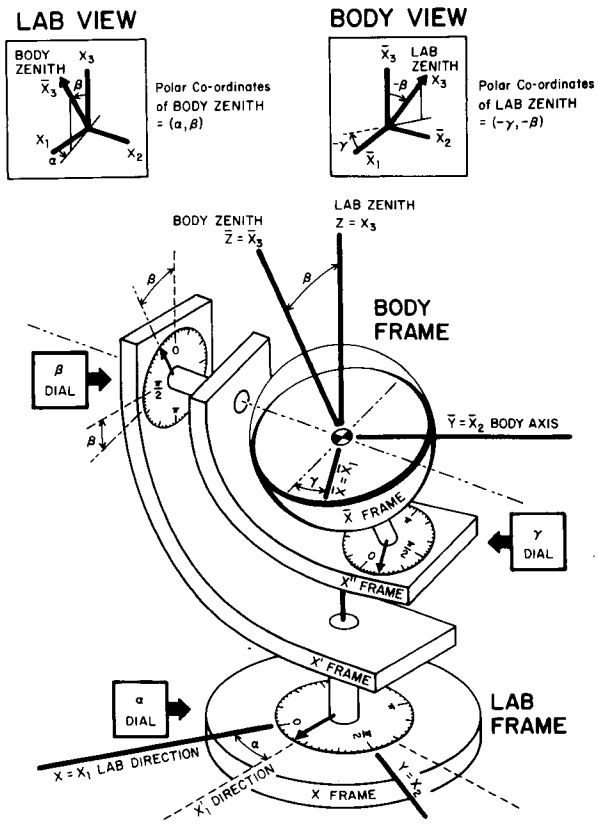

Figure 5.5.10 Mechanical definition of Euler coordinates for rotational mechanics. Laboratory and body views of the body and lab zeniths are shown in respective insets. (See also Figures 5.3.1 and 5.3.4.) [Reprinted from W. G. Harter and C. W. Patterson, *J. Chem. Phys.*, **80**, 4260 (1984).]

frame defines a coordinate axis and is supporting or supported by other frames. There is a lab $(x_1x_2x_3)$ frame supporting an $(x'_1x'_2x'_3)$ frame which in turn supports an $(x''_1x''_2x''_3)$ frame which finally supports the body $(\bar{x}_1\bar{x}_2\bar{x}_3)$ frame. Each of the frames is connected to its neighbor (or neighbors) in the sequence by pivots or bearings. Each bearing has an indicator and dial which displays one of the three Euler angles (α, β, γ). By defining Euler angles in this way one sees clearly that they are *holonomic* coordinates; that is, they depend only upon the relative orientation of the three frames and not upon the path or order of operations which yielded a given orientation.

The first two Euler angles (α, β) serve as polar coordinates for the body zenith or $\bar{x}_3$ axis in the lab frame as shown in the upper left-hand inset. The azimuth and polar angles of the lab zenith or x_3 axis in the body frame are

$(-\gamma)$ and $(-\beta)$, respectively, as indicated in the upper right-hand in set of Figure 5.5.10.

(b) Coordinate Rotation and Transformation Matrix As explained before Eq. (5.3.3), the setting of an Euler-defined position is accomplished by an ordered sequence of z, y, and z rotations. This sequence is indicated explicitly by Figure 5.5.11. The matrix representation of this sequence is given by the following:

$$\langle R(\alpha\beta\gamma)\rangle = \begin{pmatrix} \cos\alpha & -\sin\alpha & 0 \\ \sin\alpha & \cos\alpha & 0 \\ 0 & 0 & 1 \end{pmatrix} \begin{pmatrix} \cos\beta & 0 & \sin\beta \\ 0 & 1 & 0 \\ -\sin\beta & 0 & \cos\beta \end{pmatrix} \begin{pmatrix} \cos\gamma & -\sin\gamma & 0 \\ \sin\gamma & \cos\gamma & 0 \\ 0 & 0 & 1 \end{pmatrix},$$

$$= \begin{array}{c} \\ x_1 \\ x_2 \\ x_3 \end{array} \begin{array}{c} \begin{array}{ccc} \bar{x}_1 & \bar{x}_2 & \bar{x}_3 \end{array} \\ \begin{pmatrix} \cos\alpha\cos\beta\cos\gamma - \sin\alpha\sin\gamma & -\cos\alpha\cos\beta\sin\gamma - \sin\alpha\cos\gamma & \cos\alpha\sin\beta \\ \sin\alpha\cos\beta\cos\gamma + \cos\alpha\sin\gamma & -\sin\alpha\cos\beta\sin\gamma + \cos\alpha\cos\gamma & \sin\alpha\sin\beta \\ -\sin\beta\cos\gamma & \sin\beta\sin\gamma & \cos\beta \end{pmatrix} \end{array}. \tag{5.5.76}$$

Note that the $|\bar{x}_3\rangle$ ket or third column of (5.5.76) is the polar coordinate representation of the body zenith, as it should be. Similarly, the $\langle x_3|$ bra or third row of (5.5.76) is the representation of the lab zenith in the body frame where one could measure an azimuthal angle of $(-\gamma)$ and a polar angle $(-\beta)$ for the x_3 vector.

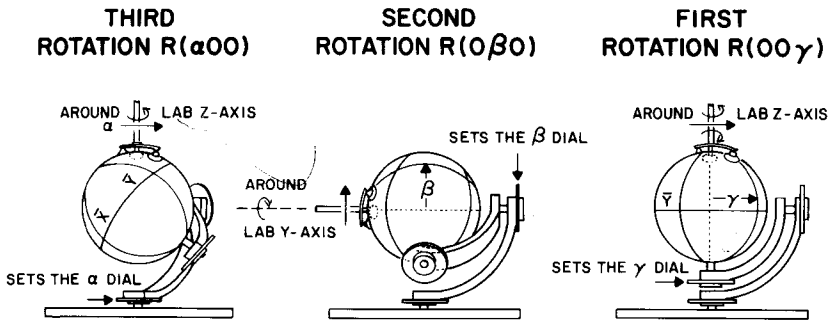

Figure 5.5.11 Operational definition of Euler coordinates. Ordered rotational sequence $R(\alpha 00)R(0\beta 0)R(00\gamma) = R(\alpha\beta\gamma)$ of lab-based operations orients the body into the $(\alpha\beta\gamma)$ position relative to the lab. Only rotations about the lab y and z axes are used. [Reprinted from W. G. Harter and C. W. Patterson *J. Chem. Phys.* **80** 4260 (1984).]

(c) Angular Velocity and Momentum in Laboratory and Body Frames

The angular velocity of the body frame relative to the laboratory may be expressed simply in terms of the angular velocities $\dot{\alpha}$, $\dot{\beta}$, and $\dot{\gamma}$ of the three dials in Figure 5.3.10. The rotation of each successive frame relative to its supporting frame depends simply upon the angular velocity of the bearing which connects them. For example, the time derivative $(d\mathbf{r}/dt)|_x$ of a vector in the lab (x) frame can be written in terms of the velocity $(d\mathbf{r}/dt)|_{x'}$ of the same vector observed in the (x') frame as follows:

$$\left.\frac{d\mathbf{r}}{dt}\right|_x = \left.\frac{d\mathbf{r}}{dt}\right|_{x'} + \boldsymbol{\omega}_\alpha \times \mathbf{r}, \tag{5.5.77a}$$

where the angular-velocity vector of the α dial is

$$\boldsymbol{\omega}_\alpha = \dot{\alpha}\mathbf{x}_3 = \dot{\alpha}\big(-\sin\beta\cos\gamma\bar{\mathbf{x}}_1 + \sin\beta\sin\gamma\bar{\mathbf{x}}_2 + \cos\beta\bar{\mathbf{x}}_3\big). \tag{5.5.77b}$$

This vector lies along the unit lab zenith $(\mathbf{x}_3)$ and is expressed in terms of the body axes using the third row of (5.5.76).

Similarly, the time derivative $(d\mathbf{r}/dt)|_{x'}$ in the (x') frame can be expressed in terms of the velocity $(d\mathbf{r}/dt)|_{x''}$ which would be observed in the (x'') frame by

$$\left.\frac{d\mathbf{r}}{dt}\right|_{x'} = \left.\frac{d\mathbf{r}}{dt}\right|_{x''} + \boldsymbol{\omega}_\beta \times \mathbf{r}, \tag{5.5.78a}$$

since these two frames are connected by the β axis which lies along the vector

$$\boldsymbol{\omega}_\beta = \dot{\beta}(-\sin\alpha\mathbf{x}_1 + \cos\alpha\mathbf{x}_2) = \dot{\beta}\big(\sin\gamma\bar{\mathbf{x}}_1 + \cos\gamma\bar{\mathbf{x}}_2\big). \tag{5.5.78b}$$

This is seen by inspecting Figure 5.5.10. Finally, the desired expression for the body frame observed velocity $(d\mathbf{r}/dt)|_{\bar{x}}$ is given in terms of $(d\mathbf{r}/dt)|_{x''}$ by

$$\left.\frac{d\mathbf{r}}{dt}\right|_{x''} = \left.\frac{d\mathbf{r}}{dt}\right|_{\bar{x}} + \boldsymbol{\omega}_\gamma \times \mathbf{r}, \tag{5.5.79a}$$

where the γ dial angular velocity vector is along the unit body zenith $\bar{\mathbf{x}}_3$:

$$\boldsymbol{\omega}_\gamma = \dot{\gamma}(\cos\alpha\sin\beta\mathbf{x}_1 + \sin\alpha\sin\beta\mathbf{x}_2 + \cos\beta\mathbf{x}_3) = \dot{\gamma}\bar{\mathbf{x}}_3. \tag{5.5.79b}$$

A combination of the preceding three relations yields lab-body velocity relations of the form

$$\left.\frac{d\mathbf{r}}{dt}\right|_x = \left.\frac{d\mathbf{r}}{dt}\right|_{\bar{x}} + \boldsymbol{\omega} \times \mathbf{r}, \tag{5.5.80a}$$

where the total angular velocity

$$\boldsymbol{\omega} = \boldsymbol{\omega}_\alpha + \boldsymbol{\omega}_\beta + \boldsymbol{\omega}_\gamma \tag{5.5.80b}$$

is a vector sum of those for the three dials. Taking the lab expressions for (5.5.77)–(5.5.79b) we derive the following matrix equation and its inverse:

$$\begin{pmatrix} \omega_x \\ \omega_y \\ \omega_z \end{pmatrix} = \begin{pmatrix} 0 & -\sin\alpha & \cos\alpha \sin\beta \\ 0 & \cos\alpha & \sin\alpha \sin\beta \\ 1 & 0 & \cos\beta \end{pmatrix} \begin{pmatrix} \dot{\alpha} \\ \dot{\beta} \\ \dot{\gamma} \end{pmatrix}, \tag{5.5.81a}$$

$$\begin{pmatrix} \dot{\alpha} \\ \dot{\beta} \\ \dot{\gamma} \end{pmatrix} = \begin{pmatrix} -\cos\alpha \cot\beta & -\sin\alpha \cot\beta & 1 \\ -\sin\alpha & \cos\alpha & 0 \\ \cos\alpha/\sin\beta & \sin\alpha/\sin\beta & 0 \end{pmatrix} \begin{pmatrix} \omega_x \\ \omega_y \\ \omega_z \end{pmatrix}. \tag{5.5.81b}$$

If the body expressions are used instead then one derives the following:

$$\begin{pmatrix} \omega_{\bar{x}} \\ \omega_{\bar{y}} \\ \omega_{\bar{z}} \end{pmatrix} = \begin{pmatrix} -\sin\beta \cos\gamma & \sin\gamma & 0 \\ \sin\beta \sin\gamma & \cos\gamma & 0 \\ \cos\beta & 0 & 1 \end{pmatrix} \begin{pmatrix} \dot{\alpha} \\ \dot{\beta} \\ \dot{\gamma} \end{pmatrix}, \tag{5.5.82a}$$

$$\begin{pmatrix} \dot{\alpha} \\ \dot{\beta} \\ \dot{\gamma} \end{pmatrix} = \begin{pmatrix} -\cos\gamma/\sin\beta & \sin\gamma/\sin\beta & 0 \\ \sin\gamma & \cos\gamma & 0 \\ \cot\beta \cos\gamma & -\cot\beta \sin\gamma & 1 \end{pmatrix} \begin{pmatrix} \omega_{\bar{x}} \\ \omega_{\bar{y}} \\ \omega_{\bar{z}} \end{pmatrix}. \tag{5.5.82b}$$

The coefficients in these matrix relations are useful for relating the lab-based angular momenta $\{J_x = \partial L/\partial\omega_x,\ J_y = \partial L/\partial\omega_y,\ J_z = \partial L/\partial\omega_z\}$ to the body-based momenta $\{J_{\bar{x}} = \partial L/\partial\omega_{\bar{x}},\ J_{\bar{y}} = \partial L/\partial\omega_{\bar{y}},\ J_{\bar{z}} = \partial L/\partial\omega_{\bar{z}}\}$, where L is a given classical Lagrangian. The connection is made through the quantities $\{J_\alpha = \partial L/\partial\dot{\alpha},\ J_\beta = \partial L/\partial\beta,\ J_\gamma = \partial L/\partial\dot{\gamma}\}$, which are the Euler canonical momenta, and one uses the chain rule

$$J_m = \frac{\partial L}{\partial \omega_m} = \frac{\partial L}{\partial \dot{\alpha}} \frac{\partial \dot{\alpha}}{\partial \omega_m} + \frac{\partial L}{\partial \dot{\beta}} \frac{\partial \dot{\beta}}{\partial \omega_m} + \frac{\partial L}{\partial \dot{\gamma}} \frac{\partial \dot{\gamma}}{\partial \omega_m} = \frac{\partial \dot{\alpha}}{\partial \omega_m} J_\alpha + \frac{\partial \dot{\beta}}{\partial \omega_m} J_\beta + \frac{\partial \dot{\gamma}}{\partial \omega_m} J_\gamma.$$

Using (5.5.81)–(5.5.82b) then gives lab and body-based momentum in terms

of Euler angles:

$$\begin{pmatrix} J_x \\ J_y \\ J_z \end{pmatrix} = \begin{pmatrix} -\cos\alpha\cot\beta & -\sin\alpha & \dfrac{\cos\alpha}{\sin\beta} \\ -\sin\alpha\cot\beta & \cos\alpha & \dfrac{\sin\alpha}{\sin\beta} \\ 1 & 0 & 0 \end{pmatrix} \begin{pmatrix} J_\alpha \\ J_\beta \\ J_\gamma \end{pmatrix}, \tag{5.5.83a}$$

$$\begin{pmatrix} J_{\bar{x}} \\ J_{\bar{y}} \\ J_{\bar{z}} \end{pmatrix} = \begin{pmatrix} -\dfrac{\cos\gamma}{\sin\beta} & \sin\gamma & \cot\beta\cos\gamma \\ \dfrac{\sin\gamma}{\sin\beta} & \cos\gamma & -\cot\beta\sin\gamma \\ 0 & 0 & 1 \end{pmatrix} \begin{pmatrix} J_\alpha \\ J_\beta \\ J_\gamma \end{pmatrix}. \tag{5.5.83b}$$

These relations become quantum operators if one represents the Euler operators by

$$J_\alpha = (h/i)\frac{\partial}{\partial\alpha}, \qquad J_\beta = (h/i)\frac{\partial}{\partial\beta}, \qquad J_\gamma = (h/i)\frac{\partial}{\partial\gamma}. \tag{5.5.84}$$

These are consistent with commutation relations

$$\begin{aligned} &[J_x, J_y] = ihJ_z \text{ (and cyclically)}, && [J_\alpha, J_\beta] \equiv 0, \text{ etc.}, \\ &[J_{\bar{x}}, J_{\bar{y}}] = -ihJ_{\bar{z}} \text{ (and cyclically)}, && [J_{\bar{x}}, J_y] \equiv 0, \text{ etc.}, \end{aligned} \tag{5.5.85}$$

which we deduced using coordinate-free arguments. One should note that the coordinates conjugate to J_x, J_y, or J_z are nonholonomic; the $d\omega_m$ are not exact differentials. Their values depend upon the rotational path history followed by the rotor to a given orientation. Euler angles depend on only the orientation.

5.6 ROTATIONAL LEVEL SPLITTING IN FINITE SYMMETRY

Consider a rotating diatomic molecule or an orbiting electron in one of the angular-momentum states $|^l_m\rangle$ belonging to a $2l + 1$-degenerate energy level ε_l. The transformation properties of these states are defined by irreps $\mathscr{D}^l$ of symmetry group R_3 or by $\mathscr{D}^{l\pm}$ of group O_3 according to the usual transformation equations:

$$R|^l_m\rangle = \sum_{m'} \mathscr{D}^l_{m'm}(R)|^l_{m'}\rangle.$$

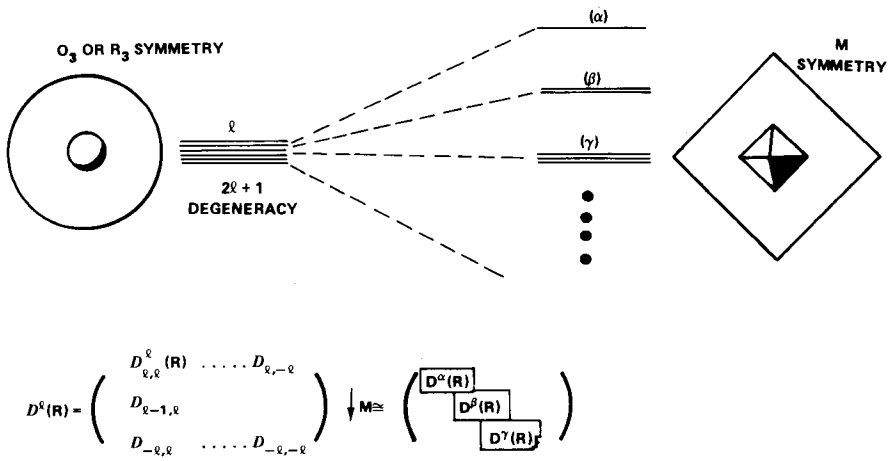

Figure 5.6.1 Molecular or crystal field splitting. l-orbital level splitting due to symmetry reduction from $O_3 \supset R_3$ to lower symmetry M corresponds to the reduction of the subduced representation $D^l \downarrow M$.

Suppose now this system is put into a lower-symmetry environment such as a crystal lattice or molecular site, where the symmetry is described by some finite group M. As a result, the energy levels will then belong to irreps $\mathscr{D}^{\alpha}, \mathscr{D}^{\beta}, \ldots$ of the new symmetry M. The corresponding degeneracies $l^{\alpha}, l^{\beta}, \ldots$ will generally be less than the free-orbital degeneracies $(2l + 1)$. Some of the orbital levels must split, as shown in Figure 5.6.1. This effect is often called CRYSTAL FIELD SPLITTING, and was first analyzed extensively by Bethe [1929].

We now see ways to determine which irreps $\mathscr{D}^{\alpha}$ of a symmetry M are correlated with a given irrep of O_3. We also discuss types of potential fields that cause splitting and show ways to obtain approximate eigenstates of them under certain conditions. These results will be used later to derive various model formulas for rotational spectra.

Of all the finite symmetries discussed in Chapters 2–4, we will treat the higher ones in each chain first, namely, O_h and D_{6h}. The properties of the others then follow relatively easily from the subgroup chain correlations.

A. Cubic Symmetry Correlations $O_3 \supset O_h$

The O_h character table was given in Eq. (4.1.16). To determine the orbital splittings, we will use these characters to find the frequencies f^{α} of O_h irrep $\mathscr{D}^{\alpha}$ in a given irrep $\mathscr{D}^{l}$ of O_3. The formula for f^{α},

$$f^{\alpha} = (1/{}^{o}G) \sum_{\substack{\text{classes} \\ c_g}} \chi_g^{\alpha *} {}^{o}c_g \,\text{Trace}\, \mathscr{D}^{l}(g) \tag{5.6.1}$$

was given in Eq. (3.5.11). We shall apply this formula to the octahedral subgroup O of $O_h = O \times C_i$ and R_3 of $O_3 = R_3 \times C_i$. It is easy to determine the inversion parity (u or g) separately. For O we know the characters x_g^α [see upper left quadrant of Eq. (4.1.16)], the order of the classes ${}^\circ c_g$ (from Figure 4.1.2, we have ${}^\circ c_1 = 1$, ${}^\circ c_{120^\circ} = 8$, ${}^\circ c_{180^\circ} = 3$, ${}^\circ c_{90^\circ} = 6$, and ${}^\circ c_{180^{\circ\prime}} = 6$) and the order of the group (${}^\circ G = 24$). We still need to find the trace of $\mathscr{D}^l$ for each rotation class.

To find the trace of an R_3 rotation by angle ω one picks the most convenient representation. The diagonal matrix

$$\mathscr{D}^l(\omega 00) = \begin{pmatrix} e^{-il\omega} & & & \\ & e^{-i(l-1)\omega} & & \\ & & \ddots & \\ & & & e^{il\omega} \end{pmatrix} \tag{5.6.2}$$

represents rotation $R(\omega 00)$ around the z axis. Any rotation $R[\omega]$ by the same angle ω around any axis $\hat{r}(\theta\phi)$ must be equivalent to $R(\omega 00)$.

$$R[\omega] = R(\phi\theta 0)R(\omega 00)R^{-1}(\theta\phi 0). \tag{5.6.3}$$

Therefore the traces of the representations must be equal.

The desired trace of Eq. (5.6.2) is evaluated by summing a geometrical series:

$$\text{Trace } \mathscr{D}^l(\omega 00) = e^{-il\omega} + e^{-i(l-1)\omega} + \cdots + e^{i(l-1)\omega} + e^{il\omega},$$

$$e^{-i\omega}\,\text{Trace } \mathscr{D}^l(\omega 00) = e^{-i(l+1)\omega} + e^{-il\omega} + e^{-i(l-1)\omega} + \cdots + e^{i(l-1)\omega}.$$

Subtracting the preceding two equations gives

$$(1 - e^{-i\omega})\text{Trace } \mathscr{D}^l(\omega 00) = e^{il\omega} - e^{-i(l+1)\omega}$$

or

$$\text{Trace } \mathscr{D}^l(\omega 00) = \frac{e^{-i\omega/2}(e^{i(l+1/2)\omega} - e^{-i(l+1/2)\omega})}{e^{-i\omega/2}(e^{i\omega/2} - e^{-i\omega/2})} = \frac{\sin(l + 1/2)\omega}{\sin \omega/2}. \tag{5.6.4}$$

From this formula one derives the trace table (5.6.5a). Substitution of each row in turn into Eq. (5.6.1) gives the correlation table (5.6.5b) of frequencies. Several examples of predicted crystal field splitting are shown in Figure 5.6.2.

	Trace $\mathscr{D}^l(\omega 00)$					Single Electron Orbital Spectroscopic Labeling
	$\omega = 0°$	$\omega = 120°$	$\omega = 180°$	$\omega = 90°$	$\omega = 180°$	
$l = 0$	1	1	1	1	1	s_g
1	3	0	−1	1	−1	P_u
2	5	−1	1	−1	1	d_g
3	7	1	−1	−1	−1	f_u
4	9	0	1	1	1	g_g
5	11	−1	−1	1	−1	h_u
6	13	1	1	−1	1	i_g
7	15	0	−1	−1	−1	k_u
8	17	−1	1	1	1	l_g
9	19	1	−1	1	−1	m_u
10	21	0	1	−1	1	n_g
11	23	−1	−1	−1	−1	o_u
12	25	1	1	1	1	q_g
13	27	0	−1	1	−1	r_u
14	29	−1	1	−1	1	t_g
15	31	1	−1	−1	−1	u_u
16	33	0	1	1	1	
17	35	−1	−1	1	−1	
18	37	1	1	−1	1	
19	39	0	−1	−1	−1	
20	41	−1	1	1	1	(5.6.5a)

	Frequency of O Irreps					
	f^{A_1}	f^{A_2}	f^E	f^{T_1}	f^{T_2}	
$l = 0$	1	·	·	·	·	A_{1g}
1	·	·	·	1	·	T_{1u}
2	·	·	1	·	1	$E_g + T_{2g}$
3	·	1	·	1	1	$A_{2u} + T_{1u} + T_{2u}$
4	1	·	1	1	1	$A_{1g} + E_g + T_{1g} + T_{2g}$
5	·	·	1	2	1	
6	1	1	1	1	2	
7	·	1	1	2	2	
8	1	·	2	2	2	
9	1	1	1	3	2	
10	1	1	2	2	3	
11	·	1	2	3	3	
12	2	1	2	3	3	
13	1	1	2	4	3	
14	1	1	3	3	4	
15	1	2	2	4	4	
16	2	1	3	4	4	
17	1	1	3	5	4	
18	2	2	3	4	5	
19	1	2	3	5	5	
20	2	1	4	5	5	(5.6.5b)

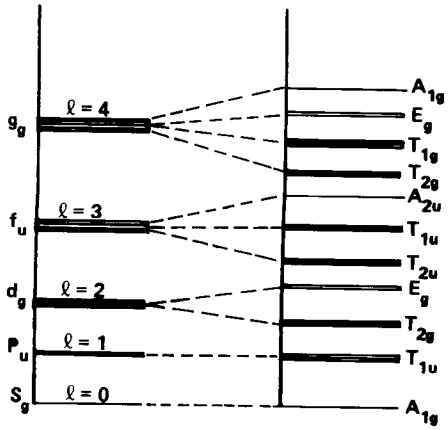

Figure 5.6.2 Octahedral splitting of s, p, d, f, and g orbitals.

The standard atomic notation $s, p, d, f, g, \ldots$ for orbital momentum $l = 0, 1, 2, 3, 4, \ldots$, respectively, is used. The inversion parities [g = even = $(+)$, u = odd = $(-)$] are assigned as they apply to one-electron (hydrogenlike) wave functions $Y_m^l(\theta\phi)$, namely, odd (even) l means odd (even) parity. However, the inversion parities for multielectronic orbitals or rotating molecules do not follow this rule, in general, as we will see later. In general, a given l may have either parity depending on the physical situation. Whichever it is, the O_h-irreps will have the same parity as their l "parent" in any $O_3 \supset O_h$ correlation.

Figure 5.6.2 is a sketch of the form, though not necessarily the order, of the O_h splittings of the lower l levels, as dictated by (5.6.5b). The convenience of the symmetry analysis which gives this so quickly should be evident. We shall see in Section 5.6.F how the ordering and spacing of the split levels can also be found easily under certain conditions.

Note that the table of (5.6.5a) for $l = 0$ repeats itself after $l = 12$. This is as far as one ever needs to calculate it. $\mathscr{D}^{12}$ contains the regular representation which has zero trace for $\omega = 0$ plus one scalar ($l = 0$ or A_{1g}) irrep whose trace is all 1. [See the first row in the table of (5.6.5a).] Therefore, the general result is

$$\mathscr{D}^l \downarrow 0 \sim [\text{integer of } l/12](\mathscr{D}^{A_1} \oplus \mathscr{D}^{A_2} \oplus 2\mathscr{D}^{E} \oplus 3\mathscr{D}^{T_1} \oplus 3\mathscr{D}^{T_2}) \oplus \mathscr{D}^{[l \bmod 12]}. \tag{5.6.6}$$

B. Cubic Eigenstates and Wave Functions

The cubic symmetry correlations (5.6.5b) indicate that a fivefold degenerate $l = 2$ level should split into a doubly degenerate E level and a triply degenerate T_2 level under the influence of O-symmetry forces. Let us

consider this example in some detail in order to understand its physical implications as well as some computational methods.

First one needs to find what combination of the five d-orbital eigenstates $\left\{\left|{2\atop 2}\right\rangle, \left|{2\atop 1}\right\rangle, \left|{2\atop 0}\right\rangle, \left|{2\atop -1}\right\rangle, \left|{2\atop -2}\right\rangle\right\}$ go together to make octahedral base states $\left\{\left|{E\atop 1}\right\rangle, \left|{E\atop 2}\right\rangle, \left|{T_2\atop 1}\right\rangle, \left|{T_1\atop 3}\right\rangle, \left|{T_2\atop 3}\right\rangle\right\}$. This is accomplished by applying appropriate octahedral projection operators P^{α}_{ij} to the orbital states:

$$\left|{E\atop e}\right\rangle = P^{E}_{ef}\left|{2\atop m}\right\rangle \Big/ (N^{E})^{1/2}, \qquad \left|{T_2\atop t}\right\rangle = P^{T_2}_{tu}\left|{2\atop m}\right\rangle \Big/ (N^{T})^{1/2}.$$

The projection factorization techniques discussed in Section 4.3.C help to simplify this projection.

Suppose the $|{l\atop m}\rangle$ states are defined with respect to the z axis which is an octahedral fourfold symmetry axis. Then the first state $|{2\atop 2}\rangle$ satisfies a local C_4 symmetry condition

$$\left|{2\atop 2}\right\rangle = P^{2_4}\left|{2\atop 2}\right\rangle = \tfrac{1}{4}(1 - R_3 + R_3^2 - R_3^3)\left|{2\atop 2}\right\rangle. \tag{5.6.7}$$

This calls for the tetragonal ($O \supset D_4 \supset C_4$) projectors P^{α}_{ij} of O, and only those for which $j = 2_4$. If you forget which components correlate with (2_4) you may construct the octahedral irreps of the local symmetry projector. We have

$$\mathscr{D}^{E}(P^{2_4}) = \begin{pmatrix} 0 & 0 \\ 0 & 1 \end{pmatrix}, \tag{5.6.8a}$$

$$\mathscr{D}^{T_2}(P^{2_4}) = \begin{pmatrix} 0 & 0 & 0 \\ 0 & 0 & 0 \\ 0 & 0 & 1 \end{pmatrix}, \tag{5.6.8b}$$

from Eq. (5.6.7), (4.2.19), and (4.2.14). (Note: We shall use the T_2 irreps which follow directly from the T_1 by sign change of R and i matrices.) The position of the unit in the matrices (5.6.8) signals that the second and third components of E and T_2, respectively, are the right ones. The desired eigenstates for E will be given by

$$P^{E}_{e2}\left|{2\atop 2}\right\rangle = \tfrac{1}{3}\sum_{R_l} \mathscr{D}^{E}_{e2}(R_l) R_l \left|{2\atop 2}\right\rangle, \tag{5.6.9a}$$

and for T_2 by

$$P^{T_2}_{t3}\left|{2\atop 2}\right\rangle = \tfrac{1}{2}\sum_{R_l} \mathscr{D}^{T_2}_{t3}(R_l) R_l \left|{2\atop 2}\right\rangle, \tag{5.6.9b}$$

where $\mathscr{D}^{\alpha}_{ij}(R_l)$ are octahedral irreps of coset leaders R_l and

$$R_l\left|\begin{matrix}2\\2\end{matrix}\right\rangle = \sum_m \mathscr{D}^2_{m2}(R_l(\alpha\beta\gamma))\left|\begin{matrix}2\\m\end{matrix}\right\rangle \tag{5.6.10}$$

depends on the R_3 $\mathscr{D}$ functions and the choice of R_l. Fortunately, there are only six cosets R_lC_4 of local subgroup $C_4 = (1, R_3, R_3^2, R_3^3)$. Hence, the sums over leaders R_l contain only six terms. Let us choose coset leaders $1 = R(000)$, $R_2^2 = R(0, \pi, 0)$, $R_1 = R(-\pi/2\pi/2\pi/2)$, $R_1^3 = R(-\pi/2 - \pi/2\pi/2)$, $R_2 = R(0, \pi/2, 0)$, and $R_2^3 = R(0, -\pi/2, 0)$. Each one of these leaders transforms a point on the local z axis onto one of the octahedral axes as explained in Section 4.3. The Euler angles $(\alpha\beta\gamma)$ are obtained by inspection of the octahedral operations in Figure 4.1.2 or by using axis-to-Euler conversion formulas (5.5.2). The representation components $\mathscr{D}^2_{m2}(\alpha\beta\gamma)$ for each of the leaders is written in the following using the $\mathscr{D}$ formula (5.4.21). Only the first column of the $\mathscr{D}$ matrix is required here. We use a single-parenthesis notation $\mathscr{D}(R = ($ to denote this.

$$\mathscr{D}^2_{0,2}(\alpha\beta\gamma = \begin{pmatrix} e^{-2i(\alpha+\gamma)}\left(\dfrac{1+\cos\beta}{2}\right)^2 \\ e^{-i(\alpha+2\gamma)}\left(\dfrac{1+\cos\beta}{2}\right)\sin\beta \\ e^{-2i\gamma}\sqrt{\dfrac{3}{8}}\sin^2\beta \\ e^{i(\alpha-2\gamma)}\left(\dfrac{1-\cos\beta}{2}\right)\sin\beta \\ e^{2i(\alpha-\gamma)}\left(\dfrac{1-\cos\beta}{2}\right)^2 \end{pmatrix},$$

$$\mathscr{D}^2(1 = \begin{pmatrix}1\\0\\0\\0\\0\end{pmatrix}, \quad \mathscr{D}^2(R_2^2 = \begin{pmatrix}0\\0\\0\\0\\1\end{pmatrix}, \quad \mathscr{D}^2(R_1 = \begin{pmatrix} 1/4 \\ -i/2 \\ -\sqrt{3/8} \\ i/2 \\ 1/4 \end{pmatrix},$$

$$\mathscr{D}(R_1^3 = \begin{pmatrix} 1/4 \\ i/2 \\ -\sqrt{3/8} \\ -i/2 \\ 1/4 \end{pmatrix}, \quad \mathscr{D}(R_2 = \begin{pmatrix} 1/4 \\ 1/2 \\ \sqrt{3/8} \\ 1/2 \\ 1/4 \end{pmatrix}, \quad \mathscr{D}(R_2^3 = \begin{pmatrix} 1/4 \\ -1/2 \\ \sqrt{3/8} \\ -1/2 \\ 1/4 \end{pmatrix}. \tag{5.6.11}$$

Substituting these into Eqs. (5.6.8)–(5.6.10) and using the T_2 octahedral irreps we find T_2 octahedral eigenstates:

$$\sum_R \mathscr{D}^{T_2}_{13}(R)\mathscr{D}^2(R = 0 + 0 + 0 + 0 - \begin{pmatrix} 1/4 \\ 1/2 \\ \sqrt{3/8} \\ 1/2 \\ 1/4 \end{pmatrix} + \begin{pmatrix} 1/4 \\ -1/2 \\ \sqrt{3/8} \\ -1/2 \\ 1/4 \end{pmatrix} = \begin{pmatrix} 0 \\ -1 \\ 0, \\ -1 \\ 0 \end{pmatrix}$$

$$\sum_R \mathscr{D}^{T_2}_{23}(R)\mathscr{D}^2(R = 0 + 0 + \begin{pmatrix} 1/4 \\ -i/2 \\ -\sqrt{3/8} \\ i/2 \\ 1/4 \end{pmatrix} - \begin{pmatrix} 1/4 \\ i/2 \\ -\sqrt{3/8} \\ -i/2 \\ 1/4 \end{pmatrix} + 0 + 0 = \begin{pmatrix} 0 \\ -i \\ 0, \\ i \\ 0 \end{pmatrix}$$

$$\sum_R \mathscr{D}^{T_2}_{33}(R)\mathscr{D}^2(R = \begin{pmatrix} 1 \\ 0 \\ 0 \\ 0 \\ 0 \end{pmatrix} - \begin{pmatrix} 0 \\ 0 \\ 0 \\ 0 \\ 1 \end{pmatrix} + 0 + 0 + 0 + 0 = \begin{pmatrix} 1 \\ 0 \\ 0. \\ 0 \\ 1 \end{pmatrix}$$

Finally we normalize T_2 column vectors and write them in terms of $\left|{}^{2}_{m}\right\rangle$ kets:

$$\begin{aligned} \left|{}^{T_2}_{1}\right\rangle &= \left(-\left|{}^{2}_{1}\right\rangle - \left|{}^{2}_{-1}\right\rangle\right)\Big/\sqrt{2}, \\ \left|{}^{T_2}_{2}\right\rangle &= \left(-i\left|{}^{2}_{1}\right\rangle + i\left|{}^{2}_{-1}\right\rangle\right)\Big/\sqrt{2}, \\ \left|{}^{T_2}_{3}\right\rangle &= \left(\left|{}^{2}_{2}\right\rangle - \left|{}^{2}_{-2}\right\rangle\right)\Big/\sqrt{2}. \end{aligned} \tag{5.6.12}$$

By applying the octahedral E irreps in the same way one obtains

$$\begin{aligned} \left|{}^{E}_{1}\right\rangle &= \left|{}^{2}_{0}\right\rangle, \\ \left|{}^{E}_{2}\right\rangle &= \left(\left|{}^{2}_{2}\right\rangle + \left|{}^{2}_{-2}\right\rangle\right)\Big/\sqrt{2}. \end{aligned} \tag{5.6.13}$$

It is instructive to examine the wave functions of the states (5.6.12) and (5.6.13) to see why their energy levels split and see the shape of the octahedral harmonics. The spherical harmonics $Y^l_m(\theta\phi)$ are functions of polar

angles or dimensionless Cartesian coordinates:

$$x/r = \cos\phi \sin\theta, \qquad y/r = \sin\phi \sin\theta, \qquad z/r = \cos\theta.$$

For example, the Y_m^2 functions are as follows:

$$\begin{aligned}
n_2\left\langle \theta\phi \middle| \begin{matrix} 2 \\ 2 \end{matrix} \right\rangle &= n_2 Y_2^2(\theta\phi) = (3/8)^{1/2} e^{2i\phi} \sin^2\theta = (3/8)^{1/2}(x+iy)^2/r^2, \\
n_2\left\langle \theta\phi \middle| \begin{matrix} 2 \\ 1 \end{matrix} \right\rangle &= n_2 Y_1^2 = -(3/2)^{1/2} e^{i\phi} \sin\theta\cos\theta = -(3/2)^{1/2}(x+iy)z/r^2, \\
n_2\left\langle \theta\phi \middle| \begin{matrix} 2 \\ 0 \end{matrix} \right\rangle &= n_2 Y_0^2 = (3\cos^2\theta - 1)/2 = (2z^2 - x^2 - y^2)/2r^2, \\
n_2\left\langle \theta\phi \middle| \begin{matrix} 2 \\ -1 \end{matrix} \right\rangle &= n_2 Y_{-1}^2 = (3/2)^{1/2} e^{-i\phi} \sin\theta\cos\theta = (3/2)^{1/2}(x-iy)z/r^2, \\
n_2\left\langle \theta\phi \middle| \begin{matrix} 2 \\ -2 \end{matrix} \right\rangle &= n_2 Y_{-2}^2 = (3/8)^{1/2} e^{-2i\phi} \sin^2\theta = (3/8)^{1/2}(x-iy)^2/r^2,
\end{aligned} \tag{5.6.14}$$

where a normalization factor $n_2 = (4\pi/5)^{1/2}$ is isolated. From Eqs. (5.6.12) and (5.6.13) the octahedral functions follows:

$$n_2\left\langle \theta\phi \middle| \begin{matrix} T_2 \\ 1 \end{matrix} \right\rangle = -n_2(Y_1^2 + Y_{-1}^2)/\sqrt{2} = (i\sqrt{3}/r^2)yz, \tag{5.6.15a}$$

$$n_2\left\langle \theta\phi \middle| \begin{matrix} T_2 \\ 2 \end{matrix} \right\rangle = n_2(-iY_1^2 + iY_{-1}^2)/\sqrt{2} = (i\sqrt{3}/r^2)xz, \tag{5.6.15b}$$

$$n_2\left\langle \theta\phi \middle| \begin{matrix} T_2 \\ 3 \end{matrix} \right\rangle = n_2(Y_2^2 - Y_{-2}^2)/\sqrt{2} = (i\sqrt{3}/r^2)xy, \tag{5.6.15c}$$

$$n_2\left\langle \theta\phi \middle| \begin{matrix} E \\ 1 \end{matrix} \right\rangle = n_2 Y_0^2 = (2z^2 - x^2 - y^2)/2r^2, \tag{5.6.15d}$$

$$n_2\left\langle \theta\phi \middle| \begin{matrix} E \\ 2 \end{matrix} \right\rangle = n_2(Y_2^2 + Y_{-2}^2)/\sqrt{2} = \sqrt{3}(x^2 - y^2)/2r^2. \tag{5.6.15e}$$

Two of the octahedral wave functions are sketched in Figure 5.6.3. The second E wave function ($\psi_2^E \sim x^2 - y^2$) is drawn adjacent to the higher-energy E-doublet level, while the third T_2 wave function ($\psi_3^{T_2} \sim xy$) is sketched below. The energy levels are the eigenvalues of the lowest-degree octahedrally symmetric Hamiltonian or potential

$$V^{(4)} = D(x^4 + y^4 + z^4 - \tfrac{3}{5}r^4). \tag{5.6.16}$$

The eigenvalues of $V^{(4)}$ and other operators will be computed in Chapter 7. However, it is easy to understand qualitatively why the states $\left|\begin{matrix} E \\ e \end{matrix}\right\rangle$ have higher-energy eigenvalues than those of states $\left|\begin{matrix} T_2 \\ t \end{matrix}\right\rangle$. If one plots the equipo-

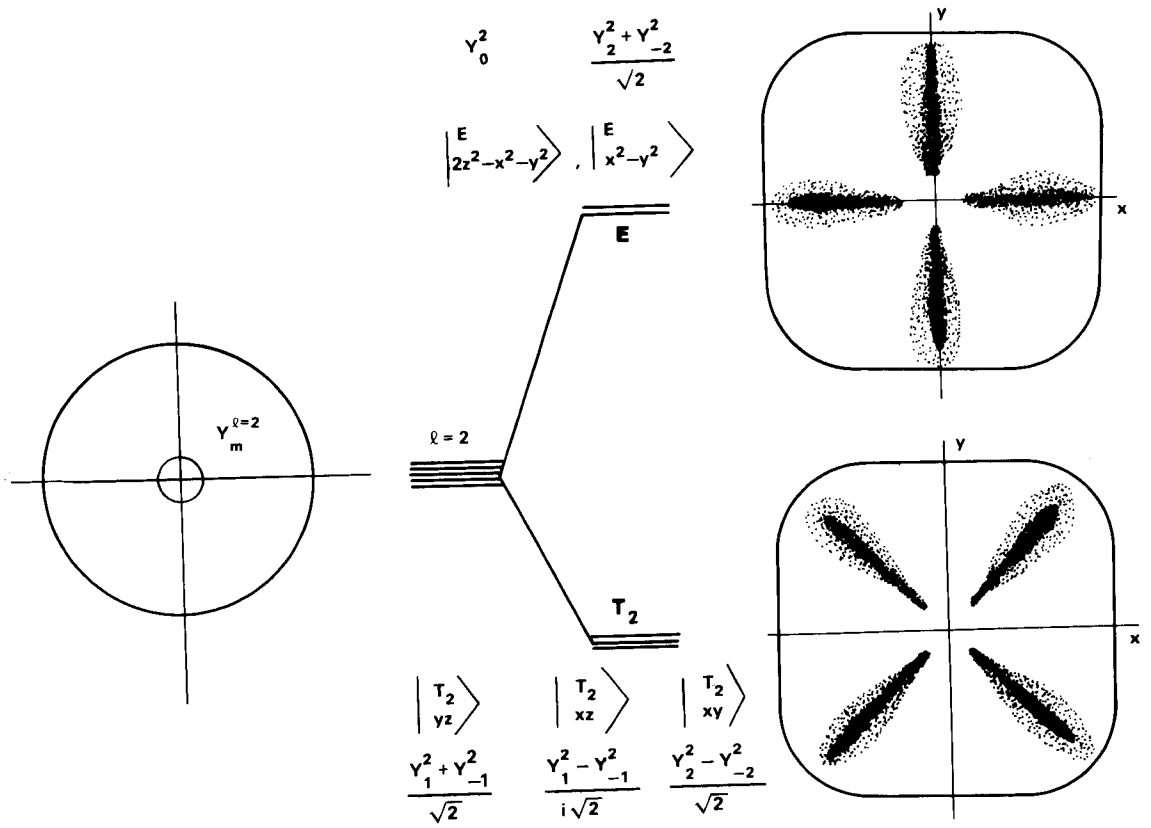

Figure 5.6.3 Detailed sketch of octahedral splitting of a d orbital. The wave functions $\left\langle \left|\begin{matrix}E\\2\end{matrix}\right\rangle \right.$ and $\left\langle \left|\begin{matrix}T_2\\3\end{matrix}\right\rangle \right.$ are sketched inside the equipotential contour $x^4 + y^4 =$ constant ($z = 0$).

tential surface $x^4 + y^4 + z^4 = 1$, then the xy contour assumes the supercircle shape of a rounded square as shown in Figure 5.6.3 (SUPERELLIPSE is the name given by the designer Piet Hein for any contour $x^n/a^n + y^n/b^n = 1$, where $n > 2$.) The T_2 waves avoid the higher potential regions by having their wave crest's lobes in the corners of the supercircle. The E waves have nodes near the T_2 crests and end up with their lobes pointing into the higher potential regions on the sides. We are studying here the generalization of the one-dimensional Bohr and Bloch waves and energy-band splitting. More discussion and examples will be given in Sections 5.6.D and 5.6.E.

C. Multipole Functions and Polynomials

Before continuing the discussion of waves and level splitting a short description of wave functions and polynomial classification will be given. Let us define the ELEMENTARY MULTIPOLE FUNCTIONS X_m by the following:

$$X_m^l \equiv \sqrt{\frac{4\pi}{2l+1}}\,(r)^l Y_m^l. \tag{5.6.17}$$

The factor $(r)^l$ converts Y_m^l into a polynomial in x, y, and z of degree l. The X_m^l are listed as explicit polynomials of x, y, and z for $l = 1$–4 in the O_3 table of Appendix F. In this table one observes $(2l + 1) = 1$, 3, 5, 7, and 9 new multipole functions appearing for each l. However, the corresponding number of independent lth-order monomials $x^a y^b z^c$ $(a + b + c = l)$ is generally greater: $(l + 1)(l + 2)/2 = 1$, 3, 6, 10, and 15. Note on the right of the table that each lth-order monomial is a combination of X^l and products $X^{l-2}(r^2)$, $X^{l-4}(r^4)$ of lower-order multipole functions with $r^2 = x^2 + y^2 + z^2$.

Suppose you want to find how many independent combinations of lth-order monomials $x^a y^b z^c$ or multipole functions X_m^l exist which transform according to a given irrep $\mathscr{D}^\alpha$ of a given symmetry such as O_h. This problem can be approached in a number of different ways.

One direct approach uses coupling coefficients to make G symmetry-defined polynomials. This will be done in Section 6.3.C and the results are listed in the tables of Appendix F for order four or less.

On the other hand, one may use $O_3 \supset G$ correlation tables such as Eq. (5.6.5b) to see how many independent functions of each type come up for each l. Let us compare these two accountings.

For example, we may make one new scalar (A_{1g}) function of fourth-order [see the $l = 4$ row and A_1 column of Eq. (5.6.5b)] and one zeroth-order polynomial [see the $l = 0$ row and A_1 column of Eq. (5.6.5b)] or a constant multiplied by r^4. This means that there are just two linearly independent A_g^1

polynomials of fourth order. Indeed, the O_h table lists

$$IV_{(1)}^{A_{1g}} = x^4 + y^4 + z^4 \quad \text{and} \quad IV_{(2)}^{A_{1g}} = x^2y^2 + x^2z^2 + y^2z^2 = \left(r^4 - IV_{(1)}^{A_{1g}}\right)/2; \qquad (5.6.18)$$

we have already encountered the first of these in Eq. (5.6.16).

Similarly, we may make two independent $(^{E_g}_1)$ polynomials or two independent $(^{E_g}_2)$ polynomials of fourth order. One set is new [see $l = 4$ row and E column of Eq. (5.6.5b)], and the other is a product of r^2 and the second-order polynomial [see $l = 2$ row and E column of Eq. (5.6.5b), which we derived in Eqs. (5.6.15d) and (5.6.15e)]. The E polynomials of fourth order in the O_h table of Appendix F are combinations of these two sets.

The relation between T_{1u} vector components (x, y, z) and $(l = 1)$ dipole functions

$$I_1^1 = -(x + iy)/\sqrt{2}, \qquad I_0^1 = z, \qquad I_{-1}^1 = (x - iy)/\sqrt{2} \qquad (5.6.19)$$

is particularly important. We have seen this sort of relation several times before when relating standing-wave and moving-wave states. The $(l = 1)$-orbital level does not split in the presence of octahedral symmetry. Note that there is just one set of fourth-order polynomials of the T_1 or T_{1g} type. [One should not make the mistake of counting functions which are products of $r = (x^2 + y^2 + z^2)^{1/2}$ or r^3 with third-order $(l = 3)$ or first-order $(l = 1)T_{1u}$ functions, since these are not polynomials.]

Some O_h irreps have to wait even longer before they appear in polynomial form. According to the table of (5.6.5b) the first odd-l A_1 (i.e., A_{1u}) polynomial is of *ninth* $(l = 9)$ order.

The even-l A_1 (i.e., A_{1g}) polynomials are more plentiful. Totally invariant A_{1g} polynomials will be very important for tensor operator theory, which is given in Chapters 6 and 7. There we will learn that the number $n^{A_{1g}}(2k)$ of scalars or invariants found between $l = 0$ and $l = 2k$ is related to the kth correlation frequencies $f^\alpha(\mathscr{D}^k \downarrow M)$ as follows:

$$n^{A_{1g}}(2k) = \sum_{\substack{M \text{ irreps} \\ \alpha}} f^\alpha(f^\alpha + 1)/2. \qquad (5.6.20)$$

For example, for angular momentum $k = 6$ we find the following number by summing over the seventh $(l = 6)$ row of the table of (5.6.5b):

$$n^{A_{1g}}(2k) = \sum_{\alpha = A_1, A_2, E, T_1, T_2} f^\alpha\left(\mathscr{D}^6 \downarrow O_h\right)\left(f^\alpha\left(\mathscr{D}^6 \downarrow O_h\right) + 1\right)/2 = 1 + 1 + 1 + 3 + 1 = 7 \qquad (5.6.21)$$

This agrees with the sum of frequencies in the A_1 column of (5.6.5b) from $(l = 0)$ to $(l = 12)$. (Do not count the A_{1u} at $l = 9$ since that is a pseudoinvariant.)

Finally, note that the number of scalar cubic polynomials of order $2l$ is simply the number of partitions of l into 1, 2, or 3 terms. For example, 6 can be written seven ways: 6, 5 + 1, 4 + 2, 4 + 1 + 1, 3 + 3, 3 + 2 + 1, and

$2 + 2 + 2$ corresponding to seven scalar polynomials

$$x^{12} + y^{12} + z^{12}, x^{10}y^2 + x^{10}z^2 + x^{10}z^2, x^8y^4 + x^8z^4 + y^8z^4,$$
$$x^8y^2z^2 + x^2y^8z^2 + x^2y^2z^8, x^6y^6 + \cdots, \text{etc.} \tag{5.6.22}$$

This last counting method is a little too special to be of direct use for other symmetries besides O_h.

D. Multipole Expansions

In Section 5.6.C the $(l = 2)$ eigenvectors of an octahedrally anisotropic potential $V^{(4)}$ were derived. A possible source of such a potential is drawn in Figure 5.6.4. There it is imagined that six point charges are brought in on the vertices of a crystal octahedron surrounding an orbiting electron. The electron is repelled by the charges. It finds the highest potential energy for a given radius r along the $\pm x$ (± 100), $\pm y$ (0 ± 10), and $\pm z$ (00 ± 1) axes where charges are sitting. It finds the lowest energy along the eight axes $(111), (-111), \ldots, (-1 - 1 - 1)$ in between.

To derive this anisotropic potential one needs to compute the following sum over the six charges:

$$\begin{aligned} V(r\theta\phi) &= \sum_{j=1}^{6} q_j/(|\mathbf{r}_j - \mathbf{r}|) \\ &= \sum_{j=1}^{6} q_j/\left[r_j^2 + r^2 - 2rr_j\cos\Theta_j\right]^{1/2} \\ &= \sum_{j=1}^{6} q_j/r_j\left[1 + (r/r_j)^2 - 2(r/r_j)\cos\Theta_j\right]^{1/2}, \end{aligned} \tag{5.6.23}$$

where Θ_j is the angle between the electronic radius r and radius r_j of charge q_j. (See Figure 5.6.4.) This can be rewritten using the Legendre generating function

$$1/(1 + h^2 - 2hz)^{1/2} = \sum_{l=0}^{\infty} h^l P_l(z) \tag{5.6.24}$$

and the addition theorem (5.5.75). The result is

$$\begin{aligned} V(r\theta\phi) &= \sum_j \sum_l q_j\left(r^l/r_j^{l+1}\right)P_l(\cos\Theta_j) \\ &= \sum_l \sum_{m=-l}^{l} y_m^l Y_m^l(\theta\phi) = \sum_l \sum_{m=-l}^{l} x_m^l X_m^l(\mathbf{r}_j), \end{aligned} \tag{5.6.25a}$$

where

$$x_m^l = (2l + 1/4\pi)^{1/2} y_m^l/r^l = \sum_j \left(q_j/r_j^{2l+1}\right)X_m^{l*}(\mathbf{r}_j) \tag{5.6.25b}$$

are constant coefficients which depend upon the charge locations. This is called the MULTIPOLE EXPANSION of a change distribution. Consider some examples for the charge octahedron with $r_j = R$ and $q_j = Q$. For $l = 0$

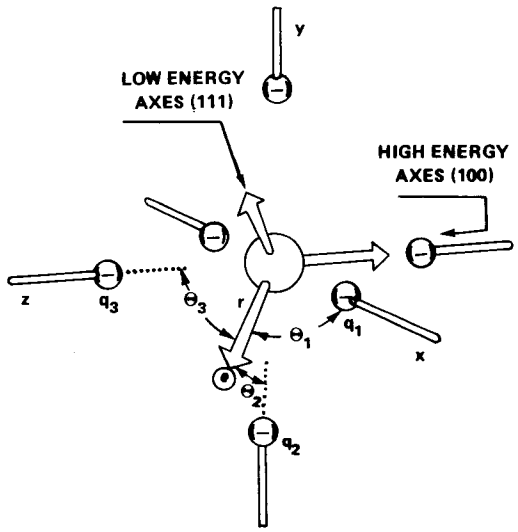

Figure 5.6.4 Octahedral arrangement of charge centers. Potential energy depends on the polar angles Θ_j between the electron and fixed charges on the octahedral axes $(\pm 1\ 0\ 0)$, $(0\ \pm 1\ 0)$, and $(0\ 0\ \pm 1)$. The least energy is had when the position vector $\mathbf{r}$ is farthest away from these axes.

we have

$$x_0^0 = (4\pi)^{1/2} 6Q/R. \tag{5.6.26}$$

For $l = 1$, 2, and 3 the sum (5.6.25b) contributes nothing. Indeed, the $O_h \subset O_3$ correlation (5.6.5b) has told us that the next octahedral invariant will be at $l = 4$. Using the X_m^4 functions in Appendix F we find only the following coefficients are nonzero:

$$\begin{aligned} x_0^4 &= (Q/8)(3R^4 + 3R^4 + 3R^4 + 3R^4 + 8R^4 + 8R^4) = (7Q/2)R^4, \\ x_4^4 = x_{-4}^4 &= Q(35/128)^{1/2}(R^4 + R^4 + R^4 + R^4 + 0 + 0) = (\sqrt{70}\,Q/4)R^4. \end{aligned} \tag{5.6.27}$$

Hence the octahedral multipole expansion has the form

$$\begin{aligned} V(r\theta\phi) &= (6Q/R) + (35Q/4R^5)\left[(2/\sqrt{70})(X_4^4 + X_{-4}^4) + \tfrac{2}{5}X_0^4\right] + \cdots \\ &= (6Q/R) + (35Q/4R^5)\left[x^4 + y^4 + z^4 - \tfrac{3}{5}r^4\right] + \cdots \end{aligned} \tag{5.6.28}$$

if we consider only terms up to the fourth order. Sixth- and higher-order terms will be discussed in Chapter 7. The first ($l = 0$) term in the foregoing gives the potential at the center of the octahedron. The second term contains

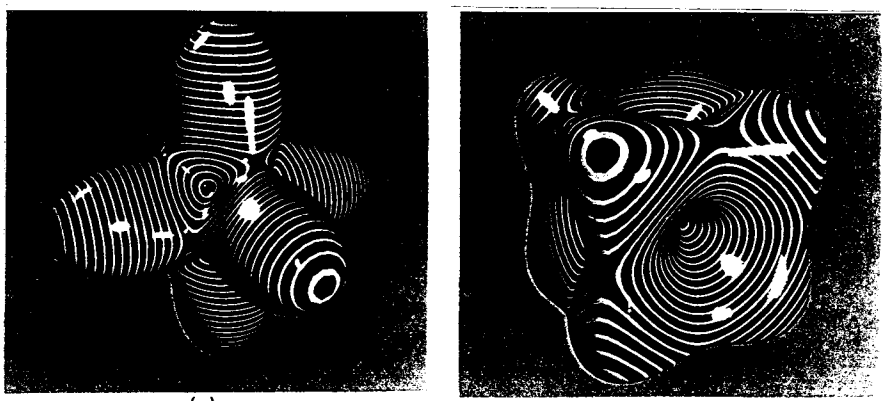

(a) (b)

Figure 5.6.5 Octahedrally anisotropic potential surfaces of fourth-degree. (a) This surface corresponds to repulsive charges placed on the octahedral axes, while (b) corresponds to attractive charges.

the potential $V^{(4)}$ from Eq. (5.6.16). It describes the octahedral potential anisotropy just outside the center. As long as x, y, and z remain small compared to R the higher-order multipole expansion terms can be neglected.

In order to visualize the fourth-order anisotropy $V^{(4)}$ it is useful to plot it as a function of (θ, ϕ) for fixed r. Expressing $V^{(4)}$ in terms of spherical harmonics gives

$$V^{(4)} = (4\pi)^{1/2} r^4 \left[(2/\sqrt{7}\,0)\left(Y_4^4 + Y_{-4}^4\right) + \tfrac{2}{5} Y_0^4 \right] /3$$

$$= r^4 \left[35\cos^4\theta - 30\cos^2\theta + 3 + 5\sin^4\theta \cos 4\phi \right] /20. \quad (5.6.29)$$

The function $(a + bV^{(4)})$ is plotted radially in Figure 5.6.5 as a function of θ and ϕ for $r = 1$, $a = 1$, and $b = \pm 5$. The positive $(b = 5)$ value in Figure (5.6.5a) corresponds to repulsive charges while the negative $(b = -5)$ value in Figure (5.6.5b) corresponds to the attractive charges. The scale factors (a, b) are chosen to clearly exhibit the anisotropic mountain and valley features while keeping the function $(a + bV^{(4)})$ positive. To visualize the potential imagine you are walking on a planet of the shape $(a + bV^{(4)})$. Then mountains and valleys are high and low potential directions, respectively. This type of spherical plot will be used for studying other multipole functions in later chapters.

E. Level Splitting for Molecular Rotors

Molecular rotational levels may split in a way that is analogous to crystal field splitting. Consider, for example, an octahedral SF_6 molecule which is sketched

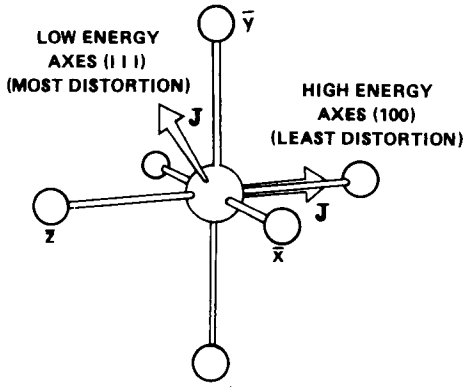

Figure 5.6.6 Octahedral rotor. Centrifugal distortion energy depends on the direction of the angular-momentum vector J relative to the octahedral axes $(\pm 1\ 0\ 0)$, $(0\ \pm 1\ 0)$, and $(0\ 0\ \pm 1)$. Greatest distortion and the least energy is had when the J vector is farthest away from these axes.

in Figure 5.6.6. If this molecule were rigid the Hamiltonian would be that of a spherical rotor as described in Eq. (5.5.48). However, the SF_6 molecule has finite spring constants and will be distorted by centrifugal forces when rotating. In Chapter 4 we showed that the radial bonds were several times stronger than the bending bonds. Therefore, we expect less centrifugal distortion when the angular-momentum vector (**J**) points along the $\bar{x}$, $\bar{y}$, or $\bar{z}$ axes than in between. If **J** is along a (111) direction as shown in Figure 5.6.6 the centrifugal distortion should be maximum. Then the centrifugal forces would exert the greatest leverage on all the bending bonds at once. Expansion causes the inertia of the molecule to increase and the energy to be lower. Hence, for a given magnitude of **J** the threefold (111) axes correspond to energy minima. If **J** points along the $\bar{x}$, $\bar{y}$, or $\bar{z}$ axes there will only be a small expansion allowed by four strong radial bonds. The fourfold symmetry axes correspond to energy maxima.

The lowest-order perturbation operator which describes anisotropic SF_6 centrifugal distortion is

$$V_{\text{cent}}^{(4)} = t\left(J_{\bar{x}}^4 + J_{\bar{y}}^4 + J_{\bar{z}}^4 - \tfrac{3}{5}J^4\right). \tag{5.6.30}$$

This is the body-based angular-momentum analog of the crystal potential (5.6.16). If you let the fourfold axes in figure 5.6.5b) be $J_{\bar{x}}$, $J_{\bar{y}}$, and $J_{\bar{z}}$ axes, then the figure is an angular plot of energy versus direction of **J** for fixed magnitude $|J| = (J_{\bar{x}}^2 + J_{\bar{y}}^2 + J_{\bar{z}}^2)^{1/2}$. For a molecule rotating freely in a laboratory vacuum the classical angular momentum is constant. However, the direction of angular momentum in the body frame may precess because of the octahedral anisotropy. An SF_6 Hamiltonian of the form $H_{\text{sphere}} + V_{\text{cent}}^{(4)}$ has $O_3 \times \bar{O}_h$ symmetry; the lab has full orthogonal O_3 symmetry, while the body symmetry is reduced to octahedral O_h symmetry of the internal structure.

The eigenstates of the octahedral centrifugal distortion Hamiltonian will have wave functions of the form

$$r_{mb}^{NB} = \sum_{n=-N}^{N} \left(\overline{\begin{array}{c|c} N & B \\ n & b \end{array}}\right) r_{mn}^{N}$$

$$= \sum_{n} \left(\overline{\begin{array}{c|c} N & B \\ n & b \end{array}}\right) \mathscr{D}_{mn}^{N*}(\alpha\beta\gamma)(2N+1)^{1/2}, \qquad (5.6.31)$$

where $\left(\begin{smallmatrix} B \\ b \end{smallmatrix}\right)$ stands for octahedral symmetry irrep labels $\left(\begin{smallmatrix} A_1 \\ \cdot \end{smallmatrix}\right)$, $\left(\begin{smallmatrix} A_2 \\ \cdot \end{smallmatrix}\right)$, $\left(\begin{smallmatrix} E \\ 1 \end{smallmatrix}\right)$, $\left(\begin{smallmatrix} E \\ 2 \end{smallmatrix}\right)$, $\left(\begin{smallmatrix} T_1 \\ 1 \end{smallmatrix}\right), \ldots, \left(\begin{smallmatrix} T_2 \\ 3 \end{smallmatrix}\right)$, and N is our new notation for total orbital momentum of the nuclei in the rotating molecule. Note that only the body momentum component n is being summed. The lab component m is still a good quantum number as long as no external crystal fields exist in the lab.

In Section 5.6.C we introduced methods which gave octahedral crystal field harmonics,

$$\left\langle \theta\phi \middle| \begin{matrix} B \\ b \end{matrix} \right\rangle = \sum_{m} \left(\begin{array}{c|c} N & B \\ m & b \end{array}\right) Y_m^N(\theta\phi), \qquad (5.6.32)$$

in terms of spherical hormonics. [Recall Eq. (5.6.15).] The same procedures can be used to derive the octahedral rotor functions r_b^B in terms of the body-defined angular-momentum functions r_n^N. Body-defined symmetry transformations obey the rules

$$\bar{R}(\alpha\beta\gamma)\left| \begin{matrix} N \\ mn \end{matrix} \right\rangle = \sum_{n'} \mathscr{D}_{n'n}^{N*}(\alpha\beta\gamma) \left| \begin{matrix} N \\ mn' \end{matrix} \right\rangle \qquad (5.6.33)$$

according to Eq. (5.5.40). The only difference in form between body- and lab-defined transformation matrices is the complex conjugation ($*$) symbol. Also, that lab transformations (5.5.31) sum over the m's while the body transformations sum over n's. Hence, the coefficient derived for crystal field problems are related to the rotor coefficients through complex conjugation:

$$\left(\overline{\begin{array}{c|c} N & B \\ n & b \end{array}}\right) = \left(\begin{array}{c|c} N & B \\ n & b \end{array}\right)^{*}. \qquad (5.6.34)$$

The symbol B^* will be used to label the irrep $\mathscr{D}^{B^*} = (\mathscr{D}^{B})^*$ of the finite subgroup. In case we are using real octahedral irreps we have $B^* = B$. For example, the E rotor eigenfunctions,

$$r_{m1}^{2E} = r_{m0}^{2},$$
$$r_{m2}^{2E} = (r_{m2}^{2} + r_{m-2}^{2})/\sqrt{2}, \qquad (5.6.35)$$

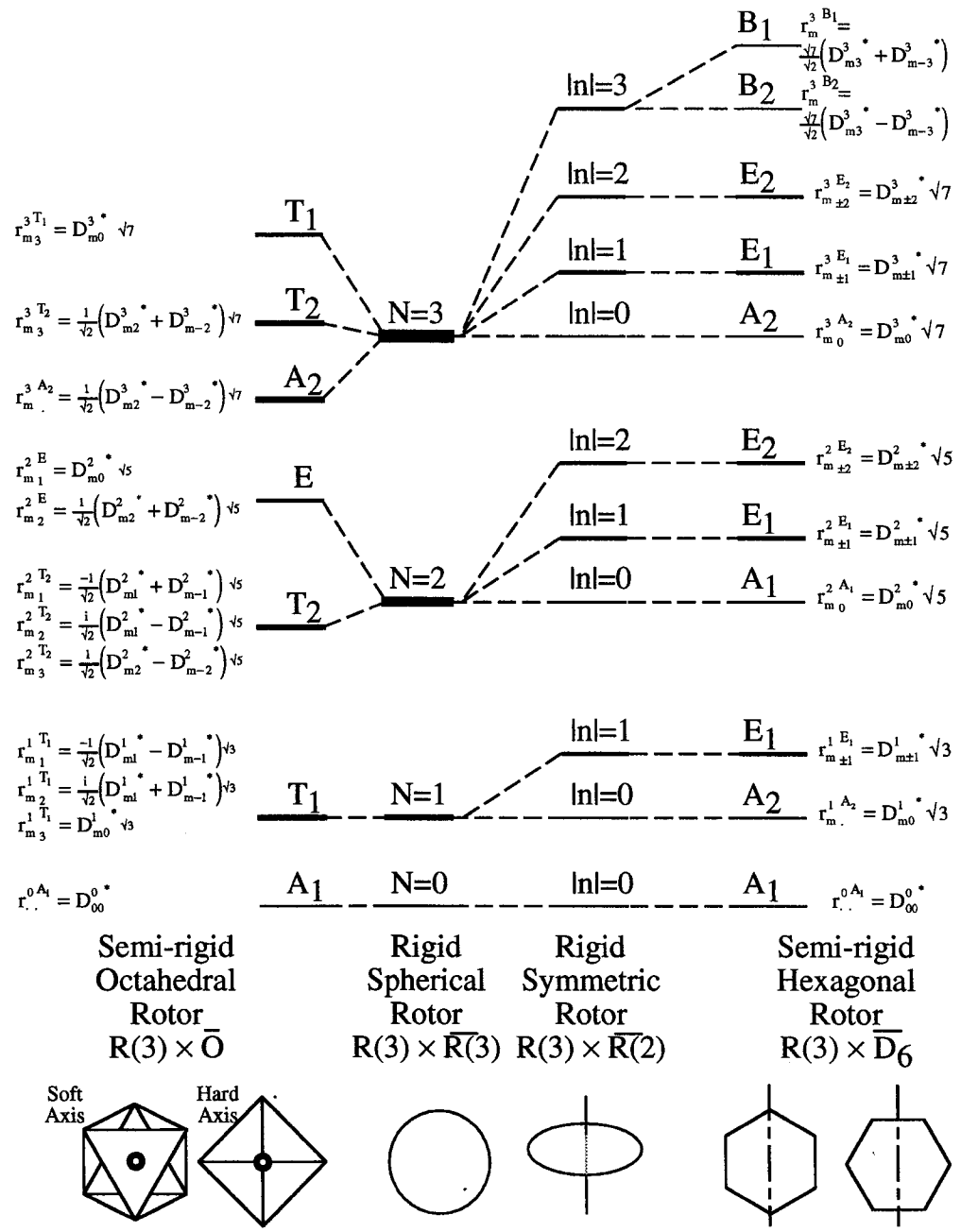

Figure 5.6.7 (a) Correlation of lowest levels of rigid spherical and symmetric rotors with semirigid rotors. (b) Centrifugal distortion of semirigid rotors. Amount of distortion depends on direction of rotation axis. Some directions are softer than others. This directional anisotropy must have the symmetry of the rotor. Hence the levels and wave functions must be defined by representations of that symmetry as shown in the figure.

follow directly from Eqs. (5.6.15d) and (5.6.15e), while the T_2 eigenfunctions

$$r_{m\,1}^{2\,T_2} = -\left(r_{m1}^2 + r_{m-1}^2\right)/\sqrt{2}\,,$$

$$r_{m\,2}^{2\,T_2} = i\left(r_{m1}^2 - r_{m-1}^2\right)/\sqrt{2}\,,$$

$$r_{m\,3}^{2\,T_2} = \left(r_{m2}^2 - r_{m-2}^2\right)/\sqrt{2}\,. \tag{5.6.36}$$

follow from Eqs. (5.6.15a)–(5.6.15c) after conjugation.

Figure 5.6.7 shows the ($N = 2$) splitting of E and T_2 on the left-hand side. The splitting is analogous to the crystal field splitting in Figure 5.6.3. The E levels favor the high-energy axes while the T_2 levels favor the low-energy axes. The latter correspond to greater distortion, as indicated at the bottom of Figure 5.6.7. Note that the energy splittings and the distortion are greatly exaggerated in the figure. Generally, the splittings are a small fraction of the spacing between N levels. Neither the splittings nor the distortions would be visible in drawing of this scale.

The $N = 3$ splittings are sketched on the upper left-hand side of Figure 5.6.7. The correlations (5.6.5b) predict an A_2, T_2, and T_1 level, though not necessarily in that order. The derivation of $r_{m\,b}^{3\,B}$ wave functions is left as an exercise. Note that all the levels shown in Figure 5.6.7 have an additional $(2N + 1)$-fold lab degeneracy which is not indicated. For example, each ($N = 2$) sublevel is fivefold degenerate with $m = 2, 1, 0, -1, -2$. To see these levels one needs to apply a lab-based perturbation such as a crystal or Zeeman field.

F. $R_3 \supset D_6$ Correlations and Level Splitting

The splittings of N levels appropriate for a hexagonal ring molecule are shown on the right-hand side of Figure 5.6.7. First the body-based symmetry is reduced from $O_3 \supset O_2$ corresponding to the rigid symmetric rotor. Then $|n|$ is a good quantum number and the levels split according to n^2 from Eq. (5.5.52). [Note that a benzenelike molecule has $(C - B) < 0$ so the levels would actually decrease with n^2.] Finally, the reduction of body symmetry from O_2 to D_6 is indicated on the extreme right-hand side of Figure 5.6.7. This could be caused by a hexagonally anisotropic centrifugal distortion potential.

The $O_3 \supset D_6$ correlations may be constructed in the same way as they were for $O_3 \supset O_h$. The D_6 characters derived and labeled in Eq. (3.6.17).

They lead to the following correlations:

	f^{A_1}	f^{A_2}	f^{E_2}	f^{B_1}	f^{B_2}	f^{E_1}
$l = 0$	1	·	·	·	·	·
1	·	1	·	·	·	1
2	1	·	1	·	·	1
3	·	1	1	1	1	1
4	1	·	2	1	1	1
5	·	1	2	1	1	2
6	2	1	2	1	1	2
7	1	2	2	1	1	3
8	2	1	3	1	1	3
9	1	2	3	2	2	3
10	2	1	4	2	2	3

(5.6.37)

It is helpful to try to understand these splittings physically. One way to do this involves the simpler Bohr orbitals and Bloch waves in Figure 3.6.5. There it is easier to see how $m = 0, \pm 1$, and ± 2 waves become A, E_1, and E_2 levels, respectively, when a D_6 symmetric perturbation is present. The same sort of labeling is done for the $n = 0, \pm 1$, and ± 2 levels on the right-hand side of Figure 5.6.7. Of course, the $|n|$ values can only be as high as the total momentum number N for the splitting of each N level. The ($N = 3$) level in Figure 5.6.7 has an $|n| = 3$ sublevel which splits into B_1 and B_2 levels under D_6 symmetric perturbations. These levels correspond to the first Brillouin-zone standing waves in Figure 3.6.5(a), i.e., sine and cosine waves. The crests of the cosine wave and the nodes of the sine wave stand in the potential valleys. This makes the latter have higher potential energy than the former. Since either wave has the same kinetic energy their levels split. The B_1 and B_2 rotor wave functions for $N = 3$ are

$$r_{m\cdot}^{3B_1} = \left(r_{m3}^3 + r_{m-3}^3\right)/\sqrt{2}\,,$$
$$r_{m\cdot}^{3B_2} = \left(r_{m3}^3 - r_{m-3}^3\right)/\sqrt{2}\,. \tag{5.6.38}$$

In order to determine which waves are B_1 or B_2 one must specify the 180° p *axis according to Eqs. (3.6.23 and 3.6.24). Whenever possible we shall let one* of the p axes be the $\bar{y}$ axis so the R_3 matrix $\mathscr{D}^N$ (0 180° 0) is real. Substituting ($\alpha = 0$, $\beta = 180°$, $\gamma = 0$) into Eq. (5.4.45) yields

$$\mathscr{D}_{mn}^{j}(0\ 180°\ 0)$$
$$= \sum_k (-1)^k \frac{[(j+n)!(n-n)!(j+m)!(j-m)!]^{1/2}(0)^{2j+m-n-2k}}{(j+m-k)!(n-m+k)!k!(j-n-k)!}\,. \tag{5.6.39}$$

The only nonzero terms are those for which the exponent is zero; i.e., $k = j + (m - n)/2$. To keep both the denominator factors $(j + m - k) = (m + n)/2$ and $(j - n - k) = -(m + n)/2$ from being negative it is necessary to have

$$m + n = 0.$$

This yields

$$\mathscr{D}^{N}_{mn}(0\ 180°\ 0) = \delta_{n,-m}(-1)^{N+m}. \tag{5.6.40}$$

Note that for odd-N and $n = 0$ this component is negative. Therefore the $n = 0$ component of the $N = 3$ level belongs to A_2:

$$r^{3A_2}_{m} = r^{3}_{m0}. \tag{5.6.41}$$

The rings in Figure 5.6.8 serve as mnemonics for the $R_3 \downarrow D_6$ level splitting. The D_6 levels contained in a particular $N = J$ level lie between the arrows which are labeled with that momentum number. For example, we read $A_2E_1E_2B_2B_1$ between the $(J = 3)$ arrow outside and the $(J = 3)$ arrow on the inside of the odd-J circle. For $J = 6n + p$ ($p < 6$ and $n = 1, 2, 3, \ldots$) one must read around the circle n times before stopping. For example, $J = 8$ gives $A_1E_1E_2B_1B_2E_2E_1A_2A_1E_1E_2$.

For low N in most molecules the ordering given by the wheel will be correct. Furthermore, the levels (A_1A_2) or (B_1B_2) enclosed by inside teeth should be very nearly degenerate. However, this may not be the case for high N. If the centrifugal potential valleys become deep enough they may trap the angular-momentum vector on the twofold symmetry axes. Then the levels will

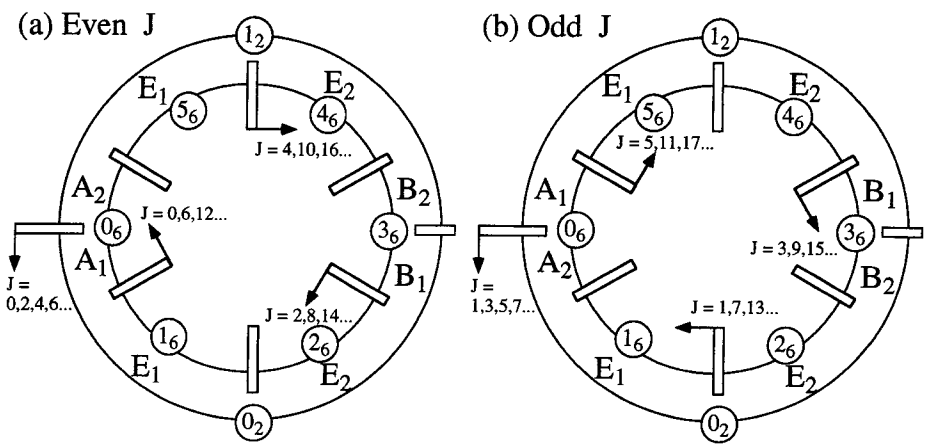

Figure 5.6.8 Mnemonic wheels for hexagonal-D_6 orbital splitting of J levels for (a) even J and (b) odd J.

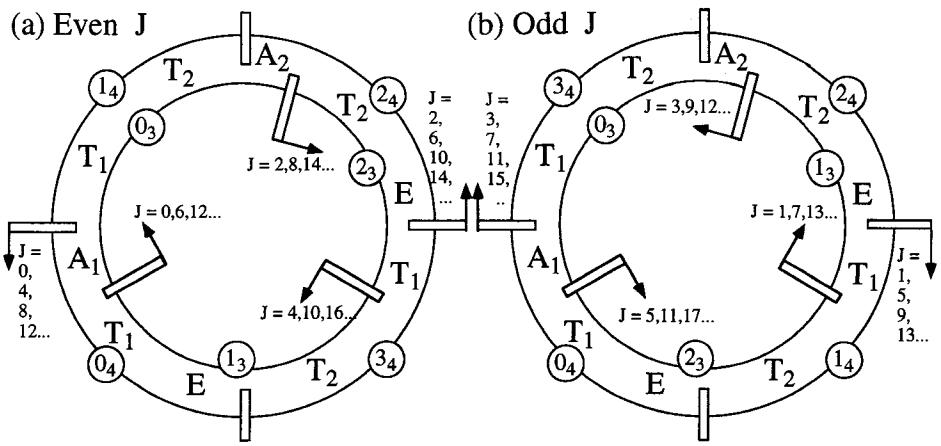

Figure 5.6.9 Mnemonic wheels for octahedral-O orbital. Splitting of J levels for (a) even J and (b) odd J.

fall into clusters $(A_1E_1E_2B_1)$ or $(A_2E_1E_2B_2)$ as they did in Figure 3.6.5(b). The clusters are indicated by the outside teeth on the mnemonic wheels.

Mnemonic wheels can be constructed easily for any D_n symmetry by appealing to the wave mechanics described in Sections 3.6.A and 3.6.B. Each wheel must contain the sequences $\{A_1E_1E_2 \cdots E_{n/2-1}B_1\}$ and $\{B_2E_{n/2-1} \cdots E_2E_1A_2\}$ for even n, or $\{A_1E_1 \cdots E_{(n-1)/2}\}$ and $\{E_{(n-1)/2} \cdots E_1A_2\}$ for odd n.

One of the surprising results of modern spectroscopy is the existence of similar mnemonic wheels for octahedral symmetry. In fact the correlation table of (5.6.5) can be replaced by the wheels in Figure 5.6.9. The octahedral wheels are read in the same way as the D_n wheels. For example, the T_2 and E states lie between the $(J = 2)$ arrows in Figure 5.6.9(a), and the A_2, T_1, and T_2 states lie between the $(J = 3)$ arrows in Figure 5.6.9(b). The examples agree with the $\mathscr{D}^2 \downarrow O$ and $\mathscr{D}^3 \downarrow O$ correlations. Furthermore, the wheels give *correct ordering* for the energy levels of the $V^{(4)}$ Hamiltonians (5.6.29) or (5.6.30). This is very convenient to have for large angular-momentum J. (The ordering was not discovered until large-J computer calculations were done by Los Alamos researchers in 1976.) For large J the teeth on the wheels indicate which levels are clustered, as explained in Chapter 7. The a_3 and a_4 teeth indicate clusters belonging to induced representations $a_3 \uparrow 0$ and $a_4 \uparrow 0$. This is also analogous to the D_6 clusters which belong to $a_2 \uparrow D_6$ or $a_6 \uparrow D_6$ induced representations.

For $J = 2$ only part of a cluster appears. If there has been *six* states satisfying (2_4) local symmetry conditions (5.6.7) then the induced representation

$$(2_4) \uparrow O \sim A_2 \oplus T_2 \oplus E$$

would result according to correlation (4.2.42b). However, A_2 is left out of the five ($J = 2$) states computed in Eqs. (5.6.15). The physical interpretation of clusters and induced representations will be taken up again in Chapter 7.

5.7 HALF-INTEGER j-LEVEL SPLITTING IN FINITE SYMMETRY

We have mentioned the peculiar double-valued transformation behavior of half-integral $j = \frac{1}{2}, \frac{3}{2}, \frac{5}{2}, \ldots$ angular-momentum states $|{}^{j}_{m}\rangle$. Any system that is composed of an odd number of electrons whose spins play some physical role will have to be described by this type of state. If such a system is put into a finite symmetry environment a peculiar splitting of the levels results. We develop the theory of this here, beginning with hexagonal D_6 symmetry as an example.

A. Ray Representations of D_6

Let us consider two methods for determining the explicit multivalued symmetry properties of half-integral spin representations. In the first method one simply calculates the $\mathscr{D}^{1/2}(R)$ representation using either Euler angles [recall Eq. (5.4.16)] or Darboux angles [recall Eq. (5.5.1)] and then forms all products of finite symmetry rotations. The second method uses Hamilton turns to obtain products geometrically. We shall compare the two methods while discussing the finite symmetry D_6.

Consider, for example, the two 180° rotations ρ_2 and ρ_3' around transverse axes shown in Figure 3.6.4. The Darboux angles of ρ_3' are ($\phi = \pi/2$, $\theta = \pi$, $\omega = \pi$) while ρ_2 has angles ($\phi = \pi/3$, $\theta = \pi$, $\omega = \pi$). Substituting these into Eq. (5.5.1) gives

$$\mathscr{D}^{1/2}(\rho_3') = \begin{pmatrix} 0 & -1 \\ 1 & 0 \end{pmatrix} \quad \text{and} \quad \mathscr{D}^{1/2}(\rho_2) = \begin{pmatrix} 0 & -ie^{-i\pi/3} \\ -ie^{i\pi/3} & 0 \end{pmatrix}. \tag{5.7.1}$$

The products $\rho_3'\rho_2$ and $\rho_2\rho_3'$ are as follows:

$$\begin{aligned} \mathscr{D}^{1/2}(\rho_3')\mathscr{D}^{1/2}(\rho_2) &= \begin{pmatrix} ie^{i\pi/3} & 0 \\ 0 & -ie^{-i\pi/3} \end{pmatrix} = -\begin{pmatrix} e^{-i\pi/6} & 0 \\ 0 & e^{i\pi/6} \end{pmatrix} \\ \mathscr{D}^{1/2}(\rho_2)\mathscr{D}^{1/2}(\rho_3') &= \begin{pmatrix} -ie^{-i\pi/3} & 0 \\ 0 & ie^{i\pi/3} \end{pmatrix} = \begin{pmatrix} e^{-i5\pi/6} & 0 \\ 0 & e^{i5\pi/6} \end{pmatrix} \end{aligned} \tag{5.7.2}$$

These results may be expressed in terms of z rotations h or h^5 for which the

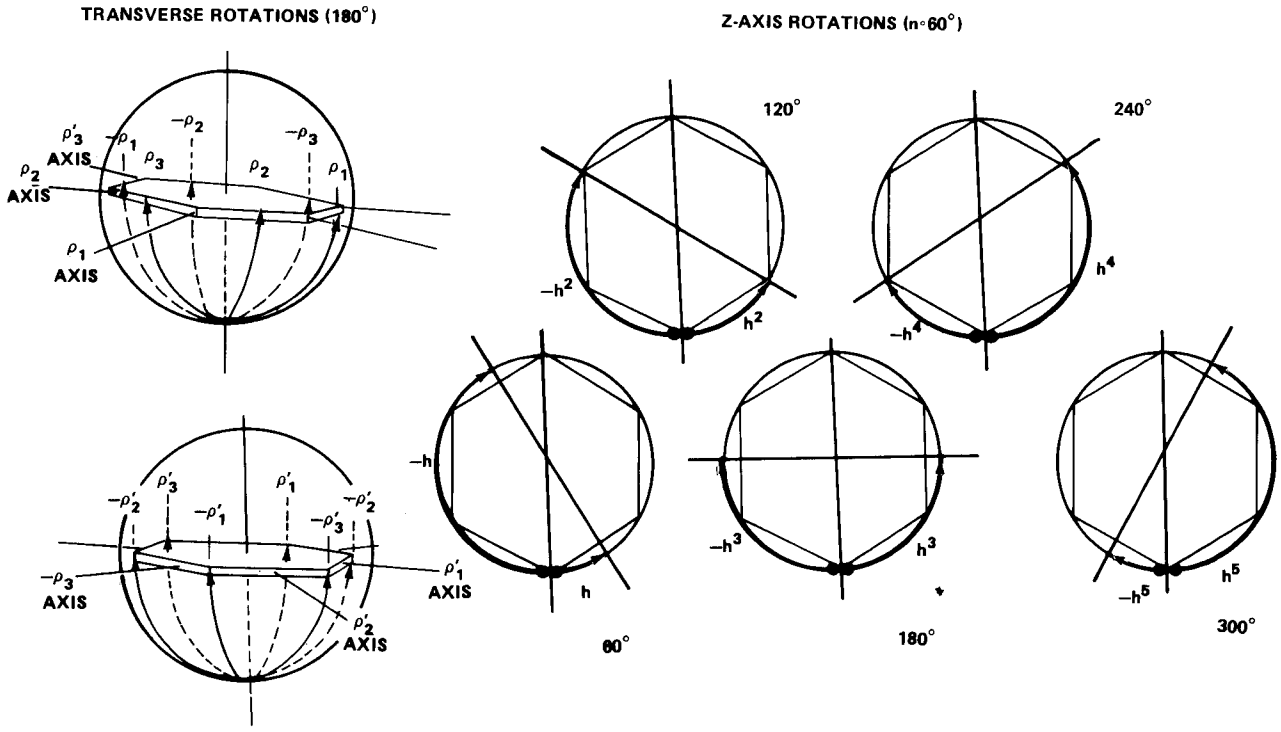

Figure 5.7.1 Hamilton-turn vectors for D_6 spin algebra.

Darboux angles are $(\theta = 0 = \phi)$ and $\omega = \pi/3$ or $5\pi/3$, respectively:

$$\mathscr{D}^{1/2}(\rho'_3)\mathscr{D}^{1/2}(\rho_2) = -\mathscr{D}^{1/2}(h), \qquad \mathscr{D}^{1/2}(\rho_2)\mathscr{D}^{1/2}(\rho'_3) = \mathscr{D}^{1/2}(h^5). \tag{5.7.3}$$

Notice the minus sign in the first product. The sign changes which appear in spin-$\frac{1}{2}$ representations make a big difference in the form of the eigenstates and group transformation properties of half-integral spin states.

Now it is possible to derive, and to a certain extent, visualize all such products using Hamilton-turn vector addition. One first assigns Hamilton-turn vectors to all the D_6 rotations as in Figure 5.7.1 using the rules given in Sections 3.1.B and 5.5.A. Each rotation by angle ω is replaced by sequential reflections through planes intersecting by angle $\omega/2$. A turn vector is a great circle arc drawn from the first plane to the second so that it is orthogonal to the planes. Let us call the vector g positive $(+g)$ or negative $(-g)$ if it goes counterclockwise or clockwise, respectively, when viewed from the chosen axis of rotation. For example, the 30° counterclockwise arc $(+h)$ in Figure 5.7.1 represents the 60° counterclockwise rotation operator h of D_6. The 150° clockwise arc $(-h)$ represents a 300° clockwise rotation. Ordinarily, this would be the same operation as h, but its effect on half-integral spin states gives the opposite phase. Hence, it is labeled $(-h)$.

The products $\rho'_3\rho_2$ and $\rho_2\rho'_3$ are performed "vectorially" in Figure 5.7.2. The operator that acts first (i.e., ρ_2 in $\rho'_3\rho_2$) has its head positioned so that it

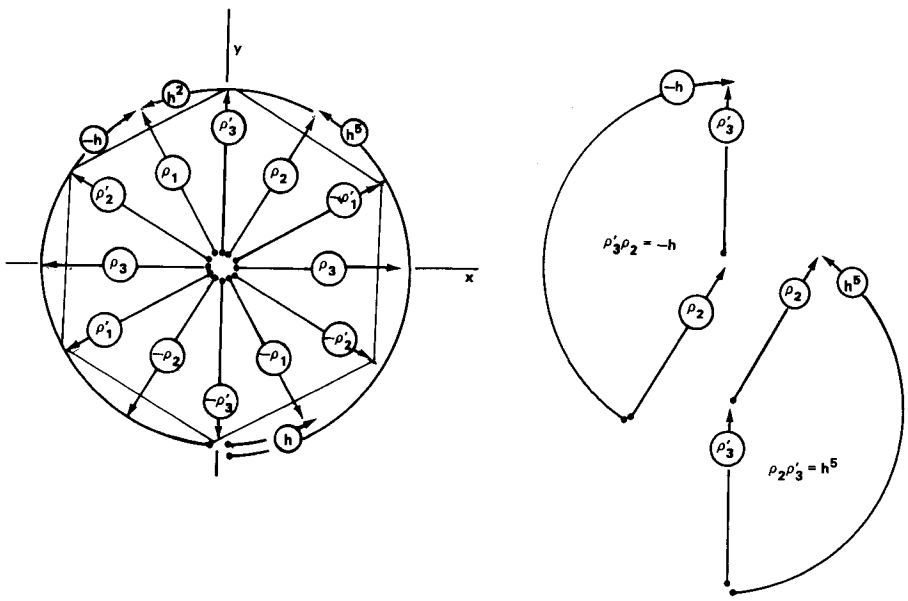

Figure 5.7.2 D_6 nomogram and example of products $(\rho'_3\rho_2 = -h)$ and $(\rho_2\rho'_3) = h^5$.

may meet the tail of the vector for the second factor. (Turn vectors can be moved anywhere on their great circles.) Then the vector sum is identified for each product.

Using either the vector sum or the matrix methods, we derive a rather different set of rules for D_6 operators which is given in the following multiplication table:

1	h^2	h^4	ρ_1	ρ_2	ρ_3	h^3	h	h^5	ρ'_1	ρ'_2	ρ'_3
h^4	-1	$-h^2$	$-\rho_2$	$-\rho_3$	ρ_1	$-h$	h^5	$-h^3$	$-\rho'_2$	$-\rho'_3$	ρ'_1
h^2	h^4	-1	$-\rho_3$	ρ_1	ρ_2	h^5	h^3	$-h$	$-\rho'_3$	ρ'_1	ρ'_2
ρ_1	ρ_2	ρ_3	-1	$-h^2$	$-h^4$	$-\rho'_1$	ρ'_3	$-\rho'_2$	h^3	h^5	$-h$
ρ_2	ρ_3	$-\rho_1$	h^4	-1	$-h^2$	$-\rho'_2$	$-\rho'_1$	$-\rho'_3$	h	h^3	h^5
ρ_3	$-\rho_1$	$-\rho_2$	h^2	h^4	-1	$-\rho'_3$	$-\rho'_2$	ρ'_1	$-h^5$	h	h^3
h^3	h^5	$-h$	ρ'_1	ρ'_2	ρ'_3	-1	h^4	$-h^2$	$-\rho_1$	$-\rho_2$	$-\rho_3$
h^5	$-h$	$-h^3$	$-\rho'_3$	ρ'_1	ρ'_2	$-h^2$	-1	$-h^4$	ρ_3	$-\rho_1$	$-\rho_2$
h	h^3	h^5	ρ'_2	ρ'_3	$-\rho'_1$	h^4	h^2	-1	$-\rho_2$	$-\rho_3$	ρ_1
ρ'_1	ρ'_2	ρ'_3	$-h^3$	$-h^5$	h	ρ_1	$-\rho_3$	ρ_2	-1	$-h^2$	$-h^4$
ρ'_2	ρ'_3	$-\rho'_1$	$-h$	$-h^3$	$-h^5$	ρ_2	ρ_1	ρ_3	h^4	-1	$-h^2$
ρ'_3	$-\rho'_1$	$-\rho'_2$	h^5	$-h$	$-h^3$	ρ_3	ρ_2	$-\rho_1$	h^2	h^4	-1

(5.7.4)

The table shown is not that of a group, since negative $(-g)$ operators are not elements of a group. The ordinary group table of D_6 is obtained if we drop all the minus signs.

Two procedures exist for analyzing this new mathematical structure with the minus signs. The first procedure defines operators $-1, -r, -r^2, \ldots, -\rho'_3$ to be elements of a group $\{1, r, r^2, \ldots, \rho'_3, -1, -r, -r^2, \ldots, -\rho'_3\}$ called the DOUBLE GROUP or COVERING GROUP which is twice as large as D_6. This involves a multiplication table with four times the number of entries shown in (5.7.4). Some of the irreps of this group can be related to the half-integral rotation matrices.

The second procedure, which we shall follow, treats a table such as that of (5.7.4) directly, in an *algebra*. The advantage of this is that, instead of doubling or quadrupling our arithmetic, we find that it is reduced to about one-half that of the original group. This makes half-integral spin analysis half as much work instead of double trouble!

There are other physical problems that require representations which obey equations of the form

$$\mathscr{D}(g)\mathscr{D}(h) = \omega_{g,h}\mathscr{D}(gh). \tag{5.7.5}$$

These are called RAY REPRESENTATIONS or PROJECTIVE REPRESENTATIONS of the group $\mathcal{G} = \{\cdots g \cdots h \cdots\}$. The theory of these is well worth the time it saves in a multitude of calculations.

In the present D_6 example the problem is to find irreducible representations of the algebra defined by the table of (5.7.4). This will be equivalent to finding irreducible *ray* representations (irreps) of D_6. It is necessary to reduce the algebra to a combination of irreducible P operators. This reduction occurs in two stages as it did for ordinary group algebras in Sections 3.2 and 3.3, respectively.

The first stage involves all-commuting operators,

$$C = \sum_g \gamma_g g, \tag{5.7.6}$$

which satisfy

$$Cg = gC$$

or

$$g^{-1}Cg = C, \tag{5.7.7}$$

for all g. Note here that the inverse g^{-1} is defined for the new algebra so that $g^{-1}g = \mathbf{1} = gg^{-1}$, and may not be the same as the group inverse. For example, in the D_6 group the inverses of h and ρ_1 are $h^{-1} = -h^5$ and $\rho_1^{-1} = -\rho_1 = \rho_1^3$, respectively, according to the table of (5.7.4). All commuting operators in spinor algebras are linear combinations of operators of the form

$$c_h = ({}^{\circ}N_h/{}^{\circ}G)\sum_g ghg^{-1}, \tag{5.7.8}$$

where ${}^{\circ}N_h$ is the number of operators which commute with h and ${}^{\circ}G$ is the order of group G. The c_h operators are analogous to the class sums introduced in Section 3.2. However, they are quite different for the spin algebra than for the group. For example, for the D_6 spin algebra only the three c_h operators are linearly independent:

$$c_1 = \mathbf{1}, \qquad c_2 = h^2 - h^4, \qquad c_3 = h - h^5. \tag{5.7.9}$$

The others are either zero ($c_\rho = c_{\rho'} = c_{h^3} = 0$) or proportional to one of these three operators.

The algebra of the all-commuting operators $\{c_1, c_h, c_{h^2}\}$ is determined by the following multiplication rules:

	$c_1 = \mathbf{1}$	$c_2 = h^2 - h^4$	$c_3 = h - h^5$
c_1	c_1	c_2	c_3
c_2	c_2	$2c_1 - c_2$	c_3
c_3	c_3	c_3	$2c_1 + c_2$

(5.7.10)

These rules follow easily from those of the table of (5.7.4). The c_3 minimal equation

$$(c_3)^3 - 3c_3 = 0$$

has three roots $(\sqrt{3}, -\sqrt{3}, 0)$, which yield in turn three all-commuting idempotents.

$$P^1 = \frac{(c_3 + \sqrt{3}\mathbf{1})(c_3 - 0)}{(\sqrt{3} + \sqrt{3})(\sqrt{3} - 0)}, \qquad P^2 = \frac{(c_3 - \sqrt{3}\mathbf{1})(c_3 - 0)}{(-\sqrt{3} - \sqrt{3})(-\sqrt{3} - 0)},$$

$$= \frac{1}{3}\mathbf{1} + \frac{1}{6}c_2 + \frac{\sqrt{3}}{6}c_3, \qquad = \frac{1}{3}\mathbf{1} + \frac{1}{6}c_2 - \frac{\sqrt{3}}{6}c_3,$$

$$P^3 = \frac{(c_3 - \sqrt{3}\mathbf{1})(c_3 + 3\mathbf{1})}{(0 - \sqrt{3})(0 + \sqrt{3})}$$

$$= \frac{1}{3}\mathbf{1} - \frac{1}{3}c_2. \tag{5.7.11}$$

These correspond to three irreducible representations whose characters follow from the coefficients of (5.7.11) according to Eqs. (3.5.5) and (3.5.7). The latter equation gives the same dimensions:

$$l^\alpha = (12/3)^{1/2} = 2 \tag{5.7.12}$$

for all three representations. The character table is given here:

$$\begin{array}{rc} g = & \begin{array}{ccc} \mathbf{1} & h^2 & h \end{array} \\ \chi_g^{E_1} = \chi_g^1 = & \begin{array}{ccc} 2 & 1 & \sqrt{3} \end{array} \\ \chi_g^{E_2} = \chi_g^2 = & \begin{array}{ccc} 2 & 1 & -\sqrt{3} \end{array} \\ \chi_g^{E_3} = \chi_g^3 = & \begin{array}{ccc} 2 & -2 & 0 \end{array} \end{array}. \tag{5.7.13}$$

A conventional notation $\{E_1E_2E_3\}$ for the ray representation will be used. Note that only three classes survived to be part of the class algebra and appear in the character table. The characters of the other classes are identically zero.

One could proceed from this point to an algebraic derivation of the twelve P_{ij}^α operators. Indeed, there are four such operators for each α. [Recall that the sum of squares $(l^\alpha)^2$ of dimensions must equal ${}^oG$. Here we have $2^2 + 2^2 + 2^2 = 12$.] However, it is easier to use the $\mathscr{D}^j(\alpha\beta\gamma)$ matrices for most applications.

Let us determine which D_6 ray representations are correlated with a given SU_2 or R_3 irrep $\mathscr{D}^j \downarrow D_6$. The same frequency formula (3.5.11) and trace formula (5.6.4) may be used. The traces and frequencies are given below.

	$\omega = 0$	$\omega = 120°$	$\omega = 60°$
$j = \frac{1}{2}$	2	1	$\sqrt{3}$
$\frac{3}{2}$	4	-1	$\sqrt{3}$
$\frac{5}{2}$	6	0	0
$\frac{7}{2}$	8	1	$\sqrt{3}$
$\frac{9}{2}$	10	-1	$\sqrt{3}$
$\frac{11}{2}$	12	0	0
⋮	⋮	⋮	⋮

,

	f^{E_1}	f^{E_2}	f^{E_3}
$j = \frac{1}{2}$	·	·	·
$\frac{3}{2}$	1	·	1
$\frac{5}{2}$	1	1	1
$\frac{7}{2}$	2	1	1
$\frac{9}{2}$	2	1	2
$\frac{11}{2}$	2	2	2
⋮	⋮	⋮	⋮

. (5.7.14)

Note that the frequency or correlation table repeats after $j = \frac{5}{2}$:

$$\mathscr{D}^j \downarrow D_6 \sim [\mathscr{D}^{E_1} + \mathscr{D}^{E_3} + \mathscr{D}^{E_2}] + \mathscr{D}^{j-3}. \tag{5.7.15}$$

Hence, the D_6 algebra for half-integral spin has exactly half as many different types of irreps as the D_6 group. That is, there are three kinds $\{E_1E_2E_3\}$ of ray representations, but six kinds $\{A_1A_2B_1B_2E_1E_2\}$ of ordinary representations for the group D_6. Most other crystal point groups also have fewer ray-irreps than irreps, as will be seen in the examples that follow. However, in all cases the sum of the squares $(l^\alpha)^2$ of dimensions equals the order of the group:

$$12 = (l^{E_1})^2 + (l^{E_2})^2 + (l^{E_3})^2 = 2^2 + 2^2 + 2^2. \tag{5.7.16}$$

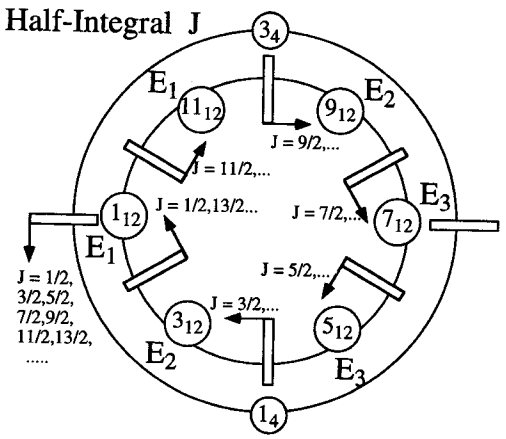

Figure 5.7.3 Mnemonic wheel for hexagonal half-integral spin splitting.

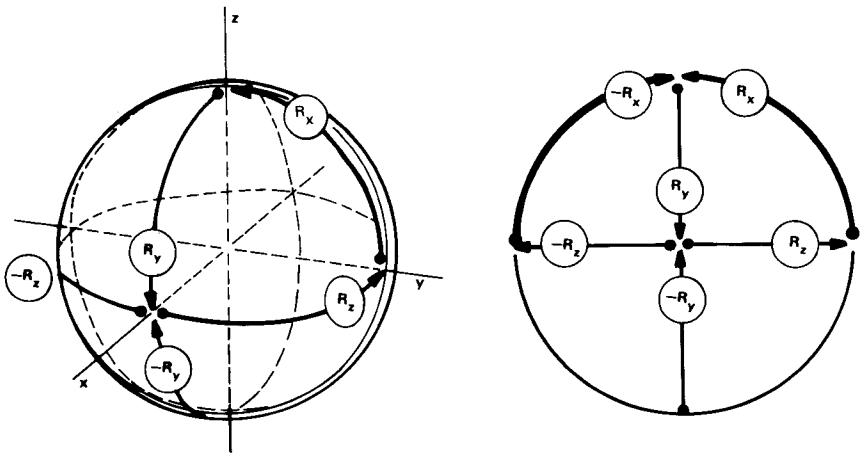

Figure 5.7.4 Hamilton arcs and vector nomogram for D_2 spin algebra.

The mnemonic wheels for the D_6 half-integral j correlations are shown in Figure 5.7.3. Similar wheels can be made for all D_n irreps.

B. Ray Representations of Other D_h Groups

The group $D_2 = C_2 \times C_2$ was the first symmetry group introduced in Chapter 2. It is an Abelian group since its three orthogonal 180° rotations commute with one another. However, the corresponding ray algebra generated by $\mathscr{D}^{1/2}$ or by Hamilton vectors is noncommutative. The D_2 Hamilton vector nomogram is shown in Figure 5.7.4. This gives the following multiplication table:

$$\begin{array}{|cccc|}\hline \mathbf{1} & R_x & R_y & R_z \\ R_x & -\mathbf{1} & R_z & -R_y \\ R_y & -R_z & -\mathbf{1} & R_x \\ R_z & R_y & -R_x & -\mathbf{1} \\ \hline \end{array} . \tag{5.7.17}$$

From this it is easy to show that the identity operator *alone* is all-commuting This implies that only one irrep of D_2 exists. The character table assumes a very simple form!

$$\begin{aligned} g &= \mathbf{1}, \\ \chi_g^E &= \boxed{2}. \end{aligned} \tag{5.7.18}$$

D_2 gives the world's simplest nontrivial ray algebra. It has a single irreducibl representation $\mathscr{D}^E$ given by the spinor representation (5.5.1) or (5.4.30):

$$\mathscr{D}^E(R_x) = \begin{pmatrix} 0 & -i \\ -i & 0 \end{pmatrix}, \quad \mathscr{D}^E(R_y) = \begin{pmatrix} 0 & -1 \\ 1 & 0 \end{pmatrix}, \quad \mathscr{D}^E(R_z) = \begin{pmatrix} -i & 0 \\ 0 & i \end{pmatrix} \tag{5.7.19}$$

Incidentally, these are just the QUATERNION q_j matrices defined by Eq. (5.5.3). In fact, the D_2 double group is called the quaternion group $Q = \{\mathbf{1}, q_x, q_y, q_z, -\mathbf{1}, -q_x, -q_y, -q_z\}$, where

$$-R_z = q_x q_y = q_z = -q_y q_x \text{ (and cyclically)},$$

and

$$q_j^2 = -\mathbf{1}. \tag{5.7.20}$$

This group Q has a character table which resembles the one for D_4. D_4 and Q account for the two eighth-order non-Abelian groups which are counted in Figure 2.2.2. (See Problems 3.3.2 and 3.4.2.)

The derivations of spin-$\frac{1}{2}$ characters and irreps for other axial groups C_n and D_n are left as exercises. However, it is interesting to note that the C_n characters can be visualized geometrically using the nth roots of negative unity (-1). It is instructive to compare the complex vector roots of positive unity in Figure 2.7.2 with the corresponding negative ones in Figure 5.7.5. There is an essential difference between odd-n groups $C_3, C_5, \ldots$, which have a (-1) representation, and even-n groups $C_2, C_4, C_6, \ldots$, which do not. This difference carrys over to the D_n groups. D_n groups with even n have only $n/2$ different two-dimensional ray representations $\{E_{1/2}, E_{3/2}, \ldots, E_{(n-1)/2}\}$. The D_n groups with odd n have $(n-1)/2$ different two-dimensional ray representations and a conjugate pair of one-dimensional ones. The number and dimension of ray representations of D_n for odd n is the same as that of ordinary representations.

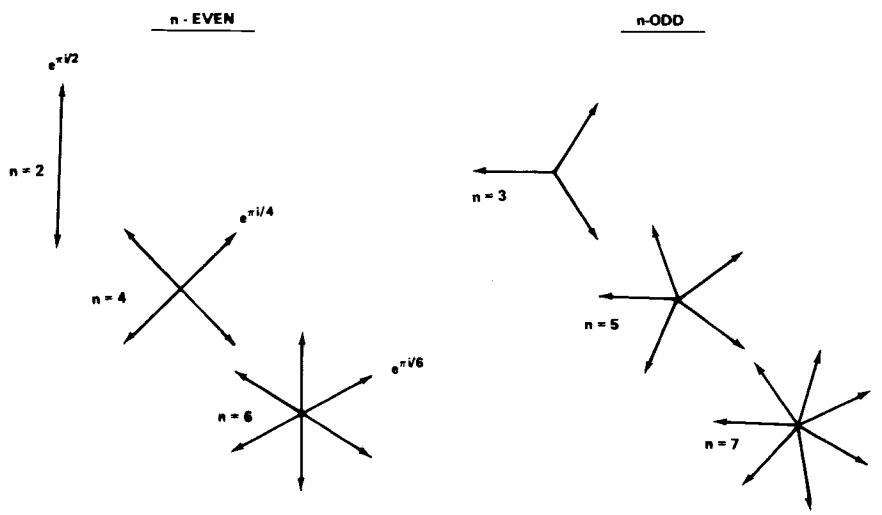

Figure 5.7.5 Representing C_n spin representations by complex nth roots of negative unity ($n = 2, 3, \ldots, 7$).

C. Ray Representations of Octahedral Symmetry

The structure of octahedral ray representations is quite different from the ordinary representations discussed in Sections 4.1 and 4.2. However, the O-group nomogram (4.1.4) gives the necessary ray algebra. Once again the 180° rotations get left out of the revised class algebra, and the only all-commuting operators are the following:

$$\begin{aligned} c_1 &= \mathbf{1}, \\ c_r &= r_1 + r_2 + r_3 + r_4 - r_1^2 - r_2^2 - r_3^2 - r_4^2, \\ c_R &= R_1 + R_2 + R_3 - R_1^3 - R_2^3 - R_3^3. \end{aligned} \tag{5.7.21}$$

When computing the class algebra one has only to compute products which give one particular element, say $\mathbf{1}$, r_1, and R_1 from each class. The other class elements copy this behavior. The necessary products are computed in the following table using Figure 4.1.4. (Also, see Appendix F, Table F.2.1.)

	r_1	r_2	r_3	r_4	$-r_1^2$	$-r_2^2$	$-r_3^2$	$-r_4^2$	R_1	R_2	R_3	$-R_1^3$	$-R_2^3$	$-R_3^3$
r_1					$\mathbf{1}$								R_1	
r_2						$\mathbf{1}$								
r_3							$\mathbf{1}$			R_1				
r_4								$\mathbf{1}$						
$-r_1^2$	$\mathbf{1}$				$-r_1$									
$-r_2^2$		$\mathbf{1}$					r_1			R_1				
$-r_3^2$			$\mathbf{1}$					r_1						
$-r_4^2$				$\mathbf{1}$		r_1								R_1
R_1									r_1		$\mathbf{1}$			
R_2										r_1		$\mathbf{1}$		
R_3									r_1					$\mathbf{1}$
$-R_1^3$									$\mathbf{1}$					
$-R_2^3$										$\mathbf{1}$				
$-R_3^3$											$\mathbf{1}$			

(5.7.22)

The desired algebra multiplication table follows:

	$c_1 = \mathbf{1}$	c_r	c_r
$c_r = \mathbf{1}$	$\mathbf{1}$	c_r	c_R
c_r	c_r	$81 + 2c_r$	$4c_R$
c_R	c_R	$4c_R$	$61 + 3c_r$

. (5.7.23)

From this one derives the minimal equation of c_R:

$$c_R^3 - 18c_R = 0.$$

Each of the three roots $(3\sqrt{2}, -3\sqrt{2}, 0)$ are identified with one of the resulting idempotents:

$$\begin{aligned} P^{E_1} &= \left(\mathbf{21} + c_r + \sqrt{2}c_R\right)/12, \\ P^{E_2} &= \left(\mathbf{21} + c_r - \sqrt{2}c_R\right)/12, \\ P^{G} &= (\mathbf{41} - c_r)/6. \end{aligned} \tag{5.7.24}$$

The usual relations (3.5.5)–(3.5.7) give the desired characters.

$$\begin{array}{c|ccc} & g = \mathbf{1} & r_1 & R_1 \\ \hline \chi_g^{E_1} = & 2 & 1 & \sqrt{2} \\ \chi_g^{E_2} = & 2 & 1 & -\sqrt{2} \\ \chi_g^{G} = & 4 & -1 & 0 \end{array}. \tag{5.7.25}$$

The splitting of half-integral angular-momentum j levels or the $\mathscr{D}^j \downarrow O$ correlations may be calculated easily from the characters (5.7.25). The R_3 trace formula (5.6.4) gives the table of traces (5.7.26a). From this one derives the frequencies $f^{\alpha}(\mathscr{D}^j \downarrow O)$ in the table of (5.7.26b).

$$\begin{array}{c|ccc} & 1 & r_1 & R_1 \\ & (\omega = 0) & (\omega = 120°) & (\omega = 90°) \\ \hline j = \frac{1}{2} & 2 & 1 & \sqrt{2} \\ \frac{3}{2} & 4 & -1 & 0 \\ \frac{5}{2} & 6 & 0 & -\sqrt{2} \\ \frac{7}{2} & 8 & 1 & 0 \\ \frac{9}{2} & 10 & -1 & \sqrt{2} \\ \frac{11}{2} & 12 & 0 & 0 \\ \vdots & \vdots & \vdots & \vdots \end{array}, \tag{5.7.26a}$$

$$\begin{array}{c|ccc} & f^{E_1} & f^{E_2} & f^{G} \\ \hline j = \frac{1}{2} & 1 & \cdot & \cdot \\ \frac{3}{2} & \cdot & \cdot & 1 \\ \frac{5}{2} & \cdot & 1 & \cdot \\ \frac{7}{2} & 1 & 1 & 1 \\ \frac{9}{2} & 1 & \cdot & 2 \\ \frac{11}{2} & 1 & 1 & 2 \\ \vdots & \vdots & \vdots & \vdots \end{array}. \tag{5.7.26b}$$

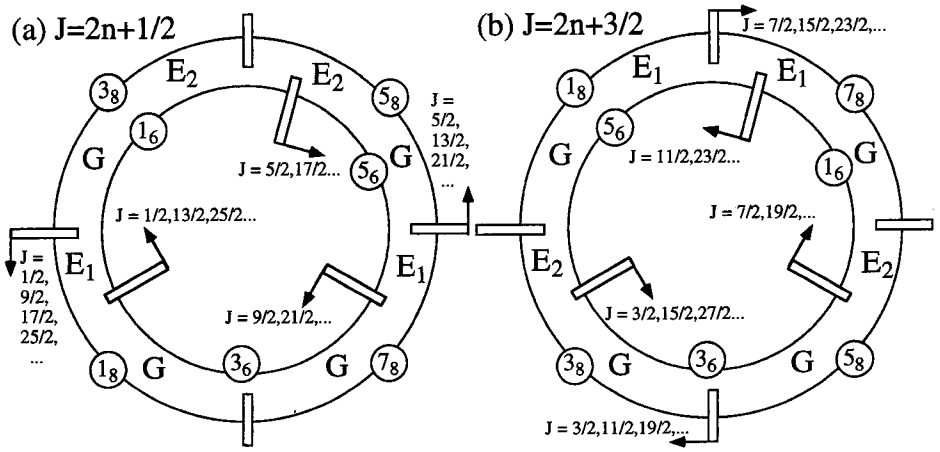

Figure 5.7.6 Mnemonic wheels for octahedral spin algebra correlation with half-integral J.

Notice that (5.7.26b) shows that $\mathscr{D}^{1/2} = \mathscr{D}^{E_1}$ and $\mathscr{D}^{3/2} = \mathscr{D}^{G}$ are both irreducible octahedral ray representations.

It is interesting to note that the preceding correlation table can be replaced by the mnemonic wheels in Figure 5.7.6. Again it happens that the ordering and clustering of half-integral eigenvalues of $V^{(4)}$ Hamiltonians are predicted by the wheels. This is very convenient to have for molecular ion problem which involve high angular momentum j.

5.8 SOME HIGHER CONTINUOUS SYMMETRIES: R_4 AND U_3

We give now a brief discussion of two Hamiltonians which have the Coulomb and oscillator potentials, respectively. The Hamiltonians possess a symmetry higher than R_3 or O_3. Their theory is very interesting but, is being developed sufficiently to have considerable practical value. We discuss it with the hope that future work will be fruitful. Also, we use the opportunity to introduce techniques for analyzing larger Lie groups, which are now being applied in modern theory. The Coulomb and oscillator symmetries were known by Pauli and others. More recently progress has been made toward applying these symmetries to atomic, molecular, and nuclear structure.

A. The Coulomb Symmetry

A particle of mass m in a Coulomb potential field k/r is described by the following Hamiltonian:

$$H = p^2/2m + k/r = \begin{cases} p^2/2m - |k|/r \text{ (attractive case)}, \\ p^2/2m + |k|/r \text{ (repulsive case)}. \end{cases} \tag{5.8.1}$$

Such a Hamiltonian obviously has spherical ($R_3 \subset O_3$) symmetry. It conserves and commutes with angular-momentum operators:

$$L_1 = x_2 p_3 - x_3 p_2, \qquad L_2 = x_3 p_1 - x_1 p_3, \qquad L_3 = x_1 p_2 - x_2 p_1. \quad (5.8.2)$$

However, there is an additional hidden symmetry of this Hamiltonian.

Consider a vector $\boldsymbol{\varepsilon}$ called the ECCENTRICITY or LENZ-RUNGE VECTOR:

$$\boldsymbol{\varepsilon} = \mathbf{r}/r - \mathbf{L} \times \mathbf{p}/km. \quad (5.8.3)$$

(The $\boldsymbol{\varepsilon}$ vector was actually discovered by Hamilton before Lenz or Runge wrote about it.) The ε vector points along the symmetry axis of the classical elliptic or hyperbolic orbit, and its length is the eccentricity of the orbit. The relation between two kinds of Coulomb orbits and their vectors $\boldsymbol{\varepsilon}$ and $\mathbf{L}$ is sketched in Figure 5.8.1.

It is easy to show that conservation of $\boldsymbol{\varepsilon}$ and $\mathbf{L}$ is consistent with the classical orbit equation

$$r = -L^2/km(1 - \varepsilon \cos\theta). \quad (5.8.4)$$

Consider the dot product of $\boldsymbol{\varepsilon}$ and $\mathbf{r}$:

$$\boldsymbol{\varepsilon} \cdot \mathbf{r} = \varepsilon r \cos\theta = r - \mathbf{L} \times \mathbf{p} \cdot \mathbf{r}/km = r + L^2/km.$$

This is the same as the orbit equation. Clearly, the eccentricity vector $\boldsymbol{\varepsilon}$ is another quantity besides $\mathbf{L} = \mathbf{r} \times \mathbf{p}$ which is conserved in a Coulomb field. Note also that its classical magnitude,

$$\begin{aligned} \varepsilon^2 = \boldsymbol{\varepsilon} \cdot \boldsymbol{\varepsilon} &= 1 - 2\mathbf{r} \cdot \mathbf{L} \times \mathbf{p}/kmr + (\mathbf{L} \times \mathbf{p}) \cdot (\mathbf{L} \times \mathbf{p})/k^2m^2 \\ &= 1 + 2L^2/kmr + L^2p^2/k^2m^2 \\ &= 1 + 2(p^2/2m + k/r)L^2/k^2m = 1 + (2H/k^2m)L^2, \end{aligned} \quad (5.8.5)$$

is expressed in terms of conserved total energy H and orbital momentum $\mathbf{L}$.

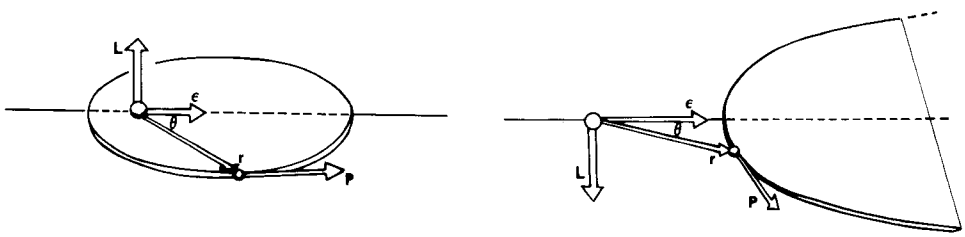

Figure 5.8.1 Location of classical eccentricity vector. The orientation of the eccentricity vector $\boldsymbol{\varepsilon}$ in an elliptical ($k < 0$) and hyperbolic repulsive ($k > 0$) Coulomb orbit is shown.

The corresponding quantum eccentricity operators are defined by

$$\varepsilon_1 = x_1/r - (L_2p_3 - L_3p_2 - p_2L_3 + p_3L_2)/2km, \quad (5.8.6a)$$

$$\varepsilon_1 = x_1/r - ([L_2p_3 - L_3p_2] - ip_1)/2km, \quad (5.8.6b)$$

$$\varepsilon_2 = x_2/r - ([L_3p_1 - L_1p_3] - ip_2)/2km, \quad (5.8.6c)$$

$$\varepsilon_3 = x_3/r - ([L_1p_2 - L_2p_1] - ip_3)/2km. \quad (5.8.6d)$$

The eccentricity operators and the angular-momentum operators (5.8.2) will be seen to generate a symmetry higher than O_3. In constructing the ε operators it is necessary to symmetrize with respect to operators that do not commute; i.e., let $\mathbf{L} \times \mathbf{p}$ equal $(\mathbf{L} \times \mathbf{p} - \mathbf{p} \times \mathbf{L})/2$ in Eqs. (5.8.6). Then one uses commutation relations such as

$$\begin{aligned}[L_1, p_2] &= [x_2p_3, p_2] - [x_3p_2, p_2] \\ &= [x_2, p_2]p_3 = ip_3\end{aligned}$$

to simplify the results wherever possible. In Chapter 7 we shall prove that commutators of L_i with any vector v_j must have the same form,

$$[L_1, v_2] = iv_3, \quad (5.8.7)$$

as the angular-momentum relations

$$[L_1, L_2] = iL_3.$$

The derivations of $\varepsilon - L$ commutators require the following commutation relations:

$$[x_i/r, p_j]\psi(x) = (x_i/r)\frac{1}{i}\frac{\partial\psi}{\partial x_j} - \frac{1}{i}\frac{\partial}{\partial x_j}(x_i\psi(x)/r) = i(\delta_{ij} + x_ix_j)\psi(x)/r$$

or

$$[x_i/r, p_j] = i(\delta_{ij} + x_ix_j)/r, \quad (5.8.8)$$

along with the derivative properties.

$$\begin{aligned}[AB, C] &= A[B, C] + [A, C]B, \\ [A, BC] &= B[A, C] + [A, B]C.\end{aligned} \quad (5.8.9)$$

After considerable algebra the following commutation relation results:

$$\begin{aligned}[\varepsilon_1, \varepsilon_2] &= -2L_3[p^2/2m + k/r]/k^2m \\ &= -i(2H/k^2m)L_3.\end{aligned} \quad (5.8.10)$$

In the case of bound states for which $\langle H \rangle = -|E|$ one may normalize ε to give

$$K_j \equiv \sqrt{-\frac{k^2 m}{2H}}\,\varepsilon_j = \sqrt{\frac{k^2 m}{2E}}\,\varepsilon_j, \tag{5.8.11}$$

whence the following commutation relations result.

$$[L_1 L_2] = iL_3, \qquad [L_1, K_2] = iK_3, \qquad [K_1, K_2] = iL_3$$
$$\cdots \qquad\qquad \cdots \qquad\qquad \cdots. \tag{5.8.12}$$

We now see that these relations are the ones for R_4 or O_4 symmetry.

(a) Introduction to the Lie Algebra of R_4 We showed in Section 5.4 that infinitesimal rotations are of the form

$$R(\cdot\cdot\,\varepsilon) = 1 + \varepsilon G = 1 + (\varepsilon/i)L,$$

where operators

$$L = iG \tag{5.8.13}$$

are the generators of rotations. The rotation operators are orthogonal:

$$R^T(\varepsilon) = R^{-1}(\varepsilon) = R(-\varepsilon).$$

This implies that

$$1 + \varepsilon G^T = 1 - \varepsilon G,$$

and that the generators are antisymmetric,

$$G^T = -G, \qquad L^T = -L. \tag{5.8.14}$$

Note that since G is real, L is Hermitian:

$$L^\dagger = L^{*T} = (iG)^{*T} = iG = L.$$

Let us generalize the treatment of R_3 to give one for R_4. According to Eq. (5.1.12), R_4 has six parameters, or three more than R_3. Therefore, we expect R_4 to have six generators. Indeed, we may construct the same representations

of the R_3 generators (5.4.5b) using 4×4 matrices: [Recall Eq. (5.4.5b).]

$$L_{32} \equiv L_x = iG_{32} \to i\mathscr{G}_{32} = \begin{pmatrix} \cdot & \cdot & \cdot & \cdot \\ \cdot & \cdot & -i & \cdot \\ \cdot & i & \cdot & \cdot \\ \cdot & \cdot & \cdot & \cdot \end{pmatrix},$$

$$L_{13} \equiv L_y = iG_{13} \to i\mathscr{G}_{13} = \begin{pmatrix} \cdot & \cdot & i & \cdot \\ \cdot & \cdot & \cdot & \cdot \\ -i & \cdot & \cdot & \cdot \\ \cdot & \cdot & \cdot & \cdot \end{pmatrix},$$

$$L_{21} \equiv L_z = iG_{21} \to i\mathscr{G}_{21} = \begin{pmatrix} \cdot & -i & \cdot & \cdot \\ i & \cdot & \cdot & \cdot \\ \cdot & \cdot & \cdot & \cdot \\ \cdot & \cdot & \cdot & \cdot \end{pmatrix}. \qquad (5.8.15a)$$

These use just the first three dimensions. Then let us make three more R_4 generators using the fourth dimension and components $(j, 4)$ or $(4, j)$:

$$K_{41} \equiv K_x = iG_{41} \to i\mathscr{G}_{41} = \begin{pmatrix} \cdot & \cdot & \cdot & -i \\ \cdot & \cdot & \cdot & \cdot \\ \cdot & \cdot & \cdot & \cdot \\ i & \cdot & \cdot & \cdot \end{pmatrix},$$

$$K_{42} \equiv K_y = iG_{42} \to i\mathscr{G}_{42} = \begin{pmatrix} \cdot & \cdot & \cdot & \cdot \\ \cdot & \cdot & \cdot & -i \\ \cdot & \cdot & \cdot & \cdot \\ \cdot & i & \cdot & \cdot \end{pmatrix},$$

$$K_{43} \equiv K_z = iG_{43} \to i\mathscr{G}_{43} = \begin{pmatrix} \cdot & \cdot & \cdot & \cdot \\ \cdot & \cdot & \cdot & \cdot \\ \cdot & \cdot & \cdot & -i \\ \cdot & \cdot & i & \cdot \end{pmatrix}. \qquad (5.8.15b)$$

Between these we find commutation relations

$$\begin{array}{lll} [L_x, L_y] = iL_z, & [L_x, K_y] = iK_z, & [K_x, K_y] = iL_z \\ \cdots & \cdots & \cdots, \end{array} \qquad (5.8.16)$$

which match those of the operators L_i and K_j of the preceding section. These relations define the Lie algebra of R_4.

We now derive the irreducible representations of the R_4 Lie algebra. This can be done by first constructing raising and lowering operators that are

eigenvectors of L_z, in much the same way that R_3 is solved in Appendix E. Let us imagine that each operator $L_x, K_x, L_y, \ldots$ corresponds to a vector $|L_x\rangle, |K_x\rangle, |L_y\rangle, \ldots$ and make a REGULAR REPRESENTATION analogous to the one for groups.

The regular representation of a Lie-algebra operator L_z is constructed by converting commutation relations,

$$[L_z, L_x] = iL_y, \quad [L_z, K_x] = iK_y, \quad [L_z, L_y] = -iL_x,$$
$$[L_z, K_y] = -iK_x, \quad [L_z, L_z] = 0, \quad [L_z, K_z] = 0,$$

into vector equations (this is permitted since commutation is a linear operation):

$$L_z|L_x\rangle = i|L_y\rangle, \quad L_z|K_x\rangle = i|K_y\rangle, \quad L_z|L_y\rangle = -i|L_x\rangle,$$
$$L_z|K_y\rangle = -i|K_x\rangle, \quad L_z|L_z\rangle = 0, \quad L_z|K_z\rangle = 0. \qquad (5.8.17a)$$

These equations define the regular representation matrix,

$$\mathscr{R}(L_z) = \begin{pmatrix} \cdot & \cdot & -i & \cdot & \cdot & \cdot \\ \cdot & \cdot & \cdot & -i & \cdot & \cdot \\ i & \cdot & \cdot & \cdot & \cdot & \cdot \\ \cdot & i & \cdot & \cdot & \cdot & \cdot \\ \cdot & \cdot & \cdot & \cdot & \cdot & \cdot \\ \cdot & \cdot & \cdot & \cdot & \cdot & \cdot \end{pmatrix}, \qquad (5.8.17b)$$

in the $\{|L_x\rangle, |K_x\rangle, \ldots\}$ basis.

The last commutation $[L_z, K_z] = 0$ indicates that a similar representation of K_z can be simultaneously diagonalized with the one for L_z. $\mathscr{R}(K_z)$ is given here:

$$\mathscr{R}(K_z) = \begin{pmatrix} \cdot & \cdot & \cdot & -i & \cdot & \cdot \\ \cdot & \cdot & -i & \cdot & \cdot & \cdot \\ \cdot & i & \cdot & \cdot & \cdot & \cdot \\ i & \cdot & \cdot & \cdot & \cdot & \cdot \\ \cdot & \cdot & \cdot & \cdot & \cdot & \cdot \\ \cdot & \cdot & \cdot & \cdot & \cdot & \cdot \end{pmatrix}. \qquad (5.8.18)$$

The simultaneous eigenvectors of $\mathscr{R}(L_z)$ and $\mathscr{R}(K_z)$ are found using the theory of Section 1.2.B(d). First we obtain the individual idempotents for

$\mathscr{R}(J_z)$ and $\mathscr{R}(K_z)$:

$$\mathscr{P}_1^J = \frac{\mathscr{R}(J_z) - (-1)1}{1-(-1)} = \tfrac{1}{2}\begin{pmatrix} 1 & \cdot & -i & \cdot & \cdot & \cdot \\ \cdot & 1 & \cdot & -i & \cdot & \cdot \\ i & \cdot & 1 & \cdot & \cdot & \cdot \\ \cdot & i & \cdot & 1 & \cdot & \cdot \\ \cdot & \cdot & \cdot & \cdot & \cdot & \cdot \\ \cdot & \cdot & \cdot & \cdot & \cdot & \cdot \end{pmatrix},$$

$$\mathscr{P}_1^K = \tfrac{1}{2}\begin{pmatrix} 1 & \cdot & \cdot & -i & \cdot & \cdot \\ \cdot & 1 & -i & \cdot & \cdot & \cdot \\ \cdot & i & 1 & \cdot & \cdot & \cdot \\ i & \cdot & \cdot & 1 & \cdot & \cdot \\ \cdot & \cdot & \cdot & \cdot & \cdot & \cdot \\ \cdot & \cdot & \cdot & \cdot & \cdot & \cdot \end{pmatrix},$$

$$\mathscr{P}_{-1}^J = \tfrac{1}{2}\begin{pmatrix} 1 & \cdot & i & \cdot & \cdot & \cdot \\ \cdot & 1 & \cdot & i & \cdot & \cdot \\ -i & \cdot & 1 & \cdot & \cdot & \cdot \\ \cdot & -i & \cdot & 1 & \cdot & \cdot \\ \cdot & \cdot & \cdot & \cdot & \cdot & \cdot \\ \cdot & \cdot & \cdot & \cdot & \cdot & \cdot \end{pmatrix},$$

$$\mathscr{P}_{-1}^K = \tfrac{1}{2}\begin{pmatrix} 1 & \cdot & \cdot & i & \cdot & \cdot \\ \cdot & 1 & i & \cdot & \cdot & \cdot \\ \cdot & -i & 1 & \cdot & \cdot & \cdot \\ -i & \cdot & \cdot & 1 & \cdot & \cdot \\ \cdot & \cdot & \cdot & \cdot & \cdot & \cdot \\ \cdot & \cdot & \cdot & \cdot & \cdot & \cdot \end{pmatrix}. \tag{5.8.19}$$

Then the products of these give the desired results. The first columns of the products $\mathscr{P}_m^J \mathscr{P}_n^K$ are

$$\mathscr{P}_1^J \mathscr{P}_1^K = \tfrac{1}{4}\begin{pmatrix} 1 \\ 1 \\ i \\ i \\ \cdot \\ \cdot \end{pmatrix}, \qquad \mathscr{P}_1^J \mathscr{P}_{-1}^K = \tfrac{1}{4}\begin{pmatrix} 1 \\ -1 \\ i \\ -i \\ \cdot \\ \cdot \end{pmatrix},$$

$$\mathscr{P}_{-1}^J \mathscr{P}_1^K = \tfrac{1}{4}\begin{pmatrix} 1 \\ -1 \\ -i \\ i \\ \cdot \\ \cdot \end{pmatrix}, \qquad \mathscr{P}_{-1}^J \mathscr{P}_{-1}^K = \tfrac{1}{4}\begin{pmatrix} 1 \\ 1 \\ -i \\ -i \\ \cdot \\ \cdot \end{pmatrix}.$$

They show that the following operators:

$$\begin{aligned} M_+ &\equiv L_x + iL_y + K_x + iK_y, & N_+ &\equiv L_x + iL_y - K_x - K_y, \\ &= L_+ + K_+, & &= L_+ - K_+, \\ N_- &\equiv L_x - iL_y - K_x + iK_y, & M &\equiv L_x - iL_y + K_x - iK_y, \\ &= L_- - K_-, & &= L_- + K_- \end{aligned} \tag{5.8.20a}$$

obey the eigencommutation relations:

$$\begin{aligned} &[L_z, M_+] = M_+, \quad [L_z, N_+] = N_+, \quad [L_z, N_-] = -N_-, \\ &[L_z, M_-] = -M_-, \quad [K_z, M_+] = M_+, \quad [K_z, N_+] = -N_+, \\ &[K_z, N_-] = N_-, \quad [K_z, M_-] = -M_-. \end{aligned} \tag{5.8.20b}$$

The $M_\pm$ and $N_\pm$ operators are the R_4 raising and lowering operators.

Now a very nice separation is possible if one redefines generators by

$$M_a \equiv (L_\alpha + K_\alpha)/2 \quad \text{and} \quad N_\alpha \equiv (L_\alpha - K_\alpha)/2. \tag{5.8.21}$$

There results two *independent* sets of R_3 commutation relations

$$[M_z, M_\pm] = \pm M_\pm, \qquad [N_z, N_\pm] = \pm N_\pm, \tag{5.8.22a}$$

and

$$[M_x, M_y] = iM_z, \qquad [N_x, N_y] = iN_z, \tag{5.8.22b}$$

where the two sets of operators are mutually commuting:

$$[M_\alpha, N_\beta] = 0. \tag{5.8.23}$$

The two commuting R_3 groups generated by M and N operators are factors of a cross-product $R_4 = R_3 \times R_3$ according to the definition in Section 2.10. This tells us that our knowledge of R_3 can be applied directly to R_4 since $R_4 = R_3 \times R_3$.

Now Cartan has developed an elegant geometrical method for treating the structure and representations of Lie algebras. We introduce some of this now as it applies to R_4. Lie-algebra operators can generally be combined to form raising and lowering operators $\{\cdots E_{+\alpha} \cdots E_{-\alpha} \cdots\}$ like the $L_\pm$ and $K_\pm$ in R_4. The E_α are eigenvectors in the sense of

$$[H_j, E_\alpha] = r_j(\alpha) E_\alpha, \tag{5.8.24}$$

for a number of mutually commuting operators $\{H_1 H_2 \cdots H_r\}$. (The H_j are $H_1 = L_z$ and $H_2 = K_z$ in R_4.) The number of mutually commuting H_i operators is called the RANK of the algebra. Then the eigenvalues or roots

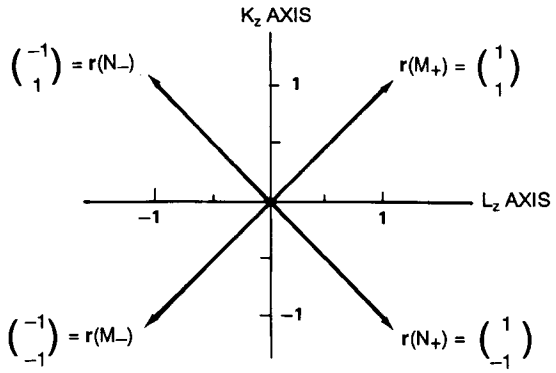

Figure 5.8.2 Root diagram of the R_4 Lie algebra.

$r_j(\alpha)$ can be taken as components of a vector called the ROOT VECTOR:

$$\mathbf{r}(\alpha) = \begin{pmatrix} r_1(\alpha) \\ r_2(\alpha) \\ \vdots \\ r_r(\alpha) \end{pmatrix} \tag{5.8.25}$$

of E_α. For example, we would have the set of four root vectors of R_4 drawn in Figure 5.8.2 according to Eqs. (5.8.20). Cartan has shown how to make root vectors into a code that defines all commutation relations and finally all irreducible representations.

For example, note that the commutation between an E_α and an E_β must give an operator whose root vector is a *sum* of $\mathbf{r}(\alpha)$ and $\mathbf{r}(\beta)$, or else zero:

$$\begin{aligned} \big[H_j, [E_\alpha, E_\beta]\big] &= \big[H_j, E_\alpha E_\beta\big] - \big[H_j, E_\beta E_\alpha\big] \\ &= \big[H_j, E_\alpha\big]E_\beta + E_\alpha\big[H_j, E_\beta\big] - \big[H_j, E_\beta\big]E_\alpha - E_\beta\big[H_j, E_\alpha\big] \\ &= \big(r_j(\alpha) + r_j(\beta)\big)\big[E_\alpha, E_\beta\big]. \end{aligned} \tag{5.8.26}$$

This implies that a commutator of a raising operator with root $\mathbf{r}(\alpha)$ and a corresponding lowering operator with root $-\mathbf{r}(\alpha)$ must give operators with zero roots, namely H_j's. In fact, it can be shown that

$$[E_{+\alpha}, E_{-\alpha}] = N\sum_j r_j(\alpha)H_j. \tag{5.8.27}$$

Here N is a normalization constant which is usually set equal to unity. For example, from Figure 5.8.2 we have

$$[M_+, M_-] = r_{L_z}(M_+)L_z + r_{K_z}(M_+)K_z = 2M_z. \tag{5.8.27}_x$$

(b) Irreducible Representations of R_4 If R_4 is an outer product $R_3 \times R_3$ of rotation groups, then the representations of R_4 are the outer products

$$\mathscr{D}^{j_m j_n} \equiv \mathscr{D}^{j_m} \otimes \mathscr{D}^{j_n}$$

of representations of R_3. The basis states must obey the standard angular-momentum relations twice: once for M_z and $M_\pm$ and once again for N_z and $N_\pm$:

$$M_z \left| \begin{matrix} j_m & j_n \\ m & n \end{matrix} \right\rangle = m \left| \begin{matrix} j_m & j_n \\ m & n \end{matrix} \right\rangle, \qquad N_z \left| \begin{matrix} j_m & j_n \\ m & n \end{matrix} \right\rangle = n \left| \begin{matrix} j_m & j_n \\ m & n \end{matrix} \right\rangle,$$

$$M_\pm \left| \begin{matrix} j_m & j_n \\ m & n \end{matrix} \right\rangle = \sqrt{(j_m \mp m)(j_n \pm m + 1)} \left| \begin{matrix} j_m & j_n \\ m \pm 1 & n \end{matrix} \right\rangle,$$

$$N_\pm \left| \begin{matrix} j_m & j_n \\ m & n \end{matrix} \right\rangle = \sqrt{(j_N \mp n)(j_N \pm n + 1)} \left| \begin{matrix} j_m & j_n \\ m & n \pm 1 \end{matrix} \right\rangle. \tag{5.8.28}$$

For a general Lie algebra there will be similar Cartan relations of the form

$$H_j |\mathbf{m}\rangle = m_j |\mathbf{m}\rangle. \tag{5.8.29}$$

Here the eigenvalues m_j are said to be components of a WEIGHT VECTOR

$$\mathbf{m} = \begin{pmatrix} m_1 \\ m_2 \\ \vdots \\ m_r \end{pmatrix}$$

for a given state. The weight vectors for states belonging to irreps $\mathscr{D}^{j_m j_n}$ of R_4 are indicated by circles in the Figure 5.8.3.

A raising (lowering) operator E_α ($E_{-\alpha}$) applied to any state with weight m gives another state of weight $\mathbf{m} + \mathbf{r}(\alpha)$ ($\mathbf{m} - \mathbf{r}(\alpha)$), or else zero:

$$H_j E_\alpha |\mathbf{m}\rangle = \big(E_\alpha H_j + [H_j, E_\alpha]\big)|\mathbf{m}\rangle,$$

$$\big(m_j E_\alpha + r_j(\alpha) E_\alpha\big)|\mathbf{m}\rangle = \big(m_j + r_j(\alpha)\big) E_\alpha |\mathbf{m}\rangle. \tag{5.8.30}$$

The beautiful theory of Cartan gives the properties of the weight vectors and the irreps of a Lie algebra in terms of its root vectors. We will study more about this later.

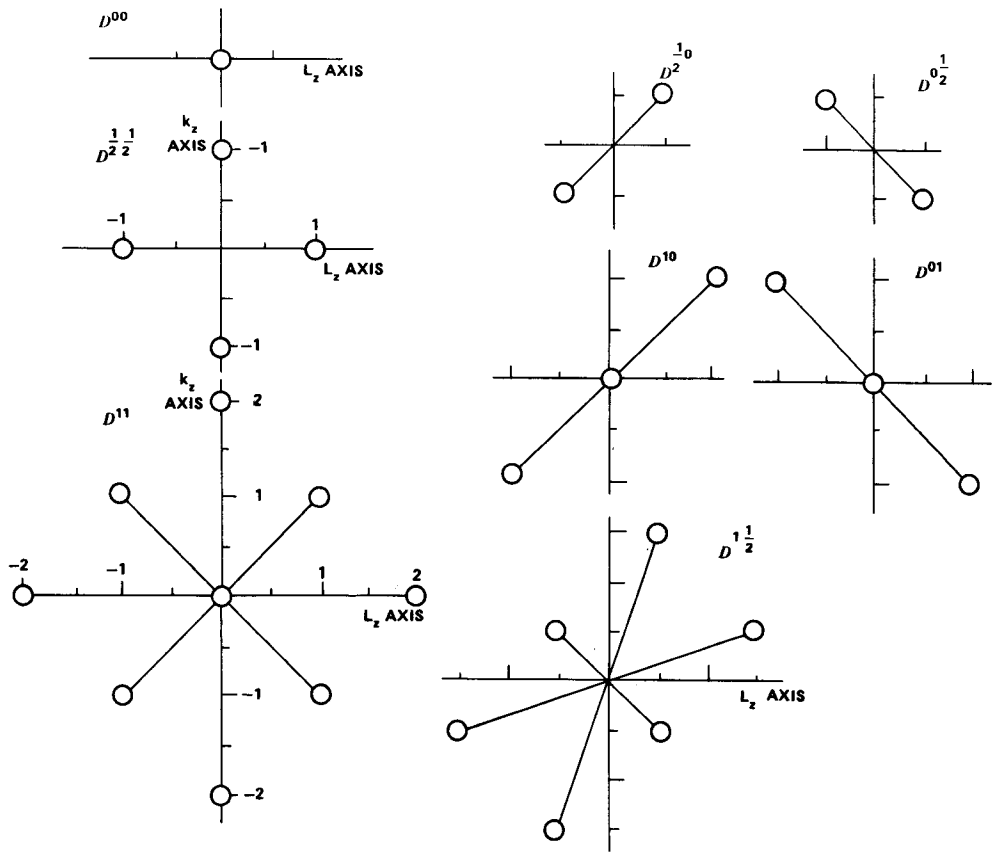

Figure 5.8.3 Examples of weight diagrams for irreducible representations for the R_4 Lie algebra. Eight examples of R_4 irreps are chosen in order to show the form of their weight diagrams.

(c) Coulomb Eigenstates The single-electron Coulomb energy levels belong only to certain irreps $\mathscr{D}^{j_m j_n}$ of R_4, namely, those for which $j_m = j_n = 0, \frac{1}{2}, 1, \ldots$ (see the left-hand side of Figure 5.8.3. This is because the vectors $\boldsymbol{\varepsilon}$ or $\mathbf{K}$ are orthogonal to L:

$$\mathbf{K} \cdot \mathbf{L} = 0,$$

which implies that

$$\mathbf{M}^2 - \mathbf{N}^2 = (\mathbf{M} + \mathbf{N}) \cdot (\mathbf{M} - \mathbf{N}) = 4\mathbf{K} \cdot \mathbf{L} = 0. \qquad (5.8.31)$$

This relation holds for the operators as well, since M and N commute. Hence we have $j_n(j_n + 1) = j_m(j_m + 1)$ or $j_m = j_n$.

The first energy level is singly degenerate corresponding to the scalar irrep $\mathscr{D}^{00}$. This would be the hydrogen 1s level. The second energy level is fourfold degenerate, corresponding to the irrep $\mathscr{D}^{(1/2)(1/2)}$. From the weight diagram in Figure 5.8.3 we see that one state has orbital momentum $L_z = +1$; two states have $L_z = 0$, while a fourth state has $L_z = -1$. Together these will make the $2p$ ($l = 1$) and $2s$ ($l = 0$) levels of hydrogen. Similarly, the ninefold degenerate $\mathscr{D}^{11}$ corresponds to the degenerate $3s$, $3p$, and $3d$ ($l = 2$) states of hydrogen.

The Coulomb energy spectrum can be given in terms of the $\langle M^2 \rangle = \langle N^2 \rangle$ eigenvalues. The classical equation (5.8.5) gives

$$-K^2 = \frac{k^2 m}{2H}, \qquad \varepsilon^2 = \frac{k^2 m}{2H} + L^2,$$

or

$$H = -(k^2 m/2)/(K^2 + L^2) = (k^2 m/2)/(2M^2 + 2N^2). \quad (5.8.32)$$

However, this fails to take account of the operator noncommutivity. After considerable algebra one obtains the correct form:

$$H = -(k^2 m/2)/(2M^2 + 2N^2 + 1), \quad (5.8.33)$$

which gives the Rydberg formula if we substitute $\langle M^2 \rangle = \langle N^2 \rangle = j_M(j_M + 1)$:

$$E^{j_m} = -(k^2 m/2)/(2j_m + 1)^2. \quad (5.8.34)$$

The form of the spectrum and wave functions is sketched some pages ahead in Figure 5.8.6.

B. The Harmonic Oscillator Symmetry

A particle of mass $m = 1$ in a three-dimensional isotropic harmonic oscillator potential is described by the following Hamiltonian:

$$H = p^2/2 + \omega^2 r^2/2 = a_x^\dagger a_x + a_y^\dagger a_y + a_z^\dagger a_z + \tfrac{3}{2}1. \quad (5.8.35a)$$

Here the creation operators

$$a_j^\dagger = \left(\sqrt{\omega}\, x_j + i p_j/\sqrt{\omega}\right)/2 \quad (5.8.35b)$$

are the standard ones introduced in Section 4.4.D.

This Hamiltonian is obviously invariant to R_3 rotations. However, the expression of it in terms of a's shows that it is also invariant to a more

general group of transformations. The full symmetry is the unitary group of transformations in three dimensions or U_3. We have that

$$\sum_j a_j^\dagger a_j \to \sum_j \left(\sum_k U_{jk}^* a_k^\dagger\right)\left(\sum_l U_{jl} a_l\right) = \sum_k \sum_l \left(\sum_j U_{jk}^* U_{jl}\right) a_k^\dagger a_l$$
$$= \sum_k a_k^\dagger a_k$$

for all unitary transformations for which

$$\sum_j U_{jk}^* U_{jl} = \sum_j U_{kj}^\dagger U_{jl} = \delta_{kl},$$

or in abstract notation

$$U^\dagger = U^{-1}.$$

We discuss this group U_3 now.

(a) Introduction to the Lie Algebra of U_3 The requirement that an infinitesimal operator

$$U = 1 + \varepsilon G = 1 + \frac{\varepsilon}{i} L$$

be a unitary operator gives the following relations:

$$U^{-1} = U^\dagger,$$
$$1 - \varepsilon G = 1 - \frac{\varepsilon}{i} L = 1 - \frac{\varepsilon}{i} L^\dagger = 1 + \varepsilon G^\dagger$$
$$G^\dagger = -G, \qquad L^\dagger = L. \tag{5.8.36}$$

In U_3 one admits complex operators U and generators G. However, G must be anti-Hermitian, or what is the same thing, $L = iG$ must be Hermitian. Translating this into matrix language the generators of U_3 include the three antisymmetric Hermitian generators of R_3:

$$L_{32} = iG_{32} \to i\mathscr{G}_{32}, \qquad L_{13} = iG_{13} \to i\mathscr{G}_{13}, \qquad L_{21} = iG_{21} \to i\mathscr{G}_{21}$$
$$= \begin{pmatrix} \cdot & \cdot & \cdot \\ \cdot & \cdot & -i \\ \cdot & i & \cdot \end{pmatrix}, \qquad = \begin{pmatrix} \cdot & \cdot & i \\ \cdot & \cdot & \cdot \\ -i & \cdot & \cdot \end{pmatrix}, \qquad = \begin{pmatrix} \cdot & -i & \cdot \\ i & \cdot & \cdot \\ \cdot & \cdot & \cdot \end{pmatrix}. \tag{5.8.37}$$

However, there are six more *symmetric* Hermitian matrices

$$K_{32} \to \mathscr{K}_{32}, \quad = \begin{pmatrix} \cdot & \cdot & \cdot \\ \cdot & \cdot & 1 \\ \cdot & 1 & \cdot \end{pmatrix}, \qquad K_{13} \to \mathscr{K}_{13}, \quad = \begin{pmatrix} \cdot & \cdot & 1 \\ \cdot & \cdot & \cdot \\ 1 & \cdot & \cdot \end{pmatrix}, \qquad K_{21} \to \mathscr{K}_{11} \quad = \begin{pmatrix} \cdot & 1 & \cdot \\ 1 & \cdot & \cdot \\ \cdot & \cdot & \cdot \end{pmatrix}$$

$$E_{11} \to \mathscr{E}_{11}, \quad = \begin{pmatrix} 1 & \cdot & \cdot \\ \cdot & \cdot & \cdot \\ \cdot & \cdot & \cdot \end{pmatrix}, \qquad E_{22} \to \mathscr{E}_{22}, \quad = \begin{pmatrix} \cdot & \cdot & \cdot \\ \cdot & 1 & \cdot \\ \cdot & \cdot & \cdot \end{pmatrix}, \qquad E_{33} \to \mathscr{E}_{33} \quad = \begin{pmatrix} \cdot & \cdot & \cdot \\ \cdot & \cdot & \cdot \\ \cdot & \cdot & 1 \end{pmatrix}. \tag{5.8.38}$$

It is convenient to define ELEMENTARY matrices or operators as follows:

$$E_{12} \to \mathscr{E}_{12} = \begin{pmatrix} \cdot & 1 & \cdot \\ \cdot & \cdot & \cdot \\ \cdot & \cdot & \cdot \end{pmatrix} = \frac{K_{21} - G_{21}}{2},$$

$$E_{13} \to \mathscr{E}_{13} = \begin{pmatrix} \cdot & \cdot & 1 \\ \cdot & \cdot & \cdot \\ \cdot & \cdot & \cdot \end{pmatrix} = \frac{K_{13} + G_{13}}{2},$$

$$E_{23} \to \mathscr{E}_{23} = \begin{pmatrix} \cdot & \cdot & \cdot \\ \cdot & \cdot & 1 \\ \cdot & \cdot & \cdot \end{pmatrix} = \frac{K_{32} - G_{32}}{2},$$

$$E_{21} \to \mathscr{E}_{21} = \begin{pmatrix} \cdot & \cdot & \cdot \\ 1 & \cdot & \cdot \\ \cdot & \cdot & \cdot \end{pmatrix} = \frac{K_{21} + G_{21}}{2},$$

$$E_{31} \to \mathscr{E}_{31} = \begin{pmatrix} \cdot & \cdot & \cdot \\ \cdot & \cdot & \cdot \\ 1 & \cdot & \cdot \end{pmatrix} = \frac{K_{13} - G_{13}}{2},$$

$$E_{32} \to \mathscr{E}_{32} = \begin{pmatrix} \cdot & \cdot & \cdot \\ \cdot & \cdot & \cdot \\ \cdot & 1 & \cdot \end{pmatrix} = \frac{K_{32} + G_{32}}{2}. \tag{5.8.39}$$

The elementary operators satisfy the following commutation relations:

$$\left[E_{ij}, E_{kl}\right] = \delta_{jk} E_{il} - \delta_{li} E_{kj}. \tag{5.8.40}$$

The elementary operators are already in a form that conforms to the Cartan root vector formalism introduced in the previous section. However, there are now three operators E_{11}, E_{22}, and E_{33} which commute with each other. Hence, there are three components for each root vector, as in the following example:

$$\begin{aligned}&[E_{11}, E_{12}] = E_{12},\\ &[E_{22}, E_{12}] = -E_{12},\\ &[E_{33}, E_{12}] = 0,\end{aligned} \qquad R(12) = \begin{pmatrix} 1 \\ -1 \\ 0 \end{pmatrix}.$$

This root vector is drawn in Figure 5.8.4(a), along with five others corresponding to the generators in Eq. (5.8.39). Note that the roots form a hexagon as indicated in Figure 5.8.4.

It is convenient to define combinations of the E_{11}, E_{22}, and E_{33} that correspond to the symmetry axes H_1, H_2, and H_3 of the hexagon:

$$\begin{aligned}H_1 &\equiv (E_{11} - E_{33})/\sqrt{2N},\\ H_2 &\equiv (E_{11} - 2E_{22} + E_{33})/\sqrt{6N},\\ H_3 &\equiv (E_{11} + E_{22} + E_{33})/\sqrt{3N}.\end{aligned} \tag{5.8.41}$$

By discarding the unit generator H_3 we obtain a Lie algebra of a group called SU_3 or A_2. By choosing the constant $N = 6$ and defining

$$\begin{aligned}E_1 &\equiv E_{12}/\sqrt{6}, \quad E_2 \equiv E_{23}/\sqrt{6}, \quad E_3 \equiv E_{13}/\sqrt{6},\\ E_{-1} &\equiv E_{21}/\sqrt{6}, \quad E_{-2} \equiv E_{32}/\sqrt{6}, \quad E_{-3} \equiv E_{31}/\sqrt{6},\end{aligned} \tag{5.8.42}$$

we obtain Cartan's standard form for the SU_3 algebra with the commutation relations given in terms of the roots in Figure 5.8.4(c):

$$[H_i, E_\alpha] = r_i(a)E_\alpha, \qquad [E_\alpha, E_{-\alpha}] = \sum_j r_j(\alpha)H_j,$$

$$[E_\alpha, E_\beta] = \sqrt{j(k+1)/2}\,|r(\alpha)|E_{\alpha+\beta}.$$

The integers j and k are given by

$$\begin{aligned}j &= \text{number of times that } \mathbf{r}(\alpha) \text{ can be raised by } \mathbf{r}(\beta),\\ &\text{and } k - j = \frac{2r(\alpha)\cdot r(\beta)}{r(\beta)\cdot r(\beta)},\\ k &= \text{number of times that } \mathbf{r}(\alpha) \text{ can be lowered by } -r(\beta).\end{aligned} \tag{5.8.43}$$

Cartan has shown that these relations are valid for an important class of Lie algebras.

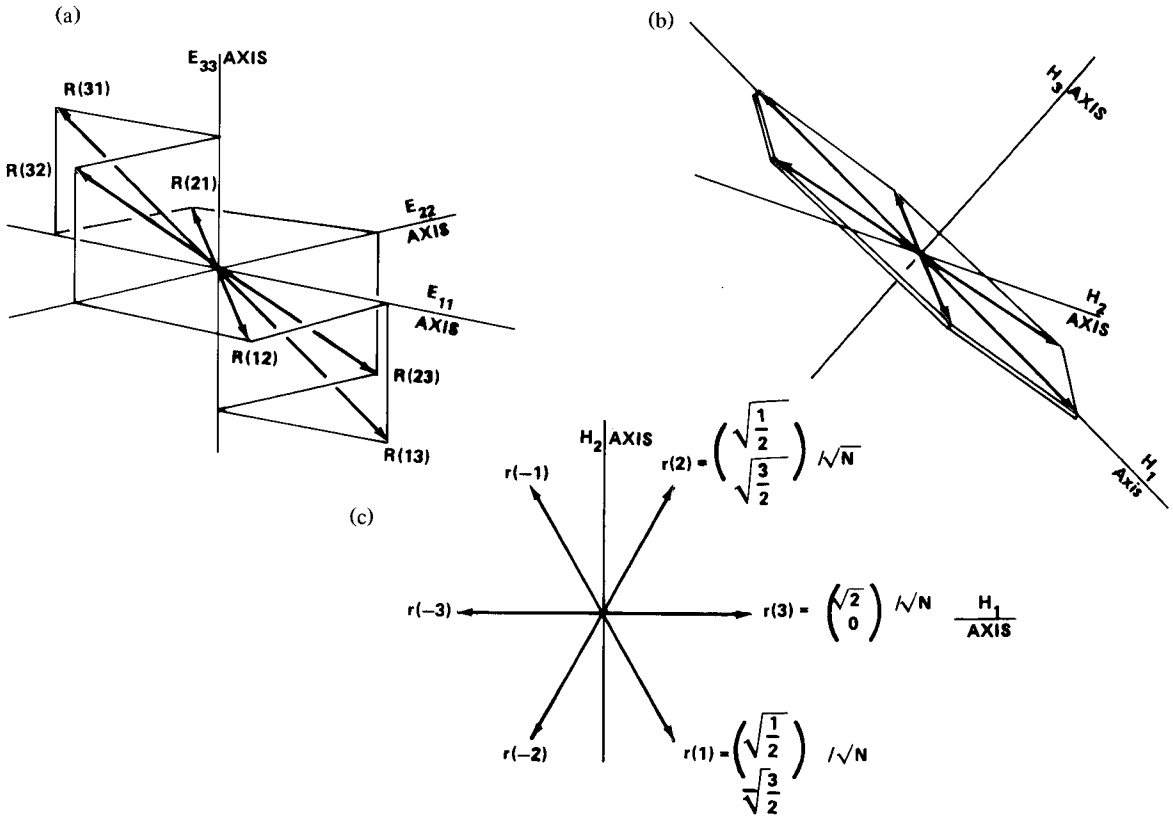

Figure 5.8.4 Root diagrams for Lie algebras of U_3 and SU_3. (a) Elementary form of U_3 root diagram is based on the commutation structure of elementary E_{ij} operators. (b) The U_3 roots $R(ij)$ lie in a hexagonal plane. (c) The normalized Cartan forms of the SU_3 roots form a hexagon.

(b) Introduction to Irreducible Representations of U_3 and SU_3 As shown in the discussion of R_4, the base states of Lie algebra irreps have weight vectors which may be raised or lowered by root vectors. In U_3 we call the vectors $r(1)$, $r(2)$, and $r(3)$ raising or POSITIVE root vectors, while $r(-1)$, $r(-2)$, and $r(-3)$ are called lowering or NEGATIVE root vectors.

Now some examples of weight vectors for SU_3 irreps are shown in Figure 5.8.5. For each set of vectors there is always one called the HIGHEST WEIGHT $M^{n_1n_2}$ which cannot be raised without going outside the set for that irrep. The Cartan theory gives the following relations between $M^{n_1n_2}$ and the positive root vectors $r(1)$ and $r(2)$,

$$\begin{aligned} n_1 &= 2M^{n_1n_2} \cdot r(1)/r(1) \cdot r(1) \\ &= \text{number of times } M \text{ can be lowered by } r(-1), \\ n_2 &= 2M^{n_1n_2} \cdot r(2)/r(2) \cdot r(2) \\ &= \text{number of times } M \text{ can be lowered by } r(-2). \end{aligned} \tag{5.8.44}$$

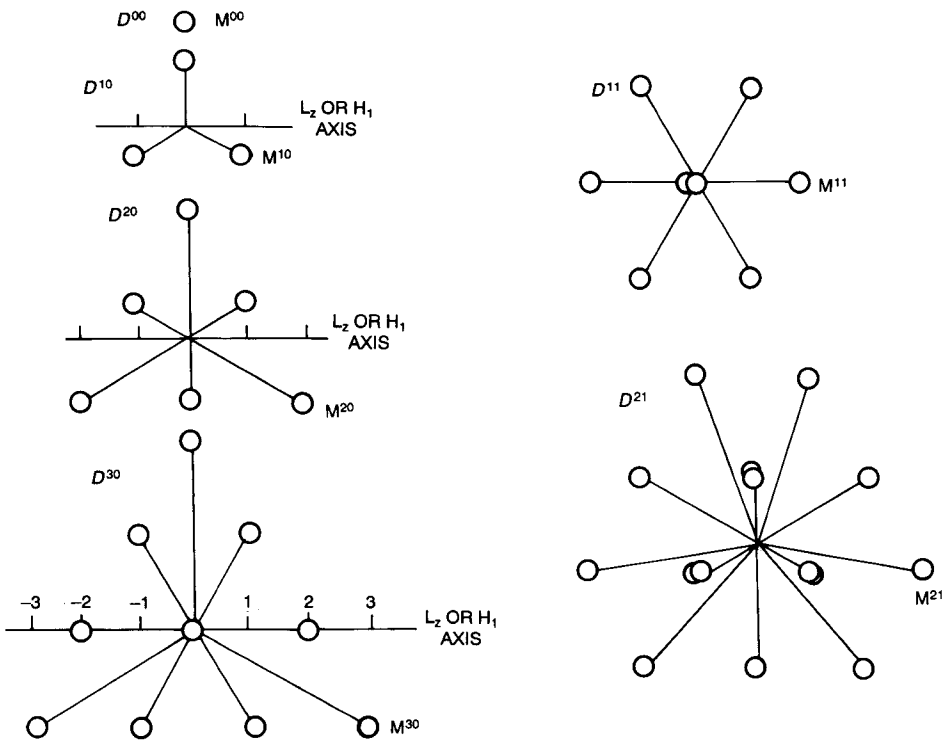

Figure 5.8.5 Examples of weight diagrams for irreducible representations of SU_3.

The vector relations determine the weight vectors of each SU_3 irrep, i.e., the eigenvalues of $\mathscr{D}^{n_1 n_2}(H_j)$. Further theory is needed to find $\mathscr{D}^{n_1 n_2}(E)$.

(c) Harmonic Oscillator Spectrum It happens that the SU_3 irreps $\mathscr{D}^{n_1 n_2}$ with $n_2 = 0$ correspond to single-particle energy levels of the three-dimensional harmonic oscillator. These correspond to weight diagrams on the left-hand side of Figure 5.8.5. The irreps with $n_2 \neq 0$ describe multiparticle states.

The first oscillator level is nondegenerate, corresponding to the irrep $\mathscr{D}^{00}$. The second level is triply degenerate corresponding to irrep $\mathscr{D}^{10}$. The states in the second level are one quantum each of excitation of motion in the x, y, or z directions. We may also describe them as angular-momentum $p(=1)$ states $\left|\begin{smallmatrix}1\\1\end{smallmatrix}\right\rangle$, $\left|\begin{smallmatrix}1\\0\end{smallmatrix}\right\rangle$ and $\left|\begin{smallmatrix}1\\-1\end{smallmatrix}\right\rangle$. In fact, we may interpret the H_1 axis as the orbital momentum (L_z) axis since operators $2\sqrt{3}H_1$, $\sqrt{6}E_1$, and $\sqrt{6}E_{-1}$ behave like ordinary angular-momentum operators L_z, L_+, and L_-, respectively.

The third oscillator level belongs to the $\mathscr{D}^{20}$ irrep and has a sixfold degeneracy: five $d(l = 2)$ states and one $s(l = 0)$ orbital, or, equivalently, the six combinations of double excitations xx, yy, zz, xy, xz, and y_z. The fourth level belongs to $\mathscr{D}^{30}$ with a $f(l = 3)$ and a $p(l = 1)$ orbital, and so forth.

(d) Comparing Coulomb and Harmonic Oscillator Spectra It is interesting to compare the oscillator and Coulomb problems. In some ways these two high-symmetry examples are extreme opposites. The Coulomb problem treats a charged particle orbiting outside a single attractive point charge. The oscillator problem treats the same particle orbiting inside a large uniform spherical cloud of attractive charge. The Coulomb problem is a good starting point for atomic and molecular structure theory. The oscillator spectrum has been shown to offer a similar, though less easily understood, starting point for the internal structure of nuclei.

In atomic shell theory we imagine filling each Coulomb level in Figure 5.8.6(a) with one pair of electrons. The *magic numbers* like 2 or 10 are the numbers of electrons which give a closed-shell atom, i.e., $(1s)^2$ = He, $(1s)^2(2s + 2p)^8$ = Ne, which have greater chemical stability. Similarly, in nuclear shell theory the magic numbers 2, 8, or 20 give the numbers of protons or neutrons which give closed-shell nuclei, i.e., ${}_2\mathrm{He}_2^4$, ${}_8\mathrm{O}_8^{16}$, ${}_{20}\mathrm{Ca}_{20}^{40}$ which have exceptionally great binding energy. The theory of nuclear shells is based upon the oscillator spectrum in Figure 5.8.6(b).

These single-particle theories work well, up to a point. For example, in potassium [next atom after argon $((1s)^2(2s)^2(2p)^6(3s)^2(3p)^6)$] it appears that the next electron does not settle in the $3d$ shell, but rather in a $4s$ level. One way to explain this is to say that the presence of the other electrons makes a deeply diving $4s$ level have lower energy than the $3d$.

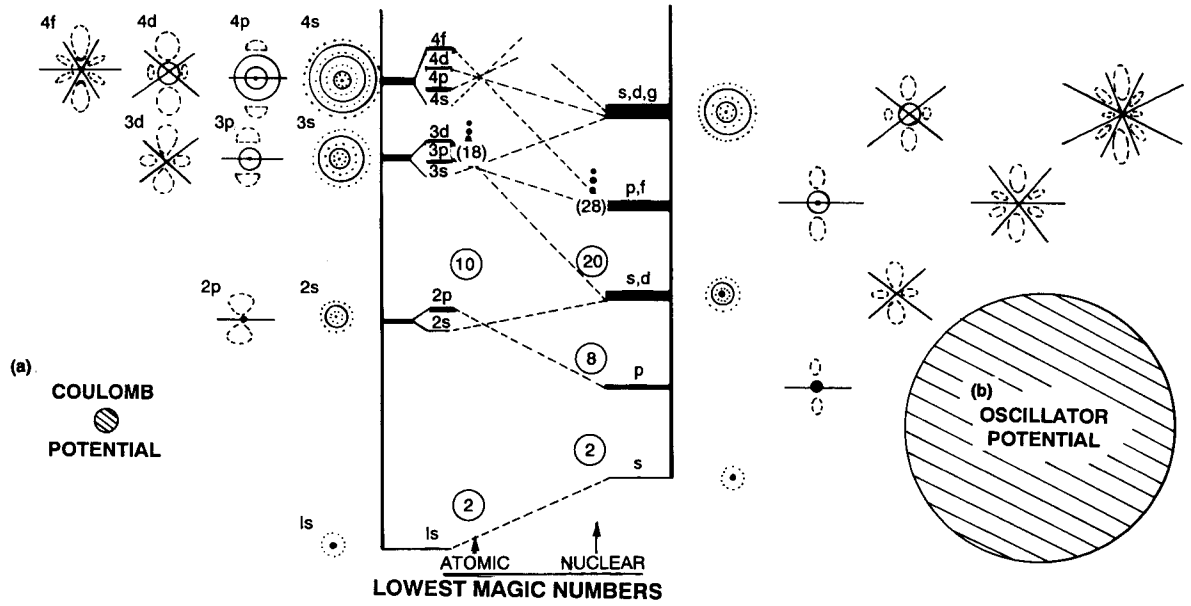

Figure 5.8.6 Sketches of single-particle eigenfunctions and levels for (a) the Coulomb ($V = k/r$) potential, and (b) the harmonic oscillator ($V = kr^2$) potential.

The explanation of higher nuclear shell structure requires a more detailed theory, too, including spin-orbit and internuclear interactions. The next nuclear magic numbers turn out to be 28, 50, 82, and 126.

APPENDIX E. DERIVATION OF ANGULAR-MOMENTUM REPRESENTATIONS

In the following the matrices representing the generators or angular-momentum operators will be derived using their commutation relations. (E.1):

$$[J_1, J_2] = i\hbar J_3, \qquad [J_2, J_3] = i\hbar J_1, \qquad [J_3, J_1] = i\hbar J_2. \tag{E.1}$$

We will choose to find the bases in which J_3 and J_z are diagonal, and therefore it will be convenient to rewrite (E.1) in the form (E.2),

$$[J_3, J_+] = \hbar J_+, \qquad [J_3, J_-] = -\hbar J_- \qquad [J_+, J_-] = 2\hbar J_3, \tag{E.2}$$

where $J_+ = J_1 + iJ_2$, and $J_- = J_1 - iJ_2$ play there the role of eigenvectors under the transformation $[J_3, \ ]$. In deriving (E.2) the relations below were used, and will be needed again shortly (let us also take $\hbar = 1$):

$$J_+J_- = J_1^2 + J_2^2 - i[J_1J_2] = J_1^2 + J_2^2 + \hbar J_3 = J_1^2 + J_2^2 + J_3, \tag{E.3}$$

$$J_-J_+ = J_1^2 + J_2^2 - \hbar J_3 = J_1^2 + J_2^2 - J_3. \tag{E.4}$$

The operator $J^2 = J_1^2 + J_2^2 + J_3^2$ can be expressed in terms of $J_\pm$ and J_3 as in (E.5) and (E.6):

$$J^2 = J_+J_- + J_3^2 - J_3 \tag{E.5}$$

$$= J_-J_+ + J_3^2 + J_3. \tag{E.6}$$

The preceding makes it easy to prove that J_3 commutes with J^2, as in the following, where Eq. (E.2) was used:

$$[J_3, J^2] = [J_3, J_+J_-] = [J_3, J_+]J_- + J_+[J_3, J_-] = 0. \tag{E.7}$$

The J_3 and J^2 are commuting Hermitian operators, and so orthonormal vectors $\left|\begin{matrix}\alpha \\ m\end{matrix}\right\rangle$ exist which are eigenvectors of both J^2 and J_3. It is necessary to find what values α and m can be:

$$J^2\left|\begin{matrix}\alpha \\ m\end{matrix}\right\rangle = \alpha\left|\begin{matrix}\alpha \\ m\end{matrix}\right\rangle, \qquad J_3\left|\begin{matrix}\alpha \\ m\end{matrix}\right\rangle = m\left|\begin{matrix}\alpha \\ m\end{matrix}\right\rangle. \tag{E.8}$$

First, note that the operators $J_\pm$ make eigenvectors with higher or lower eigenvalues of J_3:

$$J_3 J_+ \left|\begin{matrix}\alpha\\ m\end{matrix}\right\rangle = ([J_3, J_+] + J_+ J_3)\left|\begin{matrix}\alpha\\ m\end{matrix}\right\rangle = (J_+ + mJ_+)\left|\begin{matrix}\alpha\\ m\end{matrix}\right\rangle$$

$$= (m+1)J_+\left|\begin{matrix}\alpha\\ m\end{matrix}\right\rangle, \tag{E.9}$$

$$J_3 J_- \left|\begin{matrix}\alpha\\ m\end{matrix}\right\rangle = (m-1)J_-\left|\begin{matrix}\alpha\\ m\end{matrix}\right\rangle. \tag{E.10}$$

These operators $J_\pm$ are called RAISING or LOWERING operators because of this effect. We shall assure that the vector $J_\pm\left|\begin{matrix}\alpha\\ m\end{matrix}\right\rangle$ is proportional to $\left|\begin{matrix}\alpha\\ m\pm 1\end{matrix}\right\rangle$.

Let us now inquire about just how far one may "raise" or "lower." We observe from (E.5) and (E.6) that α must be equal or greater than m or $-m$:

$$\alpha - m = \left\langle\begin{matrix}\alpha\\ m\end{matrix}\right| J^2 - J_3\left|\begin{matrix}\alpha\\ m\end{matrix}\right\rangle = \left\langle\begin{matrix}\alpha\\ m\end{matrix}\right| J_- J_+ + J_3^2\left|\begin{matrix}\alpha\\ m\end{matrix}\right\rangle = \left\langle\begin{matrix}\alpha\\ m\end{matrix}\right| J_+^\dagger J_+ + J_3^\dagger J_3\left|\begin{matrix}\alpha\\ m\end{matrix}\right\rangle \geq 0, \tag{E.11}$$

$$\alpha + m = \left\langle\begin{matrix}\alpha\\ m\end{matrix}\right| J^2 + J_3\left|\begin{matrix}\alpha\\ m\end{matrix}\right\rangle = \left\langle\begin{matrix}\alpha\\ m\end{matrix}\right| J_+ J_- + J_3^2\left|\begin{matrix}\alpha\\ m\end{matrix}\right\rangle = \left\langle\begin{matrix}\alpha\\ m\end{matrix}\right| J_-^\dagger J_- + J_3^\dagger J_3\left|\begin{matrix}\alpha\\ m\end{matrix}\right\rangle \geq 0. \tag{E.12}$$

In the last step of (E.11) and (E.12) we use the fact that diagonal elements of any operator $A^\dagger A$ is positive or zero, as seen in the following:

$$\langle a|A^\dagger A|a\rangle = \sum_b \langle a|A^\dagger|b\rangle\langle b|A|a\rangle = \sum_b |\langle a|A|b\rangle|^2 \geq 0.$$

So for a given α, there is a limit to the raising process. Suppose $m = j$ is the highest value of m for a given α. Then (E.13) must hold:

$$J_+\left|\begin{matrix}\alpha\\ j\end{matrix}\right\rangle = 0. \tag{E.13}$$

Applying (E.6) and the foregoing we discover the value of α:

$$J^2\left|\begin{matrix}\alpha\\ j\end{matrix}\right\rangle = (J_- J_+ + J_3^2 + J_3)\left|\begin{matrix}\alpha\\ j\end{matrix}\right\rangle = j(j+1)\left|\begin{matrix}\alpha\\ j\end{matrix}\right\rangle. \tag{E.14}$$

This eigenvalue $\alpha = j(j+1)$ applies to all lowered states $J_-\left|\begin{matrix}\alpha\\ j\end{matrix}\right\rangle$, i.e., all states $\left|\begin{matrix}\alpha\\ m\end{matrix}\right\rangle$ since J_- commutes with J^2. But, this lowering is limited, too, say

to $m = j'$ as in Eq. (E.15):

$$J_- \left| \begin{matrix} \alpha \\ j \end{matrix} \right\rangle = 0. \tag{E.15}$$

Applying (E.5) exactly as in the foregoing we get the following:

$$J^2 \left| \begin{matrix} \alpha \\ j' \end{matrix} \right\rangle = j'(j' - 1) \left| \begin{matrix} \alpha \\ j \end{matrix} \right\rangle,$$

from which we can only conclude $j(j + 1) = j'(j' - 1)$. The two solutions $j' = j + 1$ and $j' = -j$ are indicated, but only the latter is acceptable since we said $m = j$ was the largest.

So, for a given $\alpha = j(j + 1)$, the m range in steps of 1, between $m = +j$ and $m = -j$, inclusive. We see that this is possible only if $j = 0, \frac{1}{2}, 1, \frac{3}{2}, \ldots$.

Now the representation $\mathscr{D}^j$ of $J_\pm$ in (E.16) can be produced for any j.

$$J_+ \left| \begin{matrix} j \\ m \end{matrix} \right\rangle = \mathscr{D}^j_{m+1,m}(J_+) \left| \begin{matrix} j \\ m+1 \end{matrix} \right\rangle, \qquad J_- \left| \begin{matrix} j \\ m \end{matrix} \right\rangle = \mathscr{D}^j_{m-1,m}(J_-) \left| \begin{matrix} j \\ m-1 \end{matrix} \right\rangle \tag{E.16}$$

By taking the scalar product the following relation results:

$$\left| \mathscr{D}^j_{m+1,m}(J_+) \right|^2 = \left\langle \begin{matrix} j \\ m \end{matrix} \middle| J_+^\dagger J_+ \middle| \begin{matrix} j \\ m \end{matrix} \right\rangle = \left\langle \begin{matrix} j \\ m \end{matrix} \middle| J_- J_+ \middle| \begin{matrix} j \\ m \end{matrix} \right\rangle,$$

$$\left| \mathscr{D}^j_{m-1,m}(J_-) \right|^2 = \left\langle \begin{matrix} j \\ m \end{matrix} \middle| J_-^\dagger J_- \middle| \begin{matrix} j \\ m \end{matrix} \right\rangle = \left\langle \begin{matrix} j \\ m \end{matrix} \middle| J_+ J_- \middle| \begin{matrix} j \\ m \end{matrix} \right\rangle.$$

Applying (E.5) and (E.6), respectively, gives the desired result to within a phase.

$$\begin{aligned} \left| \mathscr{D}^j_{m+1,m}(J_+) \right|^2 &= \left\langle \begin{matrix} j \\ m \end{matrix} \middle| J^2 - J_3^2 - J_3 \middle| \begin{matrix} j \\ m \end{matrix} \right\rangle \\ &= (j(j+1) - m^2 - m) = (j - m)(j + m + 1), \\ \left| \mathscr{D}^j_{m-1,m}(J_-) \right|^2 &= \left\langle \begin{matrix} j \\ m \end{matrix} \middle| J^2 - J_3^2 + J_3 \middle| \begin{matrix} j \\ m \end{matrix} \right\rangle \\ &= (j(j+1) - m^2 + m) = (j + m)(j - m + 1). \end{aligned}$$

It is conventional to choose positive real phases:

$$\begin{aligned} \mathscr{D}^j_{m+1,m}(J_+) &= \sqrt{j(j+1) - m(m+1)}, \\ \mathscr{D}^j_{m-1,m}(J_-) &= \sqrt{j(j+1) - m(m-1)}. \end{aligned} \tag{E.17}$$

ADDITIONAL READING

The most comprehensive treatment of quantum theory of angular-momentum and rotation-group theory are two volumes of the *Encyclopedia of Mathematics and Its Applications*.

L. C. Biedenharn and J. D. Louck, *Angular Momentum in Quantum Physics: Theory and Application*, Vol. 8, Encyclopedia of Mathematics, edited by G. C. Rota (Addison-Wesley, Reading, MA, 1981).

L. C. Biedenharn and J. D. Louck, *The Racah Wigner Algebra in Quantum Theory*, Vol. 9, Encyclopedia of Mathematics, edited by G. C. Rota (Addison-Wesley, Reading, MA, 1981).

These two volumes are valuable for their history and references as well as for their content. A shorter and more "user friendly" reference is the recent monograph by Zare.

R. N. Zare, *Angular Momentum: Understanding Spatial Aspects in Chemistry and Physics* (Wiley Interscience, New York, 1988).

This book is aimed at applications in atomic and molecular physics, particularly diatomic and nearly symmetric top molecules.

A slightly older and more advanced book along the same lines is by Judd. It also includes a treatment of $O(4)$.

Brian R. Judd, *Angular Momentum Theory for Diatomic Molecules* (Academic, New York, 1975).

Judd is also the author of another classic text on angular-momentum calculus.

B. R. Judd, *Operator Techniques in Atomic Spectroscopy* (McGraw-Hill, New York, 1963).

Several of the well-known older texts which treat angular-momentum theory are listed here.

E. Feinberg and G. E. Pake, *Notes on the Quantum Theory of Angular Momentum* (Addison-Wesley, Reading, MA, 1953).

M. E. Rose, *Elementary Theory of Angular Momentum* (Wiley, New York, 1957).

E. P. Wigner, *Group Theory*, (Academic, New York, 1959).

A. R. Edmonds, *Angular Momentum in Quantum Mechanics*, (Princeton University Press, Princeton, NJ, 1960).

D. M. Brink and G. R. Satchler, *Angular Momentum* (Oxford University Press, London, 1968).

A collection of famous papers on angular momentum are found in the following volumes. The first volume contains Schwinger's original boson algebraic treatment of angular momentum.

L. C. Biedenharn and H. Van Dam, Eds., *Quantum Theory of Angular Momentum* (Academic, New York, 1965).

E. M. Loebl, Ed., *Group Theory and Its Applications* (Academic, New York, 1968), Vols. I and II.

The quantum rotor and its angular-momentum theory probably originated with Casimir.

H. B. G. Casimir, *Rotation of a Rigid Body in Quantum Mechanics* (J. B. Walter's Vitgevers-Maatschappij, N. V. Gronigen den Haag Batavia, 1931).

References for the theory of quaternions and the $U(2)$ slide-rule wave given after Chapter 3. See also (if you can find it).

C. J. Joly, *Manual of Quaternions* (Macmillan, New York, 1965).

The application of $O(4)$ symmetry to the Coulomb problem is discussed in the following.

M. J. Englefield, *Group Theory and the Coulomb Problem* (Wiley Interscience, New York, 1972).

See also an article by Carl Wulfman in Volume II of Loebl (just listed). This led to a renaissance in the application of $O(4)$ and related methods to the spectra of doubly excited atoms.

C. E. Wulfman, *Chem. Phys. Lett.*, **23**, 370 (1973).

O. Sinanoglu and D. R. Herrick, *J. Chem. Phys.*, **62**, 886 (1975).

D. R. Herrick and M. E. Kellman, *Phys. Rev. A*, **21**, 418 (1980).

M. E. Kellman and D. R. Herrick, *Phys. Rev. A*, **22**, 1536 (1980).

D. R. Herrick, M. E. Kellman, and R. D. Poliah, *Phys. Rev. A*, **22** 1517 (1980).

P. Rehmus and R. S. Berry, *Chem. Phys.*, **38**, 257 (1978).

P. Rehmus, M. E. Kellman, and R. S. Berry, *Chem. Phys.*, **31**, 239 (1978).

D. R. Herrick, *Adv. Chem. Phys.*, **52**, 1 (1982).

PROBLEMS

Section 5.1

5.1.1 Suppose an n-by-n real matrix R is constructed with ($n \geq 2$) so that its columns consist of n mutually orthonormal real n-dimensional vectors $\Psi_1, \Psi_2 \cdots \Psi_n \cdots$. Suppose we construct two new vectors ϕ_1 and ϕ_2 by extracting first and second *rows*, respectively, of R.

(a) What (if anything) can we say about the values of scalar products $\phi_1 \cdot \phi_1$? Or $\phi_1 \cdot \phi_2$? Given R could you *quickly* give the values of scalar products $\phi_1 \cdot \Psi_1$? Or $\phi_1 \cdot \Psi_2$?

(b) Answer similarly worded questions involving *complex* matrix J and scalar products $\langle \phi_1 | \phi_1 \rangle$, $\langle \phi_1 | \phi_2 \rangle$, $\langle \phi_1 | \Psi_1 \rangle$, and $\langle \phi_1 | \Psi_2 \rangle$ of complex vectors.

(c) What type of matrices are R and J using the terminology of Chapter 1?

5.1.2 (a) What is the trace of a proper orthogonal 3-by-3 transformation matrix O_{ij} that performs a rotation of angle ϕ around the z axis? What is the trace if the same rotation is around the x axis? ... Or around the (111) axis?

(b) What is the trace of the corresponding *improper* operation?

(c) Suppose instead of using a set of Cartesian unit vectors $\{|1\rangle = e_1, |2\rangle = e_2, |3\rangle = e_3\}$ to construct matrix $O_{ij} = \langle i|O|j\rangle$ we use nonorthogonal vectors $|a\rangle = |1\rangle + |2\rangle$, $|b\rangle = |1\rangle + |3\rangle$, $|c\rangle = |2\rangle + |3\rangle$. By how much will the trace of matrix $O_{ab} = \langle a|O|b\rangle$ differ from that of O_{ij}?

5.1.3 A crystal symmetry group operation of translation t or rotation $\mathbf{R}$ may be defined using a basis of three primitive lattice vectors $\mathbf{l}_1$, $\mathbf{l}_2$ and $\mathbf{l}_3$ or three reciprocal vectors $\mathbf{r}_1 = \mathbf{l}_2 \times \mathbf{l}_3/v$, $\mathbf{r}_2 = \mathbf{l}_3 \times \mathbf{l}_1/v$, and $\mathbf{r}_3 = \mathbf{l}_1 \times \mathbf{l}_2/\mathbf{v}$, where $\mathbf{v} = \mathbf{l}_1 \times \mathbf{l}_2 \cdot \mathbf{l}_3$. The idea is that a symmetry operation must transform each lattice vector into an *integral* linear combination of lattice vectors, i.e., another vector in the lattice. Using characters, derive which rotational angles ω are possible for pure rotations $\mathbf{R}[\omega]$ and for improper $\mathbf{R} \cdot \mathbf{I}$ rotations around any lattice point in a two- or three-dimensional lattice. Which of the following point groups correspond to possible crystal point symmetries? D_{2h}? D_{3h}? D_{4h}? D_{5h}? D_{6h}? D_{7h}? D_{2d}? D_{3d}? D_{4d}?

5.2.1 Construct a partial correlation table involving irreps listed in Fig. 5.2.2 for the reduction of symmetry from $D_{\infty h}$ to subgroups

(a) D_{2h}.

(b) D_{3h}.

(c) D_{4h}.

(d) D_{5h}.

(e) D_{6h}.

Sketch each correlation by drawing a level-splitting diagram.

Section 5.3

5.3.1 Use the Cartesian $\{|e_1\rangle, |e_2\rangle, |e_3\rangle\}$ xyz basis to make the 3-by-3 matrix $R_{ij}(\alpha\beta\gamma) = \langle e_i|R(\alpha\beta\gamma)|e_j\rangle$ representing the Euler-angle rotation operator $R(\alpha\beta\gamma)$ defined by (5.3.4).

5.3.2 Suppose you have constructed a rotation matrix $R_{ij}(\alpha 00)$ for rotation α about the z axis and another matrix $R_{ij}(0\beta 0)$ for rotation β about the y axis.

(a) How would you combine these two operations to make one which rotated by angle α around an axis z' that lies in the xz plane at angle β from z. [Hint: z' is obtained from z by rotation

$R(0\beta 0)$. Use class conjugation transformation: $r' = trt^{-1}$.] Test your construction by making a rotation by angle α around the x axis.

(b) How would you combine these two operations to make a Darboux defined rotation $R_{ij}[\phi\theta\omega]$ by angle ω around an axis at azimuth ϕ and polar angle θ.

(c) Carry out the operations found in part (b) to construct the 3-by-3 matrix $R_{ij}[\phi\theta\omega]$.

5.3.3 **(a)** Determine the nine direction cosines $\hat{\mathbf{x}} \cdot \hat{\bar{\mathbf{x}}} = \cos(x\bar{x})$, $\hat{\mathbf{x}} \cdot \hat{\bar{\mathbf{y}}} = \cos(x\bar{y}), \ldots, \hat{\mathbf{z}} \cdot \hat{\bar{\mathbf{z}}}$ in terms of Euler angles $(\alpha\beta\gamma)$ between Cartesian systems $(\mathbf{x}, \mathbf{y}, \mathbf{z})$ and $(\bar{\mathbf{x}} = \mathbf{R}(\alpha\beta\gamma) \cdot \mathbf{x}, \bar{\mathbf{y}} = \mathbf{R} \cdot \mathbf{y}, \bar{\mathbf{z}} = \mathbf{R} \cdot \mathbf{z})$.

(b) Use these results to determine the Euler angles of the transformation

$$R(\alpha\beta\gamma) = \begin{pmatrix} \langle x|\bar{x}\rangle & \langle x|\bar{y}\rangle & \langle x|\bar{z}\rangle \\ \langle y|\bar{x}\rangle & \langle y|\bar{y}\rangle & \langle y|\bar{z}\rangle \\ \langle z|\bar{x}\rangle & \langle z|\bar{y}\rangle & \langle z|\bar{z}\rangle \end{pmatrix}$$

$$= \begin{pmatrix} 1/\sqrt{2} & 1/\sqrt{6} & 1/\sqrt{3} \\ -1/\sqrt{2} & 1/\sqrt{6} & 1/\sqrt{3} \\ 0 & -2/\sqrt{6} & 1/\sqrt{3} \end{pmatrix} = R[\phi\theta\omega]$$

(c) Find axis (Darboux) angles as well. (It may help to look at Problem 5.3.2 first.)

Section 5.4

5.4.1 Verify (5.4.30).

5.4.2 Complete the calculation of $D^1(\alpha\beta\gamma)$ and compare the resulting matrix with the result of Problem 5.3.1. Are their traces equal? Are they equivalent? What change of basis would relate them?

5.4.3 Complete the calculation of $D^2(\alpha\beta\gamma)$.

5.4.5 Suppose the spinor representation of an $U(2)$ group operation is $D^{1/2}(u) = \begin{pmatrix} u_{11} & u_{12} \\ u_{21} & u_{22} \end{pmatrix}$. Derive the formula for the angular-momentum j representation $D^j_{mn}(u)$ in terms of u_{11}, u_{12}, u_{21}, u_{22}, j, m, and n.

5.4.6 Derive phase symmetry relations for D functions.

Write: $D^j_{-m-n}(0\beta 0)$ in terms of $D^j_{mn}(0\beta 0)$.

$D^j_{nm}(0\beta 0)$ in terms of $D^j_{mn}(0\beta 0)$.

$D^j_{mn}(0 - \beta 0)$ in terms of $D^j_{mn}(0\beta 0)$.

$D^j_{mn}(0\pi - \beta 0)$ in terms of $D^j_{-mn}(0\beta 0)$, and/or D^j_{m-n}.

$D^{j*}_{mn}(\alpha\beta\gamma)$ in terms of $D^j_{-m-n}(\alpha\beta\gamma)$.

ection 5.5

5.1 Verify the expression (5.5.1) for $D^{1/2}[(\phi\theta\omega)]$ and compare with the expression (5.4.30) for $D^{1/2}(\alpha\beta\gamma)$. Verify Euler to Darboux angle relations (5.5.2).

5.2 Compute the Darboux parameterized matrix $D^1[\phi\theta\omega]$. Compare to the real vector representation found in Problem 5.3.2(c).

5.3 **(a)** Write a closed-form conversion equations for Euler angles $(\alpha\beta\gamma)$ in terms of axis (Darboux) angles $[\phi\theta\omega]$ and vice versa.

(b) For the following rotations compute Euler angles and axis angles. (These octahedral operations are shown in Figure 4.1.2.)

		Euler angles			Axis angles		
		α	β	γ	ϕ	θ	ω
180° x axis	$\mathbf{R}_{1^2}$	___	___	___	___	___	___
120° (111) axis:	$\mathbf{r}_1$	___	___	___	___	___	___
180° diagonal:	$\mathbf{i}_1$	___	___	___	___	___	___
90° x-axis:	$\mathbf{R}_1$	___	___	___	___	___	___

5.4 Determine the eigenvectors and eigenvalues of the quantum rotor Hamiltonian (5.5.52) for all levels having total angular momentum $j = 1$ and $j = 2$ for rigid molecules having the following principal inertia moments. (Let $\hbar = 1$.) Sketch spectra of levels.

(a) $I_1 = I_2 = 1$; $I_3 = 2$.

(b) $I_1 = I_2 = 10$; $I_3 = 1$.

(c) $I_1 = 1$; $I_2 = 2$; $I_3 = 3$.

5.5 Express the symmetric top Hamiltonian $BJ_{\tilde{x}}^2 + BJ_{\tilde{y}}^2 + CJ_{\tilde{z}}^2$ in terms of Euler angles and momenta $(J_\alpha J_\beta J_\gamma)$. Simplify the expression for the following cases and give classical equations of motion for each:

(a) J along lab z axis.

(b) J along body z axis.

ection 5.6

6.1 Construct a correlation table up to $l = 12$ for the symmetry breaking from $O(3)$ to D_6.

6.2 Construct a correlation table between $O(3)$ irreps $(0^+0^-1^+1^-2^+ \cdots)$ and (a) tetrahedral (T_d) irreps; and (b) icosahedral (I_h) irreps.